AN ABSTRACT IN THE DISSERTATION OF

Mark E. Nielsen for the degree of Doctor of Philosophy in Oceanography presented on December 10, 2008.

Title: Utilization of Natural and Supplemental Biofuels for Harvesting Energy from Marine Sediments

Abstract approved:

---

Clare E. Reimers

A benthic microbial fuel cell (BMFC) is an electrochemical device that generates current from the redox gradient at the sediment-water interface. Early prototypes had anodes buried in anoxic sediments and cathodes in overlying water. The BMFCs described in this dissertation are based on a chamber design that enables the use of high surface-area fiber electrodes and facilitates enhanced mass transport to the anode.

Results from Yaquina Bay, OR, show that mass transport resistance accounted for at least 93% of the total internal resistance for a particular BMFC configuration. Power output was increased 18-fold by mechanically induced fluid transport through the anode chamber. At a cold seep in Monterey Canyon, CA, naturally driven advection resulted in a five-fold increase in power from a BMFC with low-pressure check valves relative to an identical BMFC with high-pressure check valves. Enhanced transport coincided with a change in the microbial community on the anode from one dominated by epsilonproteobacteria to one with relatively even

representation from deltaproteobacteria, epsilonproteobacteria, firmicutes and flavobacterium/cytophaga/bacterioides.

Laboratory experiments investigated the effect of adding supplemental carbon sources to anode chambers. Repeated lactate injections appeared to stimulate sulfate reduction resulting in short term power gains but did not apparently shift the process responsible for baseline current. When a specific inhibitor of sulfate reduction was added, lactate-supplemented and unsupplemented BMFCs performed similarly.

BMFCs have been proposed as power sources for monitoring systems in remote locations. Practical implementation of this technology is governed by three conditions: 1) low-voltage current must be stepped up to meet the requirements of off-the-shelf electronic devices, 2) modest power production and variable power demands require integrated energy storage, and 3) BMFCs should be operated at the most efficient potential for energy production. A combination power converter/potentiostat/rechargeable battery system was described based on these considerations and tested with a chambered BMFC in Yaquina Bay, OR. The BMFC provided intermittent power to an acoustic receiver, and results highlight the need to increase power, make design improvements to better seal the chamber to the sediment and increase the capacity for energy storage.

# Utilization of Natural and Supplemental Biofuels for Harvesting Energy from Marine Sediments

by
Mark E. Nielsen

A DISSERTATION

submitted to

Oregon State University

in partial fulfillment of
the requirements for the
degree of

Doctor of Philosophy

Presented December 10, 2008
Commencement June 2009

Doctor of Philosophy dissertation of Mark E. Nielsen presented on December 10, 2008

APPROVED:

---

Major Professor, representing Oceanography

---

Dean of the College of Oceanic and Atmospheric Sciences

---

Dean of the Graduate School

I understand that my dissertation will become part of the permanent collection of Oregon State University libraries. My signature below authorizes release of my dissertation to any reader upon request.

---

Mark E. Nielsen, Author

# ACKNOWLEDGEMENTS

There are countless people to thank for help over the years that it took to complete this PhD project. First, I thank Dr. Clare Reimers for excellent mentoring and guidance throughout this project. She struck just the right balance of always being available while also letting me be self-directed. I was generously supported for much of my program by an IGERT grant from the National Science Foundation. The experience and education I gained from the Earth's Subsurface Biosphere program was a tremendous asset. Special thanks to Julie Cope, Marty Fisk and Dave Myrold for administering a great program but the true success is due to all the students who participated. I also acknowledge the Office of Naval Research for support over the years. I was aided by excellent committee members, each of whom contributed to my success. John Westall and Hong Liu provided helpful reviews of my manuscripts while Jim McManus and Jack Istok provided facilities and equipment.

I am grateful for a supportive family for instilling me with curiosity and, most importantly for a PhD, persistence. My deepest and humblest appreciation goes to my wife Stephanie, who was with me every step of the way and was nothing but supportive throughout.

# CONTRIBUTION OF AUTHORS

Dr. Clare Reimers provided guidance, advice, interpretation and reviews for all chapters of this dissertation. Dr. Hilmar "Jody" Stecher helped design the Yaquina Bay experiments described in Chapter 2. Dr. Peter Girguis, Dr. Helen White and Sonam Sharma analyzed the microbiology samples from the Monterey Canyon experiments. They contributed the clone library and microbiological methods section for Chapter 3. Diane Wu helped construct and operate the laboratory experiments described in Chapter 4. Ms. Wu collected and analyzed the early chemistry samples that are discussed in Chapter 4. Peter Kauffman designed and built the power converter/potentiostat described in Chapter 5.

TABLE OF CONTENTS

TABLE OF CONTENTS (Continued)

Page

LIST OF FIGURES

LIST OF FIGURES (Continued)

LIST OF TABLES

LIST OF APPENDIX FIGURES

LIST OF APPENDIX TABLES

# Utilization of Natural and Supplemental Biofuels for Harvesting Energy from Marine Sediments

## 1 Benthic Microbial Fuel Cells: Theory, Applications and Biogeochemical Insights

This dissertation describes the development of chambered benthic microbial fuel cells (BMFCs) and experiments designed to better understand the processes that determine their energy output. Many review papers have recently been published that focus on broader categories of microbial fuel cells (MFCs) (Larminie & Dicks, 2000; Bullen et al., 2006; Logan et al., 2006; Lovley, 2006; Du et al., 2007; Rabaey et al., 2007; Schröder, 2007; Logan, 2008). Often, BMFCs are mentioned as an interesting application and may also be referred to as sediment MFCs or environmental MFCs. The scope of this introduction is to review the underlying theory of BMFCs with particular attention to how they differ from other MFC technologies and how the work that follows in subsequent chapters was needed for the development of BMFCs into practical power supplies.

### 1.1 What is a benthic microbial fuel cell?

A BMFC is an electrochemical device that generates electrical current from the natural redox gradient that commonly occurs across the sediment-water interface (Whitfield, 1972; Reimers et al., 2001; Tender et al., 2002; Alberte et al., 2005). The redox gradient occurs as result of distinct biogeochemical zones linked to the microbial degradation of organic detritus; oxic at the sediment-water interface where aerobic respiration is the dominant process; suboxic where oxygen is depleted and nitrate, iron, and manganese reduction are the dominant processes; and anoxic where sulfate reduction and forms of fermentation and methanogenesis can be the dominant processes. The biogeochemical zonation arises because each of the processes listed above occur in sequence according to the free energy ($\Delta G^{0\prime}$) yielded by the reaction with the most energetic processes occurring first. Ideally, if all reactions were known, the difference in redox potentials between the electron-accepting and electron-donating couple ($\Delta E_0'$) could be characterized and related to $\Delta G^{0\prime}$ according to:

(1.1) $$\Delta E_0' = -nF/\Delta G^{0'}$$

where $n$ is the number of electrons transferred and $F$ is the faraday constant (96,485 coulomb $mol^{-1}$). For example, at pH 7, the $O_2/H_2O$ redox couple has a $E_0'$ of +0.82 V versus a standard hydrogen electrode (SHE) while the $SO_4^{2-}/HS^-$ redox couple has $E_0'$ of -0.22 $V_{SHE}$ (Thauer et al., 1977). Accordingly, the theoretical redox potential difference ($\Delta E_0'$) between oxic seawater and anoxic sediments is approximately 1.4 V. In practice, observed redox potential differences are 0.7 to 0.8 V as measured by redox electrodes (Schulz, 2006). The difference between theoretical and observed redox gradients arises from the fact that redox species occur at a variety of concentrations, are mixed and heterogeneously distributed in the natural environment, and their measurement depends on the nature and rates of reactions at the electrode surface (Stumm & Morgan, 1996).

### 1.2 How could BMFCs serve the oceanographic research community?

Long-term monitoring data and time series data are widely used in oceanography and other related fields. Examples of parameters for which time series data would be useful include temperature, salinity, tidal patterns, migration patterns of fish and other animals, and pollution monitoring. Long-term monitoring requires instrumentation that is powered to collect, store and transmit data. Most of the ocean is beyond the reach of the traditional power grid so batteries have been the technology of choice to power instruments, particularly subsurface sensors that cannot be powered by solar or other energy sources. However, one shortcoming of batteries is the finite amount of time before they must be replaced or recharged. Generally batteries can power a sensor for about a year in the ocean. If researchers had a widely distributed network of instruments, they would be continually changing batteries, which would require significant resources of ship time and possibly submersible time. BMFCs are proposed as a replacement for batteries since they draw fuel from the environment and are conceptually inexhaustible.

## 1.3 Principle components of a BMFC

A BMFC has few parts and operates on a simple principle. The circuit requires inert but electrically conductive electrodes located in the anoxic zone (the anode) and the oxic zone (cathode). The electrodes are connected through a load, which is usually an external resistor or potentiostat (in research applications) or a sensor (in field demonstrations). Electrons are transferred from electron donors to the anode and flow through the load to the cathode where they lead to the reduction of dissolved oxygen to water. A voltmeter is usually included to monitor cell voltage ($E_{cell}$) and a combination of a voltmeter and reference electrode is commonly used to measure individual electrode potentials ($E_{anode}$ and $E_{cathode}$). Current ($I$) may be measured directly or calculated according to Ohm's law if a known resistor is used. The most significant decisions in designing a BMFC are in the material and design of electrodes, which are discussed in more detail below.

### *1.3.1 Anodes*

The function of an anode is to accept electrons liberated by the microbial decomposition of organic substrates. Prior to the work described in this dissertation, the anodes of BMFCs were buried in the sediment. Different materials that have been investigated include platinum mesh (Whitfield, 1972; Reimers et al., 2001); graphite discs, plates or rods (Tender et al., 2002; Ryckelynck et al., 2005; Reimers et al., 2006; Donovan et al., 2008; Tender et al., 2008); stainless steel (Dumas et al., 2007); carbon cloth (Rezaei et al., 2007; Scott et al., 2008b); glassy carbon and modified graphite (Lowy et al., 2006); and carbon sponge and reticulated vitreous carbon (Scott et al., 2008a). Owing to the remote locations and long time periods for BMFC deployments, most efforts have focused on materials that have not been chemically modified.

In one of the first BMFC reports, Tender et al. (Tender et al., 2002) recognized that the slow rate of mass transfer of electron donors in sediments was a limitation of the buried anode design. Based on this observation, I and coauthors developed a

chambered BMFC design in which the anode is contained in a semi-enclosed chamber that is either pushed into the sediments or simply set on the seafloor. This design is common to all the experiments described in Chapters 2 – 5. As described in Chapter 2, the advantages of a chamber design include the use of high specific surface area electrodes and the ability to enhance mass transport either mechanically (Chapter 2; Nielsen et al., 2007) or through natural advection (Chapter 3; Nielsen et al., 2008). Chambers also allow the addition of supplemental electron donors (Chapters 4 and 5) and the sampling of anode chamber fluids for research purposes (Chapters 2 and 4).

### *1.3.2 Cathodes*

The function of cathodes is to donate electrons to available acceptors thus enabling the continuous flow of current from the anode. In most cases the terminal electron acceptor at the cathode is dissolved oxygen in the water overlying the BMFC. This electron transfer appears to be enhanced by a microbial biofilm that forms on the cathode over time, and which can contain manganese oxidizing bacteria (Bergel et al., 2005; Rhoads et al., 2005). Cathodes are as important as anodes in terms of BMFC design. However, it is unusual for the cathode to be the limiting electrode so they receive less attention. The degree of limitation can be determined by observing the potentials of the cathode and anode under varying load; if the cathode potential stays near its open circuit value as the load resistance is decreased, then it can be concluded that cathodic processes are not limiting the current. In practice, cathode surface area is easier to increase in a BMFC than is the anode surface area, because the anode is buried or placed in a chamber. Scott et al. (2008b) recently conducted a systematic comparison of 10 different cathode materials and found that a Fe-Co tetramethoxyphenyl porphyrin (FeCoTMPP) cathode produced the highest power density (62 mW $m^{-2}$) while a relatively inexpensive carbon cloth cathode produced approximately 30 mW $m^{-2}$.

### *1.3.3 Indigenous microorganisms*

The indigenous microbial community is a vital component of BMFCs. In contrast to wastewater or other laboratory MFCs, there is no inoculation procedure for field deployed BMFCs; they are restricted to the indigenous members of the sediment community (although relative proportions of species do change due to BMFC operation (Holmes et al., 2004)). Microorganisms play two key roles in the generation of current by BMFCs. First, the redox gradient described in Section 1.1 is established and maintained by microorganisms. The gradient is a result of microbially catalyzed remineralization of organic carbon and has been intensively studied for many years (Froelich et al., 1979; Nealson, 1997; Jørgensen, 2006). Second, microorganisms can facilitate the transfer of electrons between electrodes and natural donors/acceptors. The two principal modes of electron transfer are direct electron transfer (DET) and mediated electron transfer (MET). Schröder (2007) and Logan (2008) review the different mechanisms and the evidence for each. Mostly, their discussions are focused on laboratory or wastewater fuel cells. BMFCs can be more complicated because the anode is exposed to the environment rather than enclosed in a controlled reactor, and there are many possible electron donors.

Ryckelynck et al. (2005) examined the geochemical impacts of BMFCs with buried anodes and found evidence for a MET process in which dissolved and mineral forms of reduced sulfur were oxidized to $S^0$ at the anode. Isolation of sulfur disproportionating organisms similar to *Desulfobulbus* and *Desulfocapsa spp*. from buried anodes suggests that $S^0$ deposited on the anode serves as a substrate for regeneration of sulfate and sulfide (Holmes et al., 2004). In the same study, the authors report that organisms in the *Geobacteraceae* family within the group of deltaproteobacteria dominated the anode communities in marine and saltmarsh sediments. *Geobacter* species are known for their ability to oxidize acetate to $CO_2$ with an anode serving as the only electron acceptor; this process is an example of a DET process (Bond et al., 2002; Bond & Lovley, 2003). It is likely that both direct and mediated electron transfer could be occurring at the anode of a BMFC. Chapter 4

describes a laboratory experiment in which I operated six sediment MFCs for over a year and supplemented three of the MFCs in an attempt to select for one anode process over another.

### 1.4 Flow of energy

The electron source for BMFCs is usually organic material stored in sediments. Two exceptions are methane cold seeps such as those described in Chapter 3 and hydrothermal vents where a prototype MFC has been deployed directly into a vent (P. Girguis, pers. comm.). Energy is liberated through spatially separated redox half-reactions that occur at the anode and cathode. The net reaction is the oxidation of organic carbon by oxygen. However, the theoretical determination of available energy according to thermodynamics is confounded by the presence of the BMFC. Finkelstein et al. (2006) recently conducted a set of experiments that suggested as much as 95% of energy available from organic carbon oxidation can be consumed by the microbial biofilm that mediates electron transfer at the electrode surface. Apparently, microorganisms adjacent to the anode are capable of self-regulating the activity of their terminal redox enzymes so that they are poised just slightly negative of the anode potential. Therefore the amount of potential energy stored in sediment that is available for electrical work appears to have been overestimated by previous calculations (Reimers et al., 2001; Tender et al., 2002). Since current and power appear to be limited by transport processes, I and coauthors focused on such processes when predicting possible power outputs in Chapters 2 and 3. Chapter 2 (Nielsen et al., 2007) presents a study comparing BMFCs with natural and enhanced transport, and Chapter 3 (Nielsen et al., 2008) presents a study of chambered BMFCs and compares diffusive and advective transport at a deep ocean cold seep.

There is a wide range of potential electron donors for BMFCs that is not adequately described by the bulk label of "sediment organic matter". Organic matter fuels the subsurface biosphere and is highly processed in the course of doing so. The general model is that complex organic matter undergoes hydrolysis and is separated into fractions including long-chain fatty acids, aromatic compounds, fermentable sugars

and amino acids (Lovley, 2006). The latter two fractions are further processed through fermentation and produce organic acids such as acetate, lactate, propionate, butyrate, succinate and formate. These products, in turn, support the growth of dissimilatory metal reducing bacteria capable of extracellular electron transfer (e.g. *Geobacteraceae spp*.). Fermentation products may also fuel sulfate reduction resulting in dissolved sulfide and/or solid phase iron sulfide minerals, which are electrochemically active and can donate electrons to an anode (Ryckelynck et al., 2005).

It is likely that current produced by a given BMFC results from a combination of electron donors. Different processes have different chemical signatures and inherent efficiencies but are difficult to constrain when they are occurring at the same time. Chapter 4 includes results from laboratory BMFCs in which current was maintained (even slightly increased) when sulfate reduction was blocked. Two possible explanations are that 1) the primary electron donor was reduced iron rather than reduced sulfur in these cells, or 2) blocking sulfate reduction allowed hydrogen to be supplied to the BMFC from fermentative processes in the sediment.

### 1.5 Factors controlling power output

Factors that limit power production ($P$) in prototype laboratory MFCs are well described by Logan (2008). Since $P = E_{cell} \times I$, limitations are described in terms of loss factors that affect $E_{cell}$, which are related to overpotentials. Current dependent overpotentials are defined as the difference between electrode potential when current is passing and the potential at zero current. Overpotentials occur at both the anode and cathode and occur as consequences of ohmic losses, activation losses, and mass transport losses. Ohmic losses arise from the resistance to current flow through the circuit and to counter-ion flow through the electrolyte. Activation losses manifest as heat and arise from activation energy required to initiate redox reactions at the electrode surfaces. Mass transport losses arise from the depletion of electron donors at the anode and/or electron acceptors at the cathode.

A key difference between laboratory MFCs and BMFCs is the importance of mass transport losses. Mass transport is often the main limiting factor in BMFCs due to the relatively low concentration of electron donors and the slow rate of mass transport in sediments (Tender et al., 2002; Scott et al., 2008a). The experiments described in Chapter 2 (Nielsen et al., 2007) include a calculation of the internal resistance of a chambered BMFC under conditions of natural and artificially enhanced mass transport. Under the natural condition the internal resistance of the BMFC was 577Ω compared to 38Ω when pumping eliminated mass transport limitation. Conversely, mass transport limitation is not generally observed in laboratory settings and is not considered an important factor (Logan, 2008). Laboratory MFCs tend to be run either as batch reactor studies to investigate a particular aspect of the system or with a flow through system. In either case, the concentration of electron donors can be easily manipulated so as not to be a limiting factor.

Ohmic losses mainly refer to resistance to the flow of ions through the electrolyte and proton exchange membrane but also include minor resistances from the flow of current through electrode materials and connections between the electrodes and circuits. In laboratory MFCs, ohmic losses are addressed primarily by minimizing the spacing between electrodes and by careful design of the membranes. BMFCs do not have a membrane and there is a limit to how close the electrodes can be located since the oxic and anoxic zones are spatially separated (Rezaei et al., 2007). On the other hand, the electrolyte in BMFCs is seawater, which has a conductivity of approximately 25 - 40 mS $cm^{-2}$ (which is sensitive to temperature). Owing to the high conductivity of seawater, BMFC performance does not appear to be sensitive to electrode spacing.

### 1.6 Scaling issues

The relationship between performance and device size is currently being investigated for both laboratory MFCs and BMFCs. Dewan et al. (2008) recently compiled results from 20 studies, including laboratory MFCs and field-deployed BMFCs, that clearly

showed that MFCs with the largest total anode surface area had the lowest power densities. They also conducted systematic experiments and observed that maximum power density is proportional to the logarithm of the surface area of the anode. This draws into question the validity of extrapolating power densities from small-scale experiments to estimate how much power might be delivered by scaling up various MFC designs. This question is central to BMFC experiments since the underlying motivation for this research is to develop useful power supplies. Chapter 3 (Nielsen et al., 2008) describes BMFCs that produced average power levels that could power some off-the-shelf sensors. Chapter 5 describes a scaled-up BMFC that was used to power an acoustic sensor and the accompanying power management system.

### 1.7 Environmental variables

The natural environment is dynamic and not controlled like a typical laboratory setting. Accordingly, we seek to understand which natural fluctuations have the strongest influence over BMFC performance and variability. Examples of natural fluctuations include temperature changes and tidal cycles that, depending on the location, might include pressure variations, changes in water flow, salinity/conductivity changes and dissolved oxygen changes. For example Reimers et al. (2006) detected a relationship between current and temperature on the order of 1.3 mA $m^{-2}$ per °C for abiotic MFCs utilizing sulfur as the electron donor.

In estuarine field settings we observe current oscillations the frequency of which are consistent with tidal frequency (Tender et al., 2002; Nielsen et al., 2007). The oscillations can be quantified in terms of total resistance ($R$) calculated as $R = E_{cell}/I$. In the latter example, this calculation suggests that $R$ decreases by 100Ω from high tide to low tide. Over the same tidal cycle, the conductivity at the site of the BMFC deployment ranged from 35 mS $cm^{-1}$ at high tide to 20 mS $cm^{-1}$ at low tide. Based on the geometry of the BMFC it is possible that this change in conductivity could account for the change in $R$.

Even larger relative power fluctuations were observed in the power records from BMFCs deployed at cold seeps in Monterey Canyon (Chapter 3; Nielsen et al., 2008). The power records exhibited a relative standard deviation of 30 to 90% around their respective mean values. These BMFCs were deployed at a water depth of 960 m and the frequency of the power oscillations did not correlate with any observed environmental factor. The most likely explanation for the variability was variable seepage and mixing with the chambers that would control the delivery of electroactive species to the anode.

Significant power fluctuations appear to be a common feature of all chambered BMFC deployments regardless of where they are deployed. Whatever the underlying cause, variable power generation affects the requirement for power management devices in that they must be able to store fluctuating levels of power for subsequent use in powering a sensor with steady or variable demands. Chapter 5 describes a system that converts the current from a BMFC to higher voltage and then stores that charge in a rechargeable battery for subsequent use to power an acoustic sensor.

### 1.8 Practical considerations for BMFC deployment

Most BMFCs described in the literature consist of a buried anode and a cathode placed in the overlying water. As we face the challenges of scaling up BMFCs for practical use, there is a requirement to bury ever and ever larger anodes or multiple anodes. This problem is one factor that led to the development of chambered BMFCs described in Chapters 2 – 5. Chambers have the advantage of being relatively easy to deploy and they can contain electrodes of high surface area. In Chapter 3 (Nielsen et al., 2008) the performance of a buried anode BMFC and a chambered BMFC are compared at the same location. Based on the long-term power records, 600 solid anodes would be required to match the power output of the single chambered BMFC.

One of the drawbacks of chamber designs is the possibility of erosion of sediment isolating the chamber from oxygenated seawater (scouring). If scouring occurs to the extent that the anode is exposed to overlying seawater then the redox potential

collapses and the BMFC cannot produce current. This process has been an issue in highly energetic environments such as the Oregon shelf.

## 1.9 Summary

I describe five different BMFCs in the following chapters. Each experiment or demonstration had its own advantages and drawbacks (Table 1.1). Overall, BMFCs are poised to become practical power supplies for limited applications and each investigation tends to spur additional research questions for continuing work.

**Table 1.1. Summary of designs and performance of BMFC is this dissertation.**

| Chapter | BMFC Description | Power Density (mW $m^{-2}$) | Advantages | Limitations |
|---|---|---|---|---|
| 2 | Small chambers with tubes for pumping and sampling | 13 – 380 | Pumping enabled high power densities | Energy requirements of pumping offset gains |
| 3 | Solid cylindrical anode | 32 – 112 | Easy to deploy, predictable power evolution | Small cross section translates to little actual power |
| 3 | Medium-sized chambers | 30 – 200 | Easy to deploy, scaled up size produced usable amounts of power | Performance is site specific, power output highly variable |
| 4 | Core tubes in laboratory sediments (sand) | 6 – 11 | Controlled environment and replicates allow investigation of anode mechanisms | Small size, sample collection can cause artifacts in performance |
| 5 | Large-sized chamber | 8 – 48 | Scaled up prototype can produce useful levels of power, operated in sandy sediments, successfully re-charged a battery | Vulnerable to scouring which can eliminate redox gradient, relatively low power density |

## 1.10 References:

Alberte R, Bright H, Reimers C, Tender L. 2005. Method and apparatus for generating power from voltage gradients at sediment-water interfaces. *United States Patent No. US 6,913,854 B1*

Bergel A, Feron D, Mollica A. 2005. Catalysis of oxygen reduction in PEM fuel cell by seawater biofilm. *Electrochemistry Communications* 7: 900-904

Bond DR, Holmes DE, Tender LM, Lovley DR. 2002. Electrode-reducing microorganisms that harvest energy from marine sediments. *Science* 295: 483-485

Bond DR, Lovley DR. 2003. Electricity production by Geobacter sulfurreducens attached to electrodes. *Applied and Environmental Microbiology* 69: 1548-1555

Bullen RA, Arnot TC, Lakeman JB, Walsh FC. 2006. Biofuel cells and their development. *Biosensors & Bioelectronics* 21: 2015-2045

Dewan A, Beyenal H, Lewandowski Z. 2008. Scaling up microbial fule cells. *Environmental Science and Technology* 42: 7643-7648

Donovan C, Dewan A, Heo D, Beyenal H. 2008. Batteryless, Wireless Sensor Powered by a Sediment Microbial Fuel Cell. *Environmental Science & Technology* In Press

Du ZW, Li HR, Gu TY. 2007. A state of the art review on microbial fuel cells: A promising technology for wastewater treatment and bioenergy. *Biotechnology Advances* 25: 464-482

Dumas C, Mollica A, Feron D, Basseguy R, Etcheverry L, Bergel A. 2007. Marine microbial fuel cell: Use of stainless steel electrodes as anode and cathode materials. *Electrochimica Acta* 53: 468-473

Finkelstein DA, Tender LM, Zeikus JG. 2006. Effect of electrode potential on electrode-reducing microbiota. *Environmental Science & Technology* 40: 6990-6995

Froelich PN, Klinkhammer GP, Bender ML, Luedtke NA, Heath GR, et al. 1979. Early oxidation of organic matter in pelagic sediments of the eastern equatorial Atlantic: suboxic diagenesis. *Geochimica Et Cosmochimica Acta* 43: 1075-1090

Holmes DE, Bond DR, O'Neill RA, Reimers CE, Tender LR, Lovley DR. 2004. Microbial communities associated with electrodes harvesting electricity from a variety of aquatic sediments. *Microbial Ecology* 48: 178-190

Jørgensen BB. 2006. Bacteria and Marine Biogeochemistry. In *Marine Geochemistry*, ed. HD Schulz, M Zabel. Berlin: Springer

Larminie J, Dicks A. 2000. *Fuel Cell Systems Explained*. Chichester: John Wiley & Sons Ltd.

Logan BE. 2008. *Microbial Fuel Cells*. Hoboken, N.J., U.S.A.: John Wiley & Sons, Inc.

Logan BE, Hamelers B, Rozendal R, Schröder U, Keller J, et al. 2006. Microbial fuel cells: Methodology and technology. *Environmental Science & Technology* 40: 5181-5192

Lovley DR. 2006. Bug juice: harvesting electricity with microorganisms. *Nature Reviews Microbiology* 4: 497-508

Lowy DA, Tender LM, Zeikus JG, Park DH, Lovley DR. 2006. Harvesting energy from the marine sediment-water interface II - Kinetic activity of anode materials. *Biosensors & Bioelectronics* 21: 2058-2063

Nealson KH. 1997. Sediment bacteria: Who's there, what are they doing, and what's new? *Annual Review of Earth and Planetary Sciences* 25: 403-434

Nielsen ME, Reimers CE, Stecher HA. 2007. Enhanced Power from Chambered Benthic Microbial Fuel Cells. *Environmental Science & Technology* 41: 7895-7900

Nielsen ME, Reimers CE, White HK, Sharma S, Girguis PR. 2008. Sustainable energy from deep ocean cold seeps. *Energy & Environmental Science* 1: 584-593

Rabaey K, Rodriguez J, Blackall LL, Keller J, Gross P, et al. 2007. Microbial ecology meets electrochemistry: electricity-driven and driving communities. *Isme Journal* 1: 9-18

Reimers CE, Girguis P, Stecher HA, Tender LM, Ryckelynck N. 2006. Microbial fuel cell energy from an ocean cold seep. *Geobiology* 4: 123-136

Reimers CE, Tender LM, Fertig S, Wang W. 2001. Harvesting energy from the marine sediment-water interface. *Environmental Science & Technology* 35: 192-195

Rezaei F, Richard TL, Brennan RA, Logan BE. 2007. Substrate-enhanced microbial fuel cells for improved remote power generation from sediment-based systems. *Environmental Science & Technology* 41: 4053-4058

Rhoads A, Beyenal H, Lewandowski Z. 2005. Microbial fuel cell using anaerobic respiration as an anodic reaction and biomineralized manganese as a cathodic reactant. *Environmental Science & Technology* 39: 4666-4671

Ryckelynck N, Stecher HA, Reimers CE. 2005. Understanding the anodic mechanism of a seafloor fuel cell: Interactions between geochemistry and microbial activity. *Biogeochemistry* 76: 113-139

Schröder U. 2007. Anodic electron transfer mechanisms in microbial fuel cells and their energy efficiency. *Physical Chemistry Chemical Physics* 9: 2619-2629

Schulz HD. 2006. Quantification of Early Diagenesis: Dissolved Constituents in Pore Water and Signals in the Solid Phase. In *Marine Geochemistry*, ed. HD Schulz, M Zabel. Berlin: Springer

Scott K, Cotlarciuc I, Hall D, Lakeman JB, Browning D. 2008a. Power from marine sediment fuel cells: the influence of anode material. *Journal of Applied Electrochemistry* 38: 1313-1319

Scott K, Cotlarciuc I, Head I, Katuri KP, Hall D, et al. 2008b. Fuel cell power generation from marine sediments: Investigation of cathode materials. *Journal of Chemical Technology and Biotechnology* 83: 1244-1254

Stumm W, Morgan JJ. 1996. *Aquatic Chemistry: Chemical Equilibria and Rates in Natural Waters*: Wiley-Interscience

Tender LM, Gray SA, Groveman E, Lowy DA, Kauffman P, et al. 2008. The first demonstration of a microbial fuel cell as a viable power supply: Powering a meteorological buoy. *Journal of Power Sources* 179: 571-575

Tender LM, Reimers CE, Stecher HA, Holmes DE, Bond DR, et al. 2002. Harnessing microbially generated power on the seafloor. *Nature Biotechnology* 20: 821-825

Thauer RK, Jungermann K, Decker K. 1977. Energy conservation in chemotrophic anaerobic bacteria. *Bacteriological Reviews* 41: 100-180

Whitfield M. 1972. The electrochemical characteristics of natural redox cells. *Limnology and Oceanography* 17: 383-393

# 2 Enhanced Power from Chambered Benthic Microbial Fuel Cells

Mark E. Nielsen[1], Clare E. Reimers[1], Hilmar A. Stecher, III[1,2]

[1]College of Oceanic & Atmospheric Sciences, Oregon State University, Corvallis OR, 97331 USA
[2]Current address: U.S. Environmental Protection Agency, Pacific Coastal Ecology Branch, Newport OR 97365

Environmental Science & Technology
American Chemical Society, Washington D.C. 20036
2007, Vol. 41, No. 22, pp 7895-7900

## 2.1 Abstract

We describe a new chamber-based benthic microbial fuel cell (BMFC) that incorporates a suspended, high surface-area and semi-enclosed anode to improve performance. In Yaquina Bay, OR, two chambered BMFC prototypes generated current continuously for over 200 days. One BMFC was pumped intermittently which produced power densities more than an order of magnitude greater than those achieved by previous BMFCs with single buried graphite-plate anodes. On average, the continuous power densities with pumping were 233 $mW/m^2$ (2.3 $W/m^3$); peak values were 380 $mW/m^2$ (3.8 $W/m^3$) and performance improved over the time of the deployments. Without pumping, high power densities could similarly be achieved after either BMFC was allowed to rest at open circuit. A third chambered BMFC with a 0.4 $m^2$ footprint was deployed at a cold seep in Monterey Canyon, CA to test the new design in an environment with natural advection. Power density increased five fold (140 $mW/m^2$ vs. 28 $mW/m^2$) when low pressure check valves allowed unidirectional flow through the chamber.

## 2.2 Introduction

Benthic microbial fuel cells (BMFCs) generate electricity from the electropotential difference between oxic seawater and anoxic sediments (Whitfield, 1972; Reimers et al., 2001; Tender et al., 2002; Reimers et al., 2006). Electrons are delivered to the anode by microorganisms either directly from organic material or indirectly from inorganic products of organic matter degradation (Reimers et al., 2007). At the cathode, these electrons reduce dissolved oxygen to form water. Since microorganisms cause organic matter oxidation in natural anoxic environments to proceed through a variety of interactive electron acceptors (Froelich et al., 1979; Burdige, 2006), the processes at the anode can be especially complex and critical to BMFC performance.

In general, BMFCs produce relatively low levels of power due to low rates of diffusion in sediments, low concentrations of labile organic matter, and passivation of anode surfaces (Reimers et al., 2001; Tender et al., 2002; Holmes et al., 2004; Ryckelynck et al., 2005; Finkelstein et al., 2006; Lowy et al., 2006; Reimers et al., 2006; He et al., 2007). Amongst strategies attempted to increase power from BMFCs, the most successful have been 1) employing carbon cloth anodes enriched with organic substrates (Rezaei et al., 2007), and 2) using a rotating cathode (He et al., 2007). There have also been many improvements in the technology of wastewater-fueled MFCs that have been associated with pumping waste fluids through porous anode materials contained in chambers (Jang et al., 2004; He et al., 2005; Rabaey et al., 2005; Cheng et al., 2006; Moon et al., 2006). Guided by these advances, we hypothesized that power generation from BMFCs could be increased further by removing the anode from the sediments and enclosing it in a benthic chamber. Incorporating the benthic chamber would enable the use of high surface-area anodes and the advection of reductant-rich porewater to anode materials.

As BMFCs are intended to operate as long-term power sources in aquatic environments, the most relevant evaluation procedure is to conduct an extended discharge experiment under field conditions with some program of controlled cell potential ($E_{cell}$), current ($I$) or external load resistance(s) ($R_{ext}$). The system can be represented by using Ohm's law ($E_{cell} = IR_{ext}$), and internal resistance terms may be assigned to each of the processes that cause a drop in potential from the open circuit voltage ($E_{cell}$ = OCV – $IR_{int}$; Logan et al., 2006). As described by Logan et al. (2006), the three main loss categories that contribute to the steady state internal resistance ($R_{int}$) are: ohmic losses ($R_o$), activation losses ($R_a$), and mass transfer losses ($R_{mt}$); giving the relationship:

(2.1) $$R_{int} = R_o + R_a + R_{mt}$$

$R_o$ includes resistances to the flow of current through connections in the device and the resistance to counter ion flow through the electrolyte, which is seawater in ocean BMFCs (there are no proton exchange membranes). $R_a$ refers to losses due to the

activation energy required by oxidation/reduction reactions. $R_{mt}$ are losses that arise from limitations in the rate of delivery of electroactive species to the electrodes. The rate of delivery is controlled by the concentration of electroactive species in the vicinity of the electrodes and by factors that determine mass transport. Terms $R_a$ and $R_c$ may also be separated into anode and cathode components and will vary depending on the load placed on the system (Logan et al., 2006).

In this paper we present the results from two versions of chambered BMFCs developed to address the limitation of slow diffusion in sediment MFCs. We use field data to estimate the magnitude of the various loss terms, and we show that the new design of BMFC avoids the negative effects of anode passivation that have been previously observed in sediment microbial fuel cells.

## 2.3 Experimental procedures

### *2.3.1 Yaquina Bay BMFCs.*

The first version of a chambered BMFC was constructed in duplicate and evaluated in Yaquina Bay, OR (Lat. 44° 37.47', Long. 124° 02.60') at a site where the average water depth was approximately 6 m with tidal height variations of up to 3 m. These BMFCs (Figure 2.1a) differed from previous designs in three important ways: 1) the anode was enclosed in a benthic chamber and not buried in the sediments, 2) high surface area carbon-fiber brush electrodes (Hasvold et al., 1997) were used for the anodes as well as the cathodes, and 3) the cathodes were twice as long as the anodes (2 m versus 1 m). The electrodes were taken from a commercially available seawater battery (SWB 1200; Kongsberg Maritime AS, Norway). They consist of fine carbon fibers densely packed on twisted-pair titanium wires and have a manufacturer reported surface area of 26.3 $m^2$ per meter of electrode. Similar carbon brush anodes were investigated in small laboratory MFCs by Logan et al. (2007). The BMFC chambers were fabricated from hollow acrylic cylinders with an open bottom and gasket-sealed lid (0.02 $m^2$ cross-sectional area, 48 cm tall). Divers pushed the two chambers into the

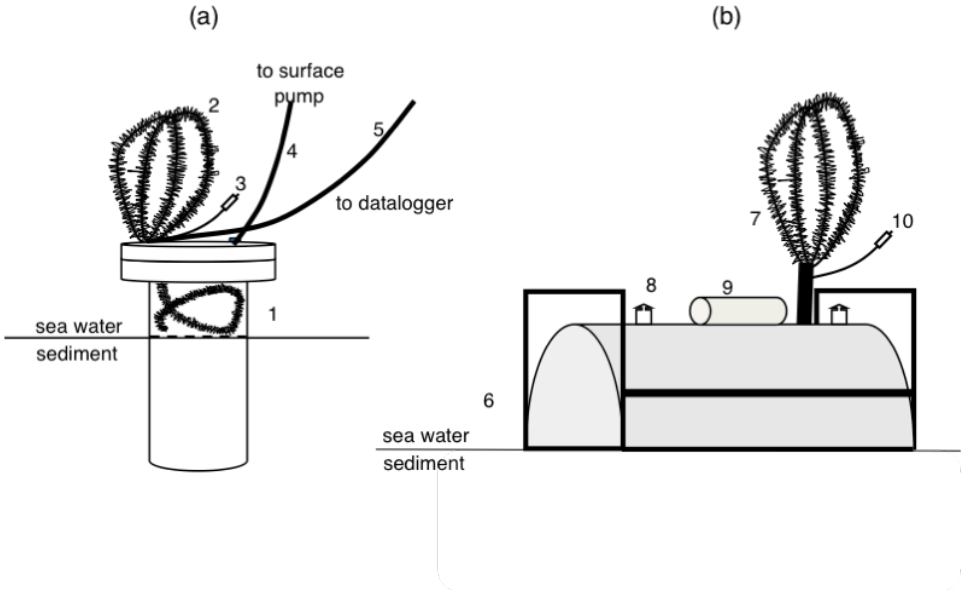


Figure 2.1 Schematic of the Yaquina Bay and Monterey Canyon BMFCs. (a) Yaquina Bay BMFC. Each BMFC included a 1 m-long carbon brush anode inside an anode chamber with a $2x10^{-3}$ $m^3$ volume (1); a 2 m-long carbon brush cathode (2); a reference electrode (3); and a sampling tube fitted to a port (4). Electrodes were connected to the data logger through 20 m of 12 gauge, 3-conductor wire (5). (b) The Monterey Canyon BMFC was constructed from a piece of plastic sewer pipe and included a 3 m-long carbon brush anode (6); a 4 m-long carbon brush cathode (7); two identical check valves (8); a titanium pressure housing containing passive potentiostat and dataloggers (9); and a reference electrode (10).

sediment, 2 meters apart, with the bottoms of the cylinders approximately 38 cm below the sediment-water interface resulting in an anode chamber volume above the sediment of approximately $2 \times 10^{-3}$ $m^3$. Each lid was equipped with a quick-connect port that allowed fluids from inside the chamber to be sampled. Samples were collected by pumping chamber fluids through 20 m of 0.43 cm (i.d.) low-density polyethylene tubing.

The whole-cell potential ($E_{cell}$), anode potential ($E_{an}$) and current ($I$) of the BMFCs were measured with a multi-channel data logger (Agilent Technologies, Santa Clara, CA). $E_{an}$ was measured versus a Ag/AgCl/seawater reference electrode mounted on the outside of the chamber lid. At an average temperature of 11.8°C, an estimated chloride activity of 320 mmol/kg and $E_o$ = 222 mV, we calculate that the reference electrode had an average potential of 248 mV vs. SHE. Cathode potential ($E_{cath}$) was calculated from the measured $E_{cell}$ and $E_{an}$. The electrodes were connected to the data logger through 20 m of 12-gauge, 3-conductor cable (WireXpress, Riverside, CA) with underwater pluggable connectors (Impulse, San Diego, CA). Power is the product of $E_{cell}$ and $I$ and is reported as power density, normalized to square meter of seafloor or anode chamber volume above the sediment, since these parameters are germane to practical applications of this technology.

The Yaquina Bay field evaluations included a long-term discharge experiment with intermittent pumping and sampling, and a set of polarization experiments. During the former, each circuit included a passive potentiostat (North-West Metasystems, Bainbridge Island, WA) set so that no current would flow at $E_{cell} < 0.5$ V, but the circuit would pass as much current as needed to maintain a 0.5 V difference between anode and cathode. No additional external resistance was applied since the potentiostat automatically controls $R_{ext}$ to maintain the set potential. During the polarization experiments, an adjustable resistor was used in place of the passive potentiostat, and $R_{ext}$ was varied manually.

### *2.3.2 Long-term discharge experiment*

After deployment, the Yaquina Bay BMFCs (denoted A and B) were left at open circuit until potentials were fully developed and stable ($E_{cell} \approx 0.8$V). Then on what is designated as "Day 0" the long-term discharge of both BMFCs was initiated and cell parameters were monitored under identical conditions except that BMFC A was pumped only to collect 2 samples (one on Day 0 prior to closing the circuits, and the other on Day 15, with 20 minutes of pumping required for each sample), whereas BMFC B was pumped for several prolonged time periods to enable slow advection of sediment porewater into the anode chamber. Three principal pumping periods were: Days 15-17, Days 35-51 and Days 153-200. During pumping periods, withdrawal rates were measured volumetrically and maintained at 6.3 mL/min ($5 \times 10^{-6}$ m/s across the sediment-water interface) whenever the pump was turned on. The residence time of fluid within the anode chamber under these conditions was 5.3 hr.

### *2.3.3 Chemical methods*

Water samples for chemical analyses were collected during pumping directly from the polyethylene tubing into 50-ml glass syringes thus avoiding contact with oxygen. The syringes were transferred to the laboratory where subsamples for various analyses were expelled. Dissolved organic carbon (DOC) subsamples were collected first and filtered through pre-combusted glass microfiber filters (GF/F). Then the syringe and remaining sample were transferred into an anaerobic nitrogen atmosphere within a glove bag where the sample water was filtered through a 0.45-$\mu$m syringe filter (Pall, Ann-Arbor, MI) and partitioned for dissolved inorganic carbon (DIC), sulfide, ammonia, sulfate, and chloride analyses.

Total sulfide and ammonia were measured spectrophotometrically (Cline, 1969; Solorzano, 1969). Sulfate and chloride were measured after a 500-fold dilution by ion chromatography (DX-500 with an AS-12 column, Dionex, Sunnyvale, CA). DOC samples were preserved with $H_3PO_4$ and analyzed on a TOC-$V_{CSH}$ analyzer (Shimadzu

Scientific Instruments, Columbia, MD). DIC samples were fixed with saturated $HgCl_2$ and analyzed coulometrically (Johnson et al., 1985).

### *2.3.4 Polarization experiments.*

Two polarization experiments were conducted with each BMFC in Yaquina Bay (275 – 285 days post-deployment), one with the pump off and one with the pump on. Beginning with the cell at a fully stabilized open circuit potential, the circuit was closed and the external resistance was stepped through 12 resistance values from 1000Ω to 5Ω, and $E_{cell}$ and $I$ were measured for 15 min at each step. Pseudo-steady state cell potentials and currents were estimated by averaging measurements over the last minute of each step (10 s interval).

### *2.3.5 Monterey Canyon BMFC.*

In order to test the chamber design in an environment with natural advection, we built a second, larger, chambered BMFC and deployed it at a methane cold seep at a water depth of 960 m in Monterey Canyon off the coast of central California (Lat. 36°46.57', Lon. 122°05.15'). This chamber was constructed from a 66 cm-long piece of 60 cm plastic sewer pipe cut lengthwise giving a volume of approximately $2.0 \times 10^{-2}$ $m^3$ and footprint of 0.4 $m^2$ (Figure 2.1b). The Monterey BMFC included 3 m of carbon brush anode suspended above the sediment within the chamber, and 4 m of carbon brush cathode (Hasvold et al., 1997) connected to the outside and suspended above the seafloor with a syntactic foam float. $E_{cell}$, and $E_{an}$ were measured directly, and $I$ was converted to a voltage and recorded with dataloggers (Volt101, Madgetech, Warner, NH). $E_{an}$ was measured versus a Ag/AgCl/seawater reference electrode. $E_{cell}$ was controlled using a passive potentiostat as described above with the voltage set at 0.4 V. The BMFC was equipped with check valves allowing unidirectional flow out of the chamber but no mechanical pumps. The BMFC was deployed and recovered by a remotely operated submersible (ROV) operated by the Monterey Bay Aquarium Research Institute. It was initially deployed for 68 days then recovered, at which time the check valves were changed and then the chamber was re-deployed at the same

location. The ROV has the navigational ability that allowed us to replace the BMFC on the same footprint (± 0.1 m) when it was re-deployed. In the first deployment, the valves were spring-loaded piston check valves with a nominal cracking pressure of 0.5 psi. In the second deployment, the valves were swing check valves with a cracking pressure of 0.1 psi.

## 2.4 Results and discussion

### *2.4.1 Evolution of power generation*

Before the long-term discharge, the Yaquina BMFCs were at open circuit for several weeks. During this time, sulfate reduction in the anode chambers led to $HS^-$ concentrations that were determined to be 5.7 and 4.1 mM, in BMFC A and B, respectively, just before their circuits were closed. After the circuits were closed, power generation proceeded in three phases (Figure 2.2). Phase I was characterized by high power resulting from electrochemical oxidation of the accumulated sulfide, and it presumably resulted in deposition of elemental sulfur at the anode. The primary feature of Phase II was a secondary power maximum peaking in BMFC A at 100 $mW/m^2$ (1 $W/m^3$) on Day 50 but partially obscured in the record of BMFC B due to pumping effects. We hypothesize that the secondary peak may have arisen because of the enrichment of microbes that can disproportionate sulfur and/or produce other previously unavailable electron donors. Similarly, a microbial succession in a laboratory MFC was described by Aelterman, et al. (2006) which was correlated to improved performance and the possible production of electron transfer mediators. More experiments are needed to test this hypothesis in chambered BMFCs, but previous experiments in Yaquina Bay showed enrichments of *Desulfobulbus, Desulfocapsa* and *Cytophagales* groups on buried anodes after six months of current generation (Holmes et al., 2004). We have observed secondary peaks in other MFC experiments, indicating that environmental forcing such as changes in temperature, salinity or tidal fluctuations specific to this experiment were not the cause. We also note that the onset of the Phase II peak occurred earlier in BMFC B, which had been

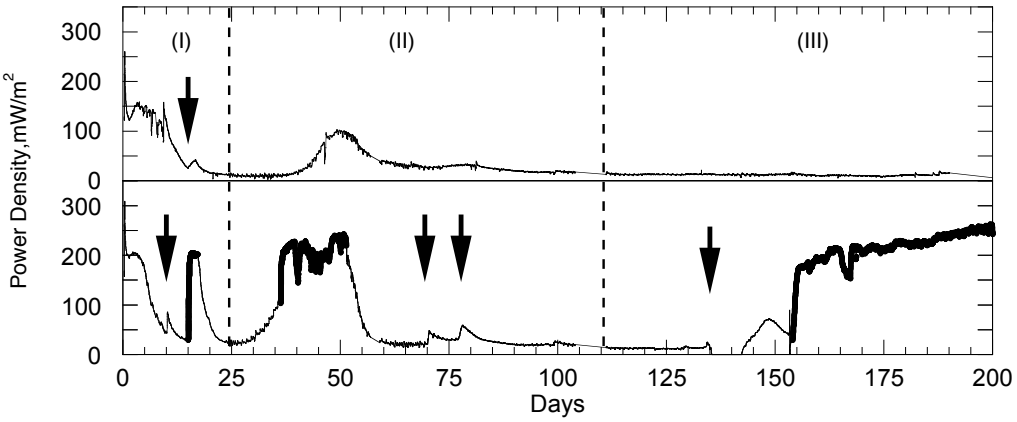


Figure 2.2 Power density from Yaquina BMFCs A (upper panel) and B (lower panel) from the long-term discharge experiment. Prolonged pumping periods are indicated by the bold sections on the record of BMFC B. Arrows represent short-duration pumping for sampling or response testing.

pumped (and thus passed more cumulative charge). In Phase III, the power densities of both cells when unpumped were steady and averaged about 13 $mW/m^2$ (0.1 $W/m^3$). Apparently, this power density represents the long-term energy available if anode reactants are supplied to the anode chamber from this sediment by diffusion and occasional bioirrigation. An exception was Days 135 – 142 in BMFC B when $E_{cell}$ temporarily dipped below 0.5 V so no current was passed.

### *2.4.2 Effect of pumping on* $\mathbf{R_{mt}}$

For the Yaquina Bay fuel cells, pumping led to approximately a 15-fold increase in sustainable power density. The effective $R_{int}$ of an unpumped BMFC at steady state was approximately 577 ohms ((0.8V-0.5V)/0.52mA) and, when pumped, $R_{int}$ was approximately 38 ohms ((0.8V-0.5V)/7.9mA). Essentially, advection enhances mass transfer of anode reactants across the sediment-water interface and it both dilutes and removes soluble reaction products. By this comparison, the anode mass transfer resistance, $R_{mt}$, in the Yaquina Bay BMFCs was at least 93% of the internal resistance when discharged continuously at 0.5 V ((577Ω-38Ω)/577Ω). This value supports the observation of Reimers et al. (2006) that mass transfer to the anode is one of the main limitations of power generation by BMFCs. Furthermore, we used the current interrupt technique (Larminie & Dicks, 2000) and determined that both BMFCs had an $R_o$ of 26-30 ohms (corroborated by the polarization experiments presented later). This leaves anodic $R_a$ and any cathode resistance terms as unknowns. These remaining losses, however, were apparently less than ohmic losses, which in turn were dwarfed by anode mass transfer losses during the long-term discharge of these BMFCs.

We attribute the power increase from pumping to an increase in the concentration of electron donors near the anode rather than to stirring or other hydrodynamic affects. This conclusion was confirmed by a 24-hour test during which the BMFC was repeatedly pumped for 1 minute and then rested for 29 minutes. The power density increased smoothly and did not show specific response to the pumping intervals (Supplemental Material, Appendix B Figure B.1).

### *2.4.3 Processes inside the chamber*

Chemical changes (Figure 2.3) illuminate processes occurring inside the anode chamber. The first sample in each time series represents water in the chamber under unpumped conditions with current being drawn. Subsequent samples reflect an increasing signature of porewater drawn from the sediments underlying the chamber. True porewater chemical concentrations were not observed because the BMFC operated as a chemical reactor and drawing current altered concentrations of electroactive species in the chamber. Porewater chemistry is also spatially and temporally variable, but representative values from the Yaquina Bay study site were reported by Ryckelynck et al. (2005). During the Day 15-17 pumping interval, the total volume pumped was 18 liters or approximately 9 times the anode chamber volume. Assuming an average porosity of 70%, the pumped fluid was drawn from approximately 26 liters of sediment.

The data in Figure 2.3 show a tight coupling between sulfide and power. When the cell was discharged without pumping, sulfide levels were drawn to below measurable concentrations. With advection produced by pumping, porewater containing sulfide was drawn from the sediments beneath the BMFC and there was a concomitant increase in power. Based on the time series of sulfate data (normalized to chloride to remove the effects of small salinity variations) sulfate reduction must have been occurring in the chamber since there was more sulfate in the porewater underlying the chamber than within the chamber. This was corroborated by elevated concentrations of DOC, DIC and ammonia relative to porewater values. Without pumping, the concentration of DOC increased in the anode chamber suggesting that this organic carbon was in a form not readily oxidized under anaerobic conditions.

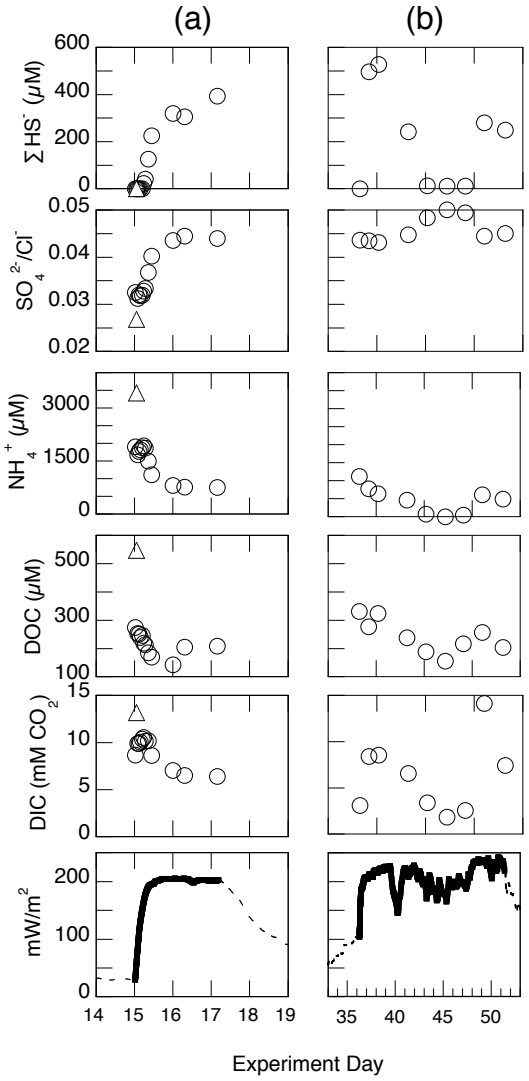


Figure 2.3 Chemistry and power density changes associated with pumping. (a) Results from the first principal pumping period. One water sample was collected for chemical analysis from BMFC A (triangle) and a time series of samples was collected from BMFC B (circles). The pumping period is highlighted in bold in the power density plot (bottom panel). (b) Time series of chemical data over a later extended period of pumping. This pumping period coincided with Phase II of the BMFC evolution so power was increasing even before the onset of pumping (see text for details).

During the next pumping period (Day 35 – 51) samples were collected over a longer time period albeit at a lower frequency (Fig. 3b). During the period from Day 43 to Day 47, it appeared that the pump may have been drawing overlying water into the chamber as evidenced by a sulfate/chloride ratio consistent with a background seawater value (0.05; Pilson, 1998) as well as low sulfide and ammonia concentrations. This may have occurred due to the temporary opening of a large burrow(s) by sediment macrofauna in the estuary (Dumbauld et al., 1996). Despite the evidence of overlying water entering the chamber and sulfide dropping below detection, the power production remained relatively high. This is evidence that electrons can be supplied by a tightly coupled sulfur cycle at the anode surface as described previously (Ryckelynck et al., 2005; Rabaey et al., 2006). In addition, the observation of power without measurable sulfide in the bulk chamber fluid could indicate electron donors other than reduced sulfur species.

### *2.4.4 Polarizations and comparison to previous BMFC designs*

We performed polarization experiments with the Yaquina Bay BMFCs to evaluate their peak power characteristics and compare them to previous BMFCs (Figure 2.4). In the case of BMFC A, pumping the anode chamber for its second polarization caused its open circuit potential to rise to 0.86V compared to an initial value of 0.80V and 0.74V after months without pumping. We speculate the shift from 0.74 to 0.86V was because the pumping flushed out oxidation products that had accumulated within the chamber during discharge phases I-III. In contrast, BMFC B was unpumped for only four days prior to its second polarization, and during this period the cell was also off, so no build up of oxidation products occurred. In all four polarizations the anode potential showed a significantly larger shift than cathode potential for each successive step in the polarization. This indicates that these BMFCs were predominantly anode limited (as was intended by 2:1 ratio of cathode to anode area).

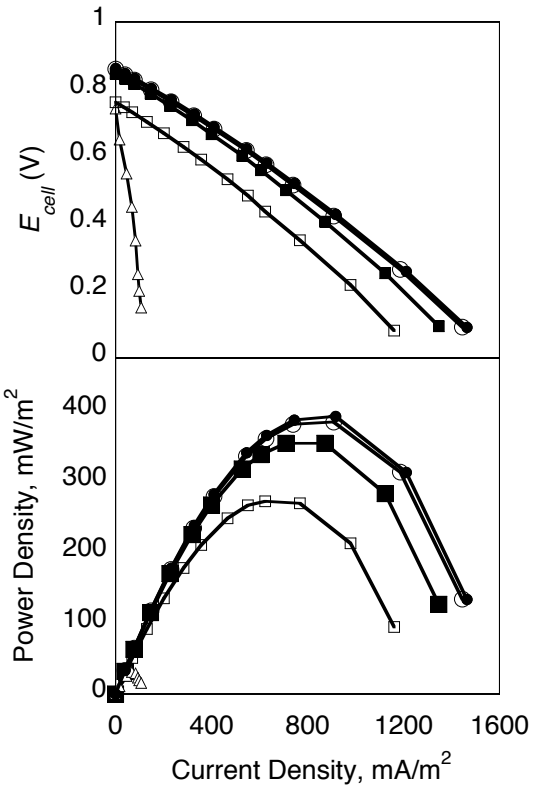


Figure 2.4 Polarization plots of Yaquina BMFC A (squares), BMFC B (circles) and a previous BMFC design (described by Tender et al., 2002, triangles). Open symbols are without pumping and filled symbols are with pumping. All polarizations were conducted starting at open circuit and then external resistance was decreased progressively with an adjustable resistor. Peak power densities in BMFCs A and B correspond to external resistances between 20 and 30 ohms.

A striking characteristic of all the plots of $E_{cell}$ *vs*. current density (Figure 2.4) is that they are close to linear, implying a nearly constant $R_{int}$ which we have calculated as equal to 18 - 27Ω by the formulation (OCV - $E_{cell}$)/$I$. This suggests that under these experimental conditions $R_o$ was dominant and the internal resistance was almost entirely dependent upon the resistance of seawater. This is concluded because using a seawater resistivity value of 0.28 Ω-m (S = 30, T = 11.8°C), an electrode spacing distance of 1.5 m and an area of 0.02 $m^2$, an independent estimate of the ohmic resistance due to seawater is approximately 21Ω. Over longer discharge periods than represented by the polarizations, the electron donors in the anode chamber would be depleted and mass transfer resistance would increase, as evidenced by the high $R_{mt}$ during steady-state discharge from the unpumped chamber.

Polarization curves are one way of comparing different fuel cell designs. In Figure 2.4, we include polarization data from a previously described BMFC in which the anodes were single graphite plates buried in Yaquina Bay sediment (Tender et al., 2002). The short-term peak power density of the plate-anode BMFC was approximately 30 $mW/m^2$ compared to 270 to 380 $mW/m^2$ (2.7 – 3.8 $W/m^3$) for unpumped and pumped chambers, respectively, with the polarizations conducted in the same way for both chambered and buried-plate anode designs. We note, however, that the long-term power densities sustainable by BMFC A (and BMFC B when unpumped) for periods of months were nearly the same as the buried-plate anode BMFC. This suggests a great advantage to operating new chambered designs in a cyclic manner. Similar advantage may be gained with a buried anode, but the high surface area carbon-fiber anodes in the chambers are able to discharge at higher current densities than the plate anodes after reactant build up.

### *2.4.5 Energy cost of pumping.*

The energy cost of pumping versus the gain in power is an important consideration for the realistic application of chambered designs. As an example, a low-power miniature peristaltic pump (e.g. P625, Instech Laboratories, Plymouth Meeting, PA) requires 225

mW of power for pumping rates up to 7.3 ml/min. This is many times greater than gains of pumping observed in Yaquina Bay (approximately 4.4 mW in terms of actual power for the 0.02 $m^2$ footprint of these chambers). This energy imbalance may be addressed several ways for full-scale BMFCs. Lower power pumps could be found, pumping rates could be optimized and/or pumps run intermittently, or a pumping system developed that does not require any electrical power such as one driven by a vacuum chamber deployed along with the BMFC. Finally, one can design chambers to take advantage of natural processes that may drive porewater advection. These processes include pressure gradients created by waves or flow over sedimentary bedforms (Huettel et al., 1998), hydrothermal venting (Elderfield & Schultz, 1996), and tidally pumped fluid venting at cold seeps (Torres et al., 2002). We tested our second version of a chambered BMFC (Figure 2.1b) in the latter environment.

Power density records from the two Monterey Canyon deployments are overlaid in Figure 2.5. The power density from the second deployment was about 5 times greater than from the first deployment. Apparently the fluid pressure from the seep fell between the cracking-pressure of the different valves, so that significant advection into the chamber was only possible with the low-pressure valves. This observation is consistent with the difference in variability between the two records. When a chamber is isolated from advection, one would expect less variability in power generation than a chamber that is open to advection forced by tidal fluctuations or other processes (see Supplemental Material, Appendix B, Figure B.2).

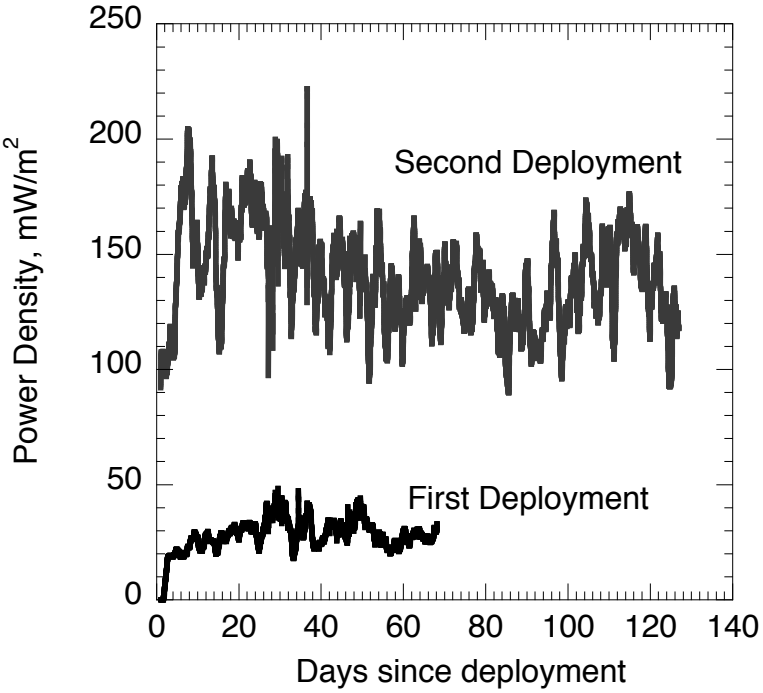


Figure 2.5 Overlay of power density records from two deployments of the Monterey BMFC. At the end of the first deployment, the check valves were changed to a model with a lower cracking pressure and then immediately redeployed. The delay was approximately 6 hours due to the transit time for the ROV to surface from 960 m and then return. During the second deployment, the BMFC began generating current immediately, suggesting that the anodic biofilm survived the trip to the surface.

Our group previously deployed BMFCs with buried graphite anodes at a nearby seep (Reimers et al., 2006). In that experiment, the maximum power density was 1100 $mW/m^2$, but that anode was a vertically oriented rod so the anode surface area does not scale with seafloor footprint. A passivation effect at the anode was also observed, which greatly reduced power over time, and it was attributed to the deposition of elemental sulfur within the pores of the solid graphite anode. The use of carbon fiber anodes inside the chambers showed no electrochemical evidence of power limitation by passivation in either the Yaquina Bay or Monterey deployments. This may be due to much higher overall surface area (relative to instrument footprint) and the lack of pores.

### *2.4.6 Acknowledgements*

This work was supported by grants from the Office of Naval Research and the National Science Foundation. We are grateful to Brian Parker, John Buchanan and Kristina McCann-Grosvenor for their diving assistance and to Joe Jennings and Andrew Ross for analytical help. Discussions with Peter Girguis helped to formulate these experiments, and he coordinated the ROV access. The Monterey deployments were made possible by the expertise of the pilots of the ROV *Ventana* and the crew of the *R/V Pt. Lobos*. This manuscript was improved through helpful conversations with John Westall, Hong Liu and reviews from several anonymous reviewers.

## 2.5 References:

Aelterman P, Rabaey K, Pham HT, Boon N, Verstraete W. 2006. Continuous electricity generation at high voltages and currents using stacked microbial fuel cells. *Environmental Science & Technology* 40: 3388-3394

Burdige DJ. 2006. *Geochemistry of Marine Sediments*: Princeton University Press. 609 pp.

Cheng S, Liu H, Logan BE. 2006. Increased power generation in a continuous flow MFC with advective flow through the porous anode and reduced electrode spacing. *Environmental Science & Technology* 40: 2426-2432

Cline JD. 1969. Spectrophotometric determination of hydrogen sulfide in natural waters. *Limnology and Oceanography* 14: 454-458

Dumbauld BR, Armstrong DA, Feldman KL. 1996. Life-History of Two Sympatric Thalassinidean Shrimps, Neotrypaea californiensis and Upogebia pugettensis, with implications for Oyster Culture. *Journal of Crustacean Biology* 16: 689-708

Elderfield H, Schultz A. 1996. Mid-ocean ridge hydrothermal fluxes and the chemical composition of the ocean. *Annual Review of Earth and Planetary Sciences* 24: 191-224

Finkelstein DA, Tender LM, Zeikus JG. 2006. Effect of electrode potential on electrode-reducing microbiota. *Environmental Science & Technology* 40: 6990-6995

Froelich PN, Klinkhammer GP, Bender ML, Luedtke NA, Heath GR, et al. 1979. Early oxidation of organic matter in pelagic sediments of the eastern equatorial Atlantic: suboxic diagenesis. *Geochimica Et Cosmochimica Acta* 43: 1075-1090

Hasvold O, Henriksen H, Melvaer E, Citi G, Johansen BO, et al. 1997. Sea-water battery for subsea control systems. *Journal of Power Sources* 65: 253-261

He Z, Haibo S, Angenent LT. 2007. Increased power production from a sediment microbial fuel cell with a rotating cathode. *Biosensors and Bioelectronics* 22: 3252-3255

He Z, Minteer SD, Angenent LT. 2005. Electricity generation from artificial wastewater using an upflow microbial fuel cell. *Environmental Science & Technology* 39: 5262-5267

Holmes DE, Bond DR, O'Neill RA, Reimers CE, Tender LR, Lovley DR. 2004. Microbial communities associated with electrodes harvesting electricity from a variety of aquatic sediments. *Microbial Ecology* 48: 178-190

Huettel M, Ziebis W, Forster S, Luther GW. 1998. Advective transport affecting metal and nutrient distributions and interfacial fluxes in permeable sediments. *Geochimica Et Cosmochimica Acta* 62: 613-631

Jang JK, Pham TH, Chang IS, Kang KH, Moon H, et al. 2004. Construction and operation of a novel mediator- and membrane-less microbial fuel cell. *Process Biochemistry* 39: 1007-1012

Johnson KM, King AE, Sieburth JM. 1985. Coulometric DIC analyses for marine studies: An introduction. *Marine Chemistry* 16: 61-82

Larminie J, Dicks A. 2000. *Fuel Cell Systems Explained*. Chichester: John Wiley & Sons Ltd.

Logan BE, Cheng S, Watson V, Estadt G. 2007. Graphite fiber brush anodes for increased power production in air-cathode microbial fuel cells. *Environmental Science & Technology* 41: 3341-3346

Logan BE, Hamelers B, Rozendal R, Schröder U, Keller J, et al. 2006. Microbial fuel cells: Methodology and technology. *Environmental Science & Technology* 40: 5181-5192

Lowy DA, Tender LM, Zeikus JG, Park DH, Lovley DR. 2006. Harvesting energy from the marine sediment-water interface II - Kinetic activity of anode materials. *Biosensors & Bioelectronics* 21: 2058-2063

Moon H, Chang IS, Kim BH. 2006. Continuous electricity production from artificial wastewater using a mediator-less microbial fuel cell. *Bioresource Technology* 97: 621-627

Pilson MEQ. 1998. *An Introduction to Chemistry of the Sea*. Upper Saddle River, NJ: Prentice Hall. 431 pp.

Rabaey K, Clauwaert P, Aelterman P, Verstraete W. 2005. Tubular Microbial Fuel Cells for Efficient Electricity Generation. *Environmental Science & Technology* 39: 8077-8082

Rabaey K, Van de Sompel K, Maignien L, Boon N, Aelterman P, et al. 2006. Microbial fuel cells for sulfide removal. *Environmental Science & Technology* 40: 5218-5224

Reimers CE, Girguis P, Stecher HA, Tender LM, Ryckelynck N. 2006. Microbial fuel cell energy from an ocean cold seep. *Geobiology* 4: 123-136

Reimers CE, Stecher HA, Westall JC, Alleau Y, Howell KA, et al. 2007. Substrate degradation kinetics, microbial diversity and current efficiency of microbial fuel cells supplied with marine plankton. *Applied and Environmental Microbiology* 73: 7029-7040

Reimers CE, Tender LM, Fertig S, Wang W. 2001. Harvesting energy from the marine sediment-water interface. *Environmental Science & Technology* 35: 192-195

Rezaei F, Richard TL, Brennan RA, Logan BE. 2007. Substrate-enhanced microbial fuel cells for improved remote power generation from sediment-based systems. *Environmental Science & Technology* 41: 4053-4058

Ryckelynck N, Stecher HA, Reimers CE. 2005. Understanding the anodic mechanism of a seafloor fuel cell: Interactions between geochemistry and microbial activity. *Biogeochemistry* 76: 113-139

Solorzano L. 1969. Determination of ammonia in natural waters by the phenolhypochlorite method. *Limnology and Oceanography* 14: 799-801

Tender LM, Reimers CE, Stecher HA, Holmes DE, Bond DR, et al. 2002. Harnessing microbially generated power on the seafloor. *Nature Biotechnology* 20: 821-825

Torres ME, McManus J, Hammond DE, de Angelis MA, Heeschen KU, et al. 2002. Fluid and chemical fluxes in and out of sediments hosting methane hydrate

deposits on Hydrate Ridge, OR, I: Hydrological provinces. *Earth and Planetary Science Letters* 201: 525-540

Whitfield M. 1972. The electrochemical characteristics of natural redox cells. *Limnology and Oceanography* 17: 383-393

# 3 Sustainable Energy from Deep Ocean Cold Seeps

Mark E. Nielsen[1], Clare E. Reimers[1], Helen K. White[2], Sonam Sharma[2] and Peter R. Girguis[2]

[1]College of Oceanic and Atmospheric Sciences, Oregon State University, Corvallis OR 97331 USA
[2]Harvard University, Biological Labs, 16 Divinity Avenue, Cambridge, MA 02138 USA

Energy & Environmental Science
The Royal Society of Chemistry
RSC Publishing, Cambridge CB4 0WF
2008, Vol. 1, No. 5, pp 513-596

## 3.1 Abstract

Two designs of benthic microbial fuel cell (BMFC) were deployed at cold seeps in Monterey Canyon, CA, unattended for between 68 and 162 days. One design had a cylindrical solid graphite anode buried vertically in sediment, and the other had a carbon fiber brush anode semi-enclosed in a chamber above the sediment-water interface. Each chamber included two check valves to allow fluid flow from the sediment into the chamber. On average, power outputs were 0.2 mW (32 mW $m^{-2}$ normalized to cross sectional area) from the solid anode BMFC and from 11 to 56 mW (27 - 140 mW $m^{-2}$) during three deployments of the chambered design. The range in power produced with the chambered BMFC was due to different valve styles, which appear to have permitted different rates of chemical seepage from the sediments into the anode chamber. Valves with the lowest breaking pressure led to the highest power production and presumably the highest inputs of electron donors. The increase in power coincided with a significant change in the microbial community associated with the anode from being dominated by epsilonproteobacteria to a more diverse community with representatives from deltaproteobacteria, epsilonproteobacteria, firmicute, and flavobacterium/cytophaga/bacterioides (FCB). The highest levels of power delivered by the chambered BMFC would meet the energy requirements of many oceanographic sensors marketed today. In addition, these BMFCs did not exhibit signs of electrochemical passivation or progressive substrate depletion as is often observed with buried anodes.

## 3.2 Introduction

Natural redox gradients between anoxic sediments and overlying water have recently been used to produce electrical power *in situ* through benthic microbial fuel cells (BMFCs; Reimers et al., 2001; Bond et al., 2002; Tender et al., 2002; Ryckelynck et al., 2005; Lovley, 2006b; Lowy et al., 2006; Dumas et al., 2007; Nielsen et al., 2007; Rezaei et al., 2007). BMFCs couple the oxidation of reduced compounds in sediments to the reduction of oxygen dissolved in the overlying water. Microorganisms play

several roles in these systems including: maintenance of the redox gradient, production of redox mediators, generation of electron-rich metabolites (e.g. sulfide ions), and in some cases, delivery of electrons to an electrode through direct electron transfer (Bond & Lovley, 2003; Chaudhuri & Lovley, 2003; Holmes et al., 2004b; Holmes et al., 2006; Lovley, 2006a; Reguera et al., 2006; Schröder, 2007).

Many ocean sensors have low power requirements, which make them appropriate applications for microbial fuel cell technology (Reimers et al., 2001; Shantaram et al., 2005; Logan & Regan, 2006; Lovley, 2006b; Tender et al., 2008). However, challenges in developing BMFCs for functional underwater applications have included: 1) relatively modest supply rates of natural fuels from the environment, 2) passivation of electrode surfaces by the adsorption of reaction products (Reimers et al., 2006), and 3) the energy cost of enhancing fuel availability (by pumping for example; Nielsen et al., 2007). Also, most microbial fuel cell experiments are performed on a small scale and do not produce useful amounts of power (i.e. when not normalized to electrode surface area, chamber volume or device cross sectional area). The most common method for addressing these challenges is refinement of the cell itself, involving testing different device configurations, electrode materials and/or schemes for delivering more fuel to the anode. Another method is to target environments where natural phenomena can help drive the transport of reduced compounds to the anode of the BMFC.

In this paper we describe an experimental program of BMFC testing at seafloor locations with chemical seepage. Results from two tests described in this paper were presented previously in a different form as ancillary data (Nielsen et al., 2007). Here they are discussed in-depth with additional measurements and attention paid to environmental processes that control the supply of electron donors to the anode (diffusion and/or advection). Without the input of energy to pump fluid (or otherwise manipulate parts of the fuel cell) one BMFC produced usable amounts of power, relying on natural processes in marine sediments to provide electron donors to the

anode. The microbial phylogeny of biofilms sampled from anode materials was investigated, and the highest diversity was observed in the BMFC with the highest power production.

### *3.2.1 Power targets for BMFCs*

Long-term monitoring is important to many environmental and oceanographic investigations. To meet this objective, sensors and supporting communication devices are evolving to use less and less power, thus extending available deployment times in remote, "off grid", locations. Table 3.1 presents examples of sensors and a telesonar modem with low power requirements that are relevant to oceanographic studies. Power requirements for such devices are typically not static and depend on the duty cycle and the extent of data processing, storage and/or communication. Currently, batteries are the power supply of choice in deep ocean settings where other alternatives such as wind or solar are not available. Batteries have a finite life, however, so a development goal for benthic microbial fuel cells is to replace batteries in selected long-term monitoring applications. The sensors listed in Table 3.1 typically consume from 20 mW to a little less than 500 mW during periods of peak demand. This range of power is the context in which the performance of the BMFCs described in this paper need to be evaluated.

Table 3.1 Examples of power requirements for oceanographic sensors and communication devices

| Instrument | Manufacturer | Voltage (V) | Power Requirement (mW) |
|---|---|---|---|
| Turbidity meter | Seapoint Sensors, Inc. | 7 - 20 | 24.5 avg, 42 peak |
| Chlorophyll-a fluorometer | Seapoint Sensors, Inc. | 8 - 20 | 120 avg, 216 peak |
| Conductivity, temperature and depth | Ocean Sensors, Inc. | 6 | 1.2 sleep mode, 420 peak |
| Backscattering meter | Wetlabs, Inc. | 7 - 15 | 0.6 sleep mode, 560 peak |
| Wireless Temperature Probe/Transmitter | Madgetech, Inc. | 3.3 | 49.5 |
| Acoustic receiver | Sonotronics, Inc. | 3.5 | 14 standby, 28 peak |
| Acoustic Modem | Teledyne Benthos | 14 - 28 | 12 standby, 500 active, 20 W transmit |

### *3.2.2 Regional setting*

The locations for these experiments were within the Monterey Submarine Canyon, CA (Figure 3.1). This canyon is a prominent geomorphic feature on the west coast of North America. The canyon system begins near shore and extends to a water depth of approximately 3.5 km. Cold seeps characterized by vesicomyid clams and chemoautotrophic bacterial mats are ubiquitous in the canyon (Barry et al., 1996; Orange et al., 1999; Paull et al., 2005). It has been suggested that the seepage is driven by tectonic compression from transform faults between the Pacific and North American plates or by "slow mud-diapirism" (Reimers et al., 2006). The canyon cuts into the organic-rich Monterey Formation, which is thought to be the source of organic carbon in the seep fluid (Martin et al., 1997). The study area for these experiments is known as Extrovert Cliff (36° 46.6'N, 122° 05.1'W) and is characterized by a muddy

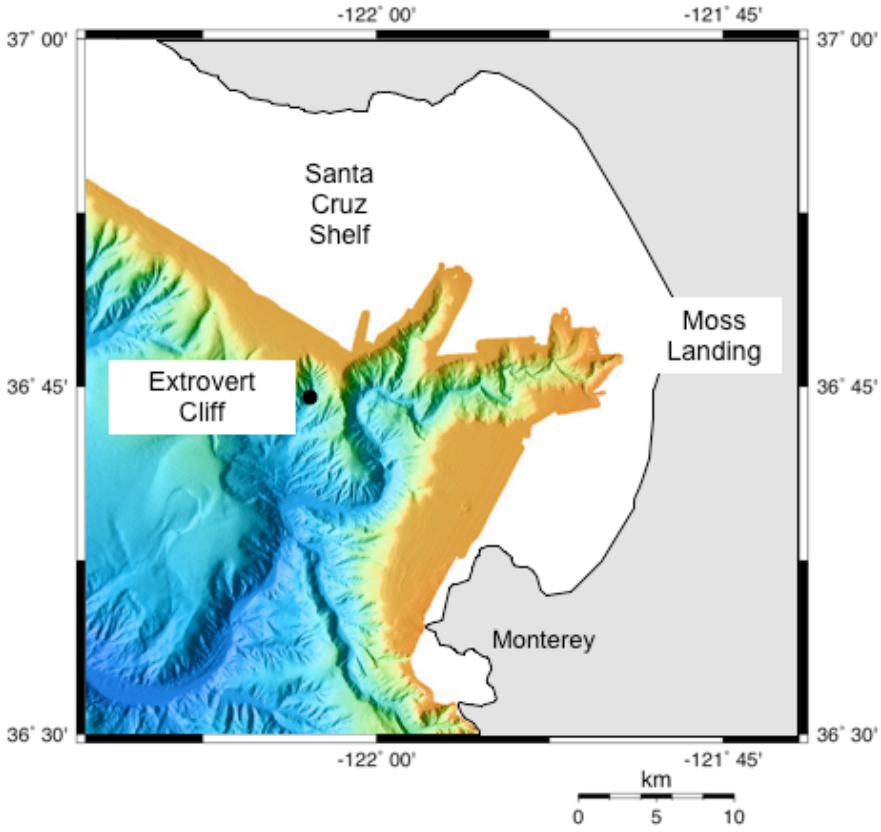


Figure 3.1 Location of study site within Monterey Canyon. Adapted from bathymetry survey by Monterey Bay Aquarium Research Institute (http://www.mbari.org/data/mapping/monterey/default.htm).

slope with cold seeps that affect patches of seafloor (~1 - 10 $m^2$) spaced 10's of meters apart, at a depth of about 960 m (Figure 3.2). Flow intensity from the seeps varies spatially and temporally with some seeps exhibiting little detectable advection and others having a discrete conduit where active flow results in a shimmering fluid expulsion across the sediment-water interface. Sensors mounted on a remotely operated vehicle (ROV) used during these experiments indicated a bottom water temperature of 4°C, a salinity of 34.5 and dissolved oxygen concentration of approximately 11 μM directly over the seeps.

### *3.2.3 Seeps as energy sources*

Reduced compounds in pore fluids from cold seeps can be converted to electrical power by a BMFC by both biological and chemical mechanisms of electron transfer (Reimers et al., 2006). The amount of electrical power produced depends on fluid composition, transport of electrochemical reactants and products to and from the electrodes, and the design of the BMFC including size and electrode surface area. Furthermore, these factors can depend on each other; for example, the dominant transport process may be affected by the design of the BMFC. In previous experiments at these seeps, we used a solid graphite anode buried in the sediment (Reimers et al., 2006). The power record from that experiment was characterized by a peak (about 25 days into the deployment) and then decay to a low quasi-steady state level of power production. Decaying production of power over time is consistent with diffusion as the dominant mode of transport of electron donors to the anode, resulting in depletion of electron donors at the electrode surface and/or passivation of the electrode. It also implies that advective transport through fluid seepage was insufficient to prevent these effects. Entering into this study we hypothesized that: 1) burying an anode may restrict or redirect localized advection through the sediment; and 2) a BMFC design which allowed natural seepage to influence the anode environment should produce significantly more power.

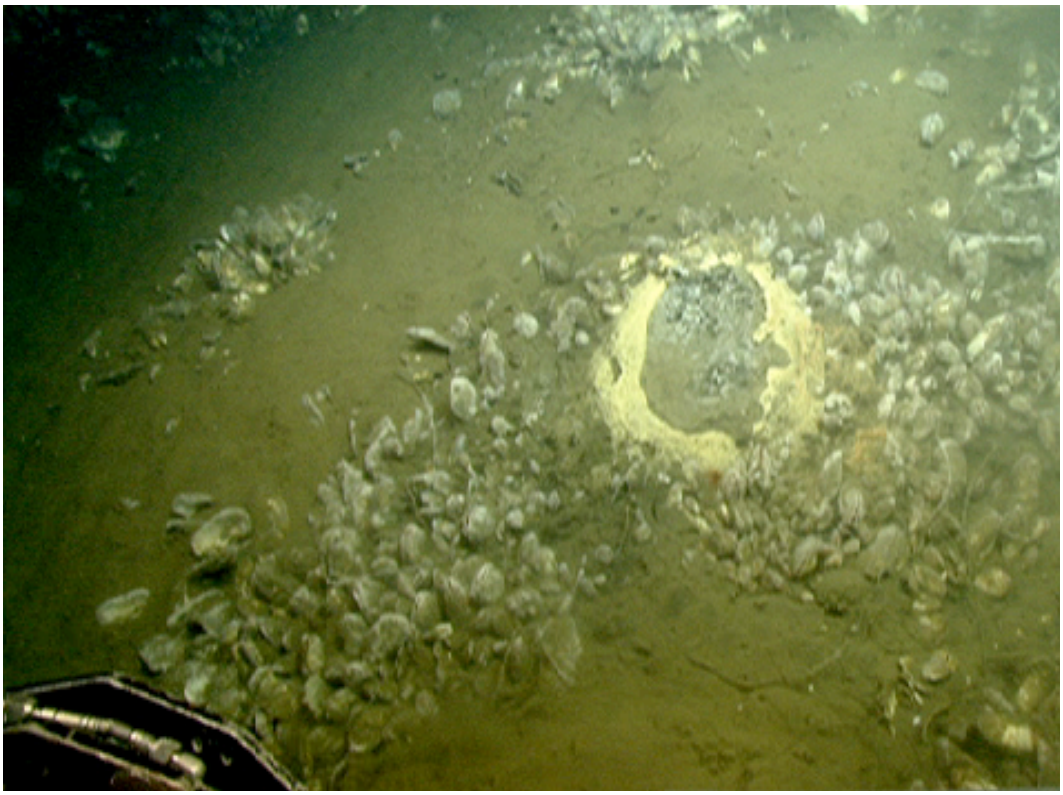

Figure 3.2 Image of seeps at Extrovert Cliff in Monterey Canyon. Clams indicate seepage areas along a sloped seabed. A conduit for vigorous fluid flow is visible in the right portion of the photo ringed with a bacterial mat.

Labonte et al. (2007) recently deployed benthic flux chambers in Monterey Canyon over seeps very close to the areas that we targeted in this experimental program. The chambers that covered 640 $cm^2$ of seafloor did not impede flow and measured fluid flow rates of $2 – 6 \times 10^3$ cm $y^{-1}$ for the most vigorous seeps (corresponding to volumetric fluxes of 2.4 – 7.3 $cm^3$ $s^{-1}$ per seep). The concentration of sulfide in the seep fluids is approximately 12 mM (Reimers et al., 2006). Thus if we assume that sulfide is the primary electron donor, the maximum current (*I,* A) that might be generated by a BMFC designed similar to a flux chamber placed over an active seep may be estimated as:

(1) $$I = Q \times C_0 \times n \times F$$

where $Q$ is the volumetric fluid flux ($cm^3$ $s^{-1}$), $C_0$ is the concentration of electron donor in the fluid (mol $cm^{-3}$), $n$ is the number of electrons involved in electrochemical reaction (*2,* in the case of sulfide oxidation to sulfur) and $F$ is Faraday's constant (96,485 C/mol). Assuming 100% current efficiency and a BMFC voltage fixed at 0.4V, the maximum power sustainable by Monterey Canyon seeps can be calculated as the product of current and voltage. These calculations predict power outputs of 37 to 112 mW.

In contrast, in the absence of seepage the current would be limited by diffusion across the sediment-water interface and proportional to the seafloor area enclosed by a chambered BMFC ($A$). In this case, the current can be approximated using:

(2) $$I = n \times F \times \varphi D_s \frac{d\overline{C}}{dz} \times A$$

where $\varphi$ represents the sediment porosity ($cm^3_{porewater}/cm^3_{sediment}$), $\frac{d\overline{C}}{dz}$ denotes a spatially averaged concentration gradient of the dominant electron donor $C$ across the sediment-water-interface (mol $cm^{-3}$/cm), and $D_s$ is the diffusion coefficient ($cm^2$ $s^{-1}$)

for *C* corrected for sediment tortuosity effects (Boudreau, 1997; Schulz, 2006). Beneath a chambered BMFC, concentration gradients may grow or shrink depending the rate of electron donor oxidation at the anode, the volume of the subsurface fluid reservoir supplying the sediment gradient, and perturbations caused by bioirrigation. We estimate that a diffusive flux across the sediment water interface according to equation (2) would result in power output ranging from 1 to 26 mW (again assuming a current efficiency of 100% and an operating voltage of 0.4 V). The large range is due to expected variability in $\varphi$ (0.6 – 0.9) (Reimers et al., 1992) which leads to a range in $D_s$ from 5.6 to 9.3 × $10^{-6}$ (calculated according to Schulz, 2006) and variability in $\frac{d\overline{C}}{dz}$. We estimated $\frac{d\overline{C}}{dz}$ would range from 1 to 10 × $10^{-6}$ mol $cm^{-3}$ $cm^{-1}$ based on sulfide profiles measured in sediment cores of seep sediments by Rathburn et al. (2003).

## 3.3 Methods and instrumentation

### *3.3.1 Benthic microbial fuel cells*

The BMFCs in this study were deployed with the *ROV Ventana* operated by the Monterey Bay Aquarium Research Institute. Vigorous seeps with visible fluid flow were targeted for all deployments. The fuel cells differed primarily in their anodes: BMFC 1 had a single solid graphite anode buried in the mud, and BMFCs 2-4 had carbon-fiber brush anodes suspended above the sediment-water interface inside a benthic chamber. BMFC 4 was a re-deployment of BMFC 2 with a slightly different configuration (details below).

The anode of BMFC 1 was constructed from a cylindrical piece of solid graphite (50 cm long with one end milled into a tip) and a diameter of 0.04 m (geometric surface area = 0.05 $m^2$). A titanium bolt wrapped with the exposed end of an insulated copper wire was threaded into the upper end of the graphite and potted in a PVC sleeve with marine grade epoxy in order to make a connection to the circuit. The cross sectional area of the anode assembly (including the PVC sleeve) was 6.2 × $10^{-3}$ $m^2$. The

cathode was a 0.5 m length of carbon-fiber brush electrode (Hasvold et al., 1997) fastened to a post that extended approximately 0.3 m above the sediment-water interface. A bare-wire Ag/AgCl reference electrode was also fastened to the cathode post. A pressure housing containing the control and measurement circuitry (described below) was attached with the cathode to a stainless steel frame placed on the seafloor. The anode was pushed vertically into the sediment into an active seepage conduit with a manipulator arm of the ROV.

The chambers (Figure 3.3) were constructed from a section of acrylonitrile butadiene styrene (ABS) plastic sewer pipe (0.61 m I.D.) cut lengthwise giving a rectangular cross sectional area of 0.4 $m^2$ (and an estimated chamber volume above the sediment of $2.0 \times 10^{-2}$ $m^3$ after it was pushed into the sediment). The ends of the chambers were made from 1.25 cm-thick acrylic, glued to the pipe section, and reinforced with stainless steel screws. Two one-way valves were installed on the top of each chamber to allow flow from the sediment into and through the chamber. Each chamber had a single anode consisting of three 1-m sections of carbon-fiber brush electrode (Hasvold et al., 1997) connected end to end. The anode sections were spaced side-by-side evenly inside the chamber and attached to the chamber walls with polypropylene hardware. The cathode for each BMFC was made from four 1-m sections of identical carbon-fiber brush electrodes connected to each other by attaching one end to a common titanium bolt with an insulated copper wire from the BMFC circuit. The bolt was potted in epoxy to protect the copper wire from corrosion. The other ends of the cathodes were connected to another titanium bolt at a common point. The cathodes were fastened to posts that extended approximately 0.5 m above the sediment-water interface from one corner of each chamber. The manufacturer-reported surface area of the brush electrodes is 26 $m^2$ per meter of length, giving total surface areas of approximately 78 and 104 $m^2$, for the anode and cathode, respectively. Bare-wire Ag/AgCl reference electrodes (for monitoring anode and cathode potentials) were

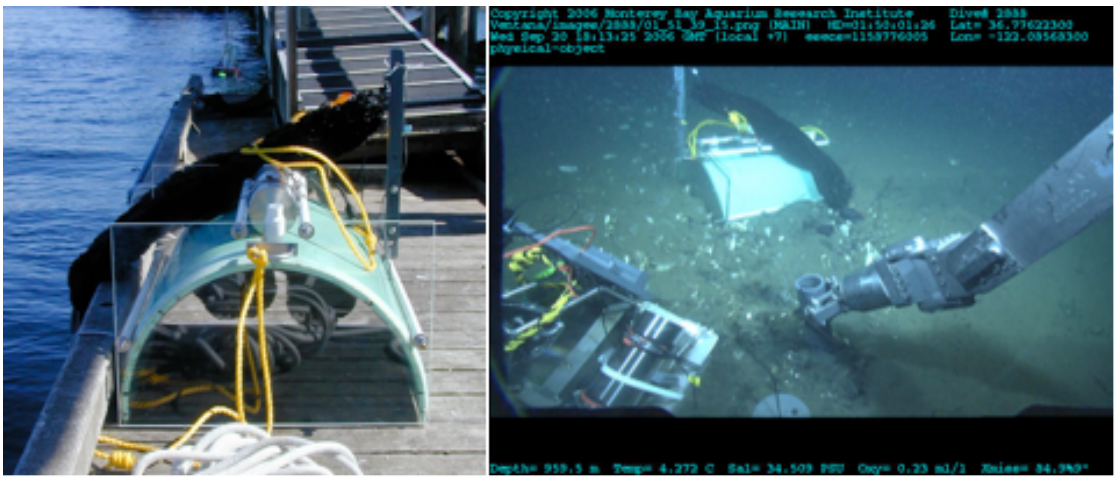

Figure 3.3 Photographs of the chambered BMFC: A) On the dock prior to a test deployment. The anodes can be seen suspended inside the chamber. The one-way valves, and the pressure housing that contains the controlling potentiostat and voltage loggers can be seen on top of the chamber. B) Just after deployment on the seafloor in Monterey Canyon (photograph is a screen grab from the *ROV Ventana* high definition video system). In the foreground, the PVC sleeve supporting the solid anode from BMFC 1 is being pushed into the sediment.

attached to the posts supporting the cathode just below the electrodes (approximately 40 cm above the sediment-water interface). The potential of the bare-wire Ag/AgCl reference electrode in seawater under the conditions at this site is estimated to be approximately 236 mV versus the standard hydrogen electrode (Reimers et al., 2006). Titanium pressure housings contained the measurement and control circuitry (described below) and were attached to the top of each chamber.

Figure 3.4 depicts the pressure housing, electrical controls and data loggers for these BMFCs. Whole-cell potential (cathode versus anode), anode potential (anode versus Ag/AgCl) and current (after conversion to a voltage) were measured every 10 minutes with voltage recorders (Madgetech, Warner, NH). Whole-cell potential was controlled with a potentiostat (NW Metasystems, Bainbridge Island, WA) to allow enough current to flow to maintain the whole cell potential at some predetermined setpoint (0.4 V for these experiments). If/when the whole-cell potential falls below the setpoint, the potentiostat opens the circuit allowing the natural redox gradient to recover until the setpoint is met again. In effect, the potentiostat acts as a variable external load that is automatically manipulated to maintain the predetermined voltage. Cathode potential was calculated from the whole-cell and anode potentials. Power was normalized to cross-sectional area for both.

When BMFC 2 was recovered, we attached a syntactic foam float to the cathode assembly and replaced the spring loaded check valves with swing check valves that have a lower cracking pressure (0.7 kPa compared to 3.4 kPa) and re-deployed the BMFC on the same footprint (± 0.1 m). This deployment is denoted BMFC 4.

Prior to the field deployments in Monterey Canyon, the chambered BMFCs (configured as BMFC 2 and 3) were tested in Yaquina Bay, OR. The tests in the bay served not only to verify proper operation of the BMFCs but also to condition the electrodes. The solid-anode BMFC was not tested and therefore the electrodes were not conditioned. BMFCs 1-3 were deployed in Monterey Canyon on a single cruise in

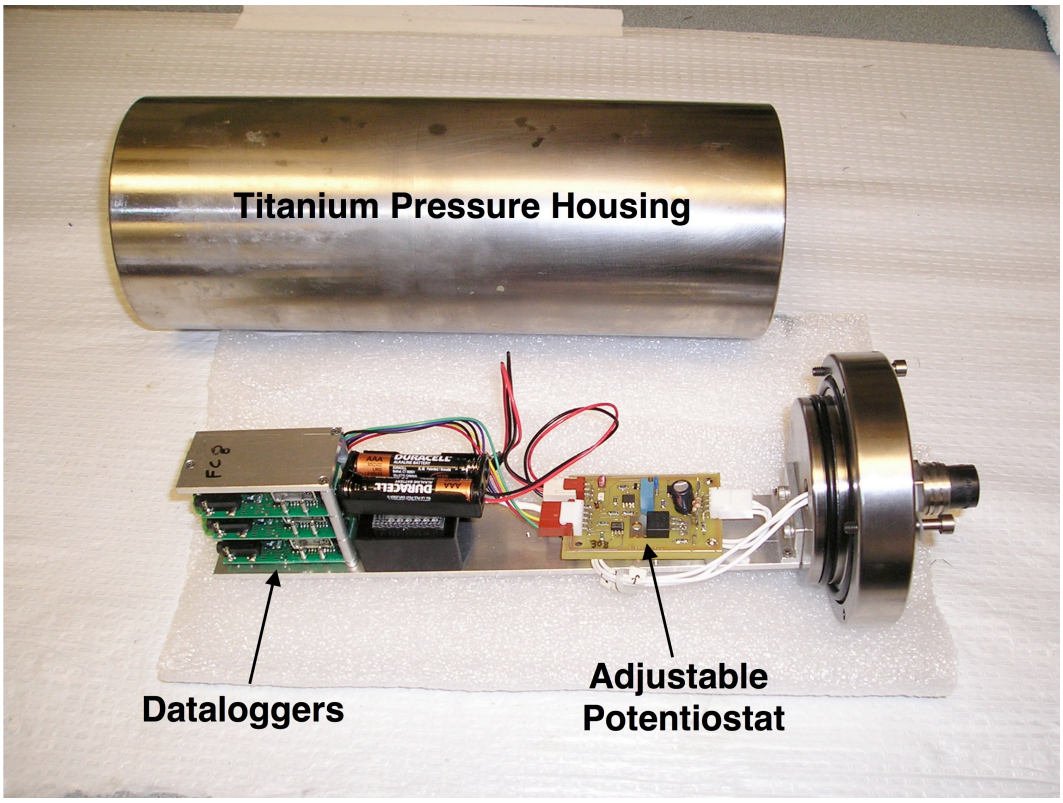


Figure 3.4 Photograph of potentiostat that controls the whole-cell potential and the titanium pressure housing.

September 2006. BMFC 1 was deployed for 162 days, and BMFCs 2 and 3 were deployed for 68 and 69 days, respectively. BMFC 2 was subsequently redeployed as BMFC 4 for an additional 127 days.

### *3.3.2 Microbiological community analysis*

Clippings from the carbon fiber brush anodes from BMFC 2 and BMFC 4 were collected at the conclusion of the respective deployments. The samples were collected with flame-sterilized forceps and shears immediately upon recovery of the BMFCs to the deck of the ship. Approximately 2 g of fibers were clipped and preserved in a filter-sterilized 1:1 solution of ethanol and iso-osmotic, phosphate buffered saline and frozen at –50 °C. The anode of BMFC 1 could not be sampled because it broke off from its PVC sleeve and was lost during recovery.

Nucleic acids were extracted with the PowerSoil DNA extraction kit (MoBio Inc., San Diego, CA), modified to maximize yields (Girguis et al., 2003). Small-subunit (SSU) rRNA bacterial genes from all samples were amplified by PCR with a bacterial targeted forward primer (B27f, 59-AGAGTTTGATCCTGGCTCAG-39) and a universal reverse primer (U1492r, 59-GGTTACCTTGTTACGACTT-39). Environmental rRNA clone libraries were constructed by cloning amplicons into a pCR4 TOPO vector and transforming into chemically competent Escherichia coli according to the manufacturer's protocol (TOPO TA cloning kit; Invitrogen Inc.). Transformants were screened on LB–kanamycin–X-Gal plates using blue-white selection. Plasmids were purified with the Montage miniprep kit (Millipore, Inc.) and sequenced with BigDye chemistry (version 3.1) on an ABI 3730 capillary sequencer. Ninety-six plasmids were sequenced and compared in both directions from each anode sample. SSU rRNA sequences were trimmed to remove the vector using Sequencher 4.0 (Gene Codes Inc., Ann Arbor, MI). SSU rRNA sequence data were compiled and aligned to full-length sequences obtained from GenBank with the FASTALIGNER alignment utility of the ARB program package (www.arb-home.de). Alignments were verified by comparison of the sequences of secondary structure with those of

Escherichia coli and closely related phylotypes. Phylogenetic analysis of the bacterial SSU rRNA sequences was accomplished with MrBayes version 3.1.2.

## 3.4 Results and discussion

### *3.4.1 Power production*

Table 3.2 and Figure 3.5 summarize power and power density for all the BMFC deployments. Power density was normalized to cross-sectional area of the respective designs because this dimension has implications for scaling up the power output of BMFCs through enlargement or by deploying an array of devices. BMFC 1 produced an average power of 0.2 mW (32 mW $m^{-2}$). As in our previous experiments, this design of BMFC did not produce a sustained level of power. It peaked on day 23 at about 0.7 mW (113 mW $m^{-2}$) and then decayed to approximately 0.1 mW (16 mW $m^{-2}$) after day 100. BMFCs 2 and 3 produced significantly more power. The average power for this configuration (n = 2) was about 11 ± 1 mW (27 ± 2 mW $m^{-2}$). BMFC 4 produced an average of 56 mW (140 mW $m^{-2}$) over a deployment of 127 days that began at the end of the BMFC 2 deployment.

Table 3.2 Summary of Monterey Canyon BMFC Experiments

| BMFC | Description | Length of Deployment (days) | Peak Power (mW) | Average Power (mW) | Average Power Density (mW $m^{-2}$) | Rel. St Dev. |
|---|---|---|---|---|---|---|
| 1 | Anode buried in sediment | 162 | 0.7 | 0.2 | 32 | 76% |
| 2 | Anode enclosed in chamber | 68 | 20 | 12 | 30 | 38% |
| 3 | Anode enclosed in chamber | 69 | 20 | 11 | 27 | 90% |
| 4 | Anode enclosed in chamber | 127 | 80 | 56 | 140 | 30% |

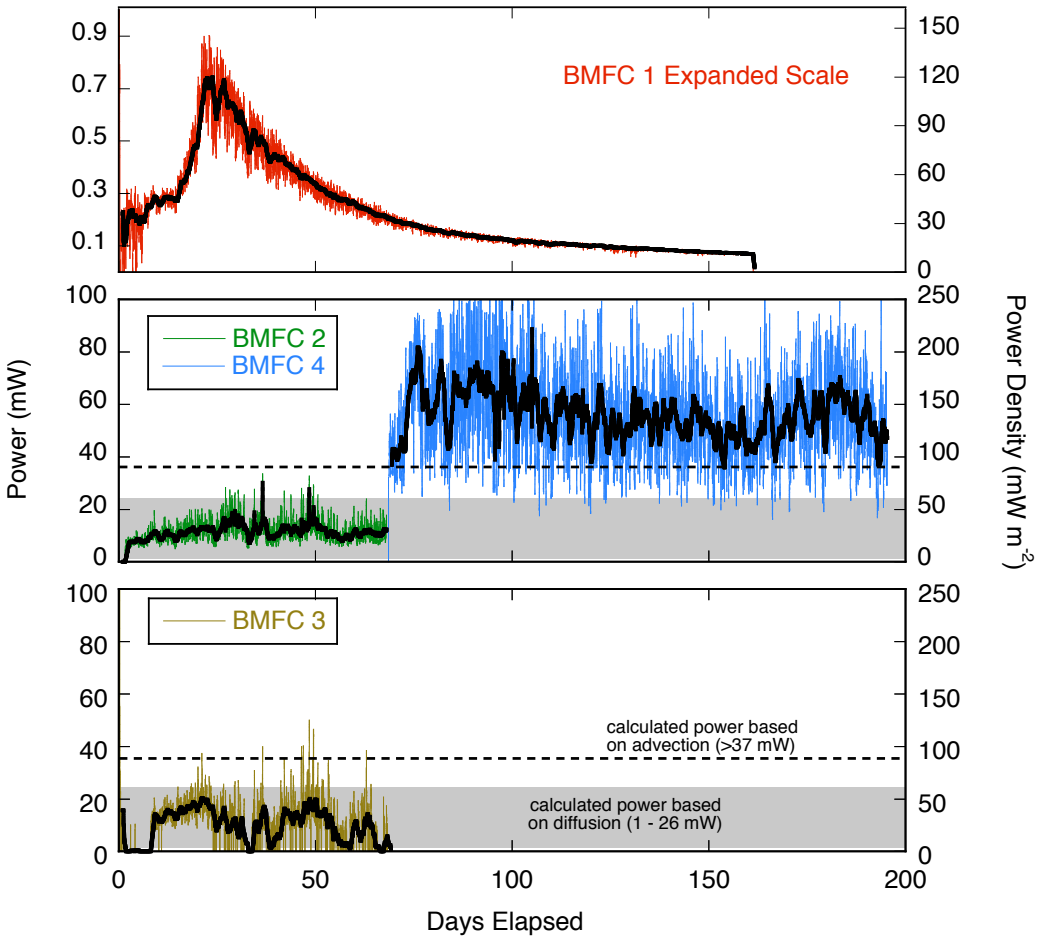


Figure 3.5 Power records from all BMFC deployments (raw data is shown with an overlay showing the 24-hour running average in bold). Left axis shows actual power output and right axis shows power normalized to cross-sectional area. The upper panel has a magnified scale and shows the BMFC 1 results. Data from BMFCs 2-4 are shown in the lower panels. Shaded area is range of power predicted by diffusion calculations. Dashed line shows lower bound of power expected from advective flux (details in text).

The power records from the three chamber deployments are highly variable and show normal distributions around the respective mean values with relative standard deviations ranging from 30 to 90 percent. We speculated in an earlier report (Nielsen et al., 2007) that part of the variability might be due to tidal pumping resulting from transient pressure anomalies and elastic properties of the sediment matrix (Wang & Davis, 1996; Tivey et al., 2002; Jupp & Schultz, 2004; LaBonte et al., 2007). However, a power spectral density (Trauth, 2006) plot did not show peaks corresponding with a tidal frequency and suggested that the variability was due to random noise. We also attempted a cross-spectral analysis between power and wave height, including a distributed lag analysis to look for delayed effects of pressure gradients, but did not identify any significant correlation. Wave height data were obtained from NOAA, National Data Buoy Center Site 46042.

The lack of correlation with tides is in contrast to previous findings in Yaquina Bay in which power was correlated and in phase with the tidal signal (Nielsen et al., 2007). However, Yaquina Bay is an estuary and tidal fluctuations are accompanied by changes in pressure, salinity (and therefore conductivity), dissolved oxygen and temperature. In the deep ocean, tidal fluctuations would only cause pressure changes, which we hypothesized might result in power fluctuations due to changes in seepage rates. Since variations in power were not significantly correlated to tidal pressure, changes in power output are probably due to a combination of factors. Other possible factors that might contribute to the variable power output include environmental factors affecting the cathode, bioirrigation (especially by clams living within the seep sediments), heterogeneous fluid composition, and random stirring events that facilitate transport of electroactive species to the electrode surface.

### *3.4.2 Electrode potentials*

Overpotential is the difference between observed electrode potential and potential at equilibrium conditions (Bard & Faulkner, 2001). Open circuit potentials are always lower than theoretical cell potentials due to overpotentials at the cathode and anode.

There are additional current dependent overpotentials at each electrode due to activation losses, ohmic losses and mass transport (or concentration losses) (Logan et al., 2006). Current dependent overpotentials are the difference between electrode potential at open circuit and under load. They are useful indicators of which electrode is most affected by current limiting processes (e.g., mass transfer of reactants or passivation) in a given experiment. A departure from zero (positive for the anode and negative for the cathode) is correlated with apparent limitation at the electrode. The BMFCs in this study were not equipped with devices that allowed direct measurements of the open circuit potential of the electrodes (circuits were closed at the time of deployment and remained so for the entire experiment). However, using average open circuit values observed during previous experiments with buried anodes at a nearby seep (–0.43 and 0.38 V vs. Ag/AgCl for the anode and cathode, respectively) (Reimers et al., 2006), we can estimate the current dependent overpotentials (potential under load – potential at open circuit, $\eta$) for the electrodes in each BMFC (Figure 3.6). In doing so, we note that from our experience the assumed open circuit values are very typical for sulfide-rich marine sediment/seawater based MFCs plus or minus 0.03 V (Ryckelynck et al., 2005). Because the cell potential is maintained at 0.4 V by the potentiostat the difference in overpotentials remains constant.

BMFC 1 began cathode limited and shifted to apparent anode limitation over the course of its deployment. This change can be attributed to a typical 1-2 week period of cathode conditioning during which cathode potential versus Ag/AgCl rises sigmoidally (Reimers et al., 2006). In contrast, BMFC 2 (and its redeployment as BMFC 4) exhibited slightly greater anode overpotential than cathode overpotential (0.3 V vs. –0.2 V, respectively) during most of the record (the datalogger recording anode potential failed early in the BMFC 4 deployment). BMFC 3 exhibited a

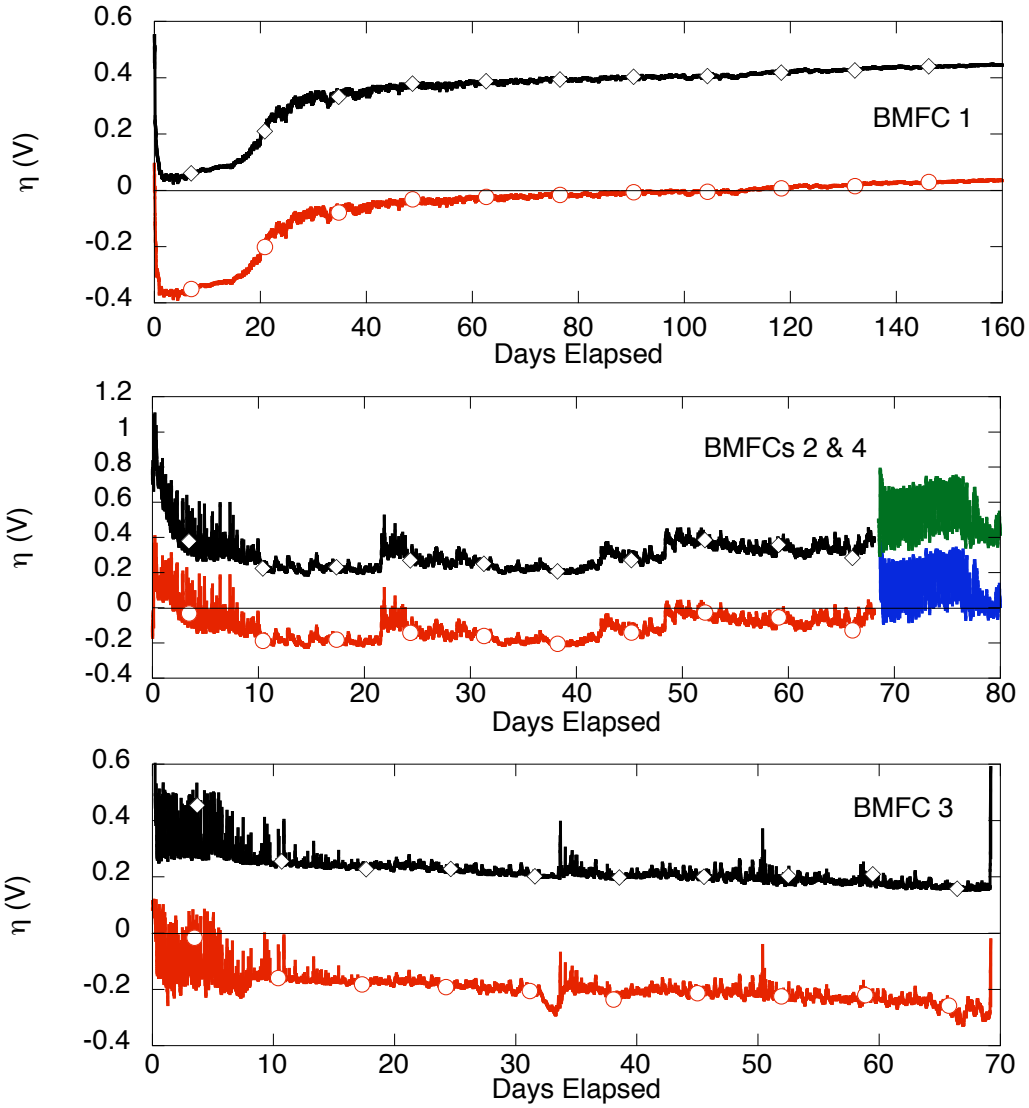


Figure 3.6 Cathode (○) and anode (◇) overpotentials (η) for all BMFC deployments based on open circuit potentials (vs. Ag/AgCl) observed during previous experiments at nearby seeps. BMFCs 2 and 4 are shown on the same plot (middle panel) since they are the same device that was recovered and then redeployed. The datalogger monitoring anode potential failed during the BMFC 4 deployment, so the record is incomplete.

systematic progression from predominantly anode limitation towards cathode limitation. The first 10 to 14 days of each chamber deployment shows a noisy signal for both the cathode and anode potential. This characteristic is shared by the data from all of the chamber configurations but is probably not related to electrode conditioning since the chambers were tested in Yaquina Bay prior to the Monterey Canyon deployments. The cause of the noisy signal does not appear to have limited or inhibited the onset of power generation.

### *3.4.3 Comparison between buried solid anode and chamber design*

The average power density from the chambered BMFCs was similar to the power density from the buried anode. However, the chambers had a cross section (or footprint) that was approximately 65 times larger than the buried anode. Thus, in terms of actual power output, the chambered BMFCs produced 60 to 280 times more power than the buried anode BMFC and thus had superior performance according to the criteria of producing useful power for oceanographic sensors. The different designs required similar resources for deployment in terms of ROV time and capacity. Scaling up the solid anode in size or deploying a complex array of them to produce greater power would not be as practical as deploying a single chamber.

The power records from the different BMFC designs have distinct patterns related to the transport processes that control the delivery of electron donors in the sediment and to the anode in the respective BMFCs. The power record from BMFC 1 showed a peak on day 23 followed by a decay over time. This pattern is similar to previous results (Reimers et al., 2006) and is consistent with an electrochemical system for which 1) the cathode requires a conditioning period, 2) long-term power production is limited by anode processes and anode area, and 3) the medium surrounding the anode is stagnant (or unstirred) and thus the electron donor supply is dependent on molecular diffusion in the absence of bioirrigation. In this case the apparent diffusive supply is at odds with the observed seepage from the seafloor. Therefore, we conclude that the solid anode buried in the sediment effectively plugged the advective transport of the

seep. Conversely, the records from BMFCs 2-4 show no systematic decay in the amount of power produced over time. For power levels to have remained approximately constant (i.e. not decay) we conclude that there was a sustained supply of electron donors to the chambers.

When the spring-loaded check valves on BMFC 2 were replaced with swing check valves, power increased by a factor of five (Table 3.2, Figure 3.5). The other alteration we made at the redeployment was to use syntactic foam to suspend the cathode above the BMFC. However, because BMFC 2 had greater anode overpotential than cathode overpotential we infer that the alteration that affected the anode (changing the valve) probably had a larger effect. The higher power associated with the lower pressure valves suggests that seep fluid was able to pass through the chamber and out the check valves on BMFC 4 (0.7 kPa cracking pressure) but was often restricted by the valves on BMFCs 2 and 3 (3.4 kPa cracking pressure).

The power predictions based on equations (1) and (2), independent measurements of fluid flow and composition, and BMFC dimensions are consistent with the different transport mechanisms in the sediments beneath the various chambers. We predicted a range of 37 to 112 mW could be sustained by advective fluxes. These predictions bracket the power produced by BMFC 4 but are far greater than what was generated by BMFCs 2 and 3. BMFCs 2 and 3 produced power in the middle of our predicted range (1 to 26 mW) based on diffusive transport of sulfide across the sediment-water interface. However, current was highly variable suggesting advective inputs were at times non-zero.

### *3.4.4 BMFC efficiency*

A common measure of fuel cell efficiency is the amount of electrons passed through the circuit divided by the amount of available electrons added to the system as fuel; this quantity is known as coulombic or current efficiency (Kim et al., 2000; Logan et al., 2006). Coulombic efficiency is challenging to measure in BMFC field

experiments because it is difficult to constrain the delivery of electron donors from the natural system. As noted earlier, predictions for the Monterey Canyon seep environment depend on the presumed transport mechanism and bracket the current and therefore power generated by all the chambered BMFCs. Taking the upper bound of the predicted range (112 mW) and the performance of BMFC 4 gives an efficiency of approximately 50 percent. This may indicate ~50% of the sulfide (and other electron donors) transported into the chamber exits unreacted. If this is verified in future experiments, the BMFCs can be re-designed to lower the fraction of unreacted electron donor and to produce more power.

Two changes that may lower the fraction of unreacted electron donor are increasing the residence time of fluid in the chamber (by changing the volume), and/or changing ratio of anode surface area (in $m^2$) to chamber volume (L). By comparison, our earlier experiments with mechanically pumped chambered BMFCs in Yaquina Bay had a residence time of approximately 5 hr and 26 $m^2$ of anode area within a 2 L chamber volume (13:1 ratio) (Nielsen et al., 2007). In Monterey Canyon (an environment with higher sulfide fluxes) we estimate a residence time of 8 – 22 hours based on fluid flux measurements from Labonte et al. (2007), and we had 78 $m^2$ of anode surface area within a 20 L volume (3.9:1 ratio). Peak power densities in Yaquina Bay were 380 mW $m^{-2}$ of seafloor during polarization experiments under pumped conditions. The maximum power density observed in the Monterey Canyon experiments was approximately 200 mW $m^{-2}$. Because this is an environment with a higher flux of sulfide across the sediment water interface we conclude that the residence time was not as limiting as the ratio of anode surface area to volume. We predict higher power densities may be achieved by increasing the amount of anode area within the chambers to ensure that all the potential electron donors are oxidized before leaving the chamber (assuming advective transport). Improvement may also be achieved by altering anode positioning to insure electrode area is evenly distributed relative to the preferential flow-path through the chamber. This might be accomplished by adding bulkheads within the chamber to direct fluid flow past all of the electrode material.

Performance may also be improved by linking a series of BMFCs rather than scaling up the size of a single device. Aelterman et al. (2006) and Ieropoulos et al. (2008) demonstrated the benefits of connecting laboratory fuel cells in series or parallel to boost voltage or current, respectively. In the latter case, the authors conclude that compartmentalizing a fuel cell into many units results in more efficient operation than a single large unit. In oceanic settings the entire fuel cell is immersed in conductive fluid and electrode pairs cannot be isolated from one another so they cannot be connected in series. Multiple distinct fuel cells could be linked together in parallel to boost current (Tender et al., 2008) but it is unknown how BMFCs in such a configuration would affect each other (if at all). The higher power density from our Yaquina Bay experiments compared to our Monterey Canyon experiments is consistent with the observation that smaller BMFCs may be inherently more efficient than larger BMFCs. However, based on the metric of producing enough power to operate an instrument, the larger fuel cell was the best performer.

Each chamber deployment exhibited some degree of cathode limitation as evidenced by current dependent overpotentials reaching -0.3 V (Figure 3.6). This result is not surprising since bottom seawater in Monterey Canyon is very low in dissolved oxygen (11 μM) and bottom currents are relatively slow. One possible solution is to increase the amount of cathode surface area. Other measures that could be considered include catalysts to promote oxygen reduction or reduction of alternate electron acceptors such as dissolved nitrate. It is likely that oxygen reduction at the cathode is already catalyzed by naturally occurring catalysts such as Mn-oxidizing bacteria for example (Rhoads et al., 2005). Any alternative catalysts would need to be studied and compared to naturally occurring processes. We also noticed a difference between seeps in this study. BMFC 2 and 4 showed less cathode overpotential than BMFC 3, which showed a constant decline over time. Upon recovery of the BMFCs we noted that the cathode and the outside of BMFC 3 was noticeably more covered with a white bacterial mat that might have been sulfide-oxidizing bacteria. It is possible that the

seep we selected for the BMFC 3 deployment had more diffuse flow than the seep at which BMFC 2 (and then 4) was deployed, resulting in the development of a bacterial mat that progressively fouled the cathode. Therefore, site selection may also play a role in maintaining cathode electroactivity, but this consideration is secondary to the requirement of targeting active seeps in order to maximize delivery of fuel to the anode chamber.

### *3.4.5 Comparison of microbial communities*

Based on the 16s rRNA analysis of clone libraries, which provide a robust index of microbial community composition, the bacteria within the biofilm on the BMFC 2 anode were dominated by epsilonproteobacteria (Table 3.3). The phylotypes recovered from the BMFC 4 anode were significantly more varied in phylogenetic diversity and contained sequences allied to the deltaproteobacteria, epsilonproteobacteria, and flavobacterium/cytophaga/bacteriodes (FCB).

The difference in phylogenetic diversity between BMFC 2 and 4 likely reflects different chemical environments inside the respective anode chambers. For BMFC 2, we have shown that the fuel delivery to the chamber was at a rate in keeping with transport predominantly by diffusion. Without advective flow, the chamber would approximate a batch reactor in which the products of anode reactions accumulate. The dominance of epsilonproteobacteria in BMFC 2 suggests that these organisms may help drive the electron transfer process in this environment under fuel-limited conditions. In contrast, previous sediment fuel cell experiments have shown that deltaproteobacteria become the dominant phylotype in anode biofilms (Figure 3.7). The epsilonproteobacteria were most closely related to *Arcobacter nitrofigilis* which are commonly found at oxygen-sulfide transitions in marine systems (Campbell et al., 2006). This association is consistent with our understanding that sulfide is the major electron donor for BMFCs in these environments.

Table 3.3 Microbial community analysis of anode fibers.

| Bacterial Group | Most Closely Related Species | Proportion of phylotypes found | |
|---|---|---|---|
| | | BMFC 2 | BMFC 4 |
| alphaproteobacteria | *Roseobacter denitrificans* | 1% | 0% |
| betaproteobacteria | *Brachymonas denitrificans* | 1% | 6% |
| deltaproteobacteria | *Desulfobulbus propionicus, Desulfuromonas acetoxidans* | 1% | 23% |
| gammaproteobacteria | *Solemya reidi symbiont* | 0% | 9% |
| epsilonproteobacteria | *Arcobacter nitrofigilis* | 93% | 23% |
| Firmicute | -- | 1% | 11% |
| Deferribacteres/Flexistipes | *Flexistipes sinus* | 2% | 0% |
| Myxobacteria | -- | 0% | 2% |
| Fusobacter | *Propionigenium modestum* | 0% | 4% |
| Flavobacterium/Cytophaga/Bacterioides | *Cytophaga fermentans* | 0% | 17% |
| Mycoplasma | *Asteroleplasma* | 0% | 2% |
| Planctomycetes | *Vercomicrobium* | 0% | 2% |

In BMFC 4, it appeared that fluid flowed through the chamber and was episodically refreshed. This configuration led to a more diverse community, possibly due to more concentrated electron donors. The samples recovered from the BMFC 4 anode also included representatives from the FCB groups which are known to process complex organic compounds and produce secondary metabolites that might be used as electron donors for power generation (Covert & Moran, 2001; Kirchman, 2002). We cannot be certain about the phylogenetic differences between BMFC 2 and 4 since there are only two samples to compare. However, they suggest a more systematic experiment relating fluid transport, microbial community analysis and power production could produce new insights about the role of certain groups of organisms in benthic fuel cells.

Figure 3.7 compares the phylogenetic communities from BMFCs 2 and 4 with other experiments. In all cases shown in the comparison, the phylogenetic communities

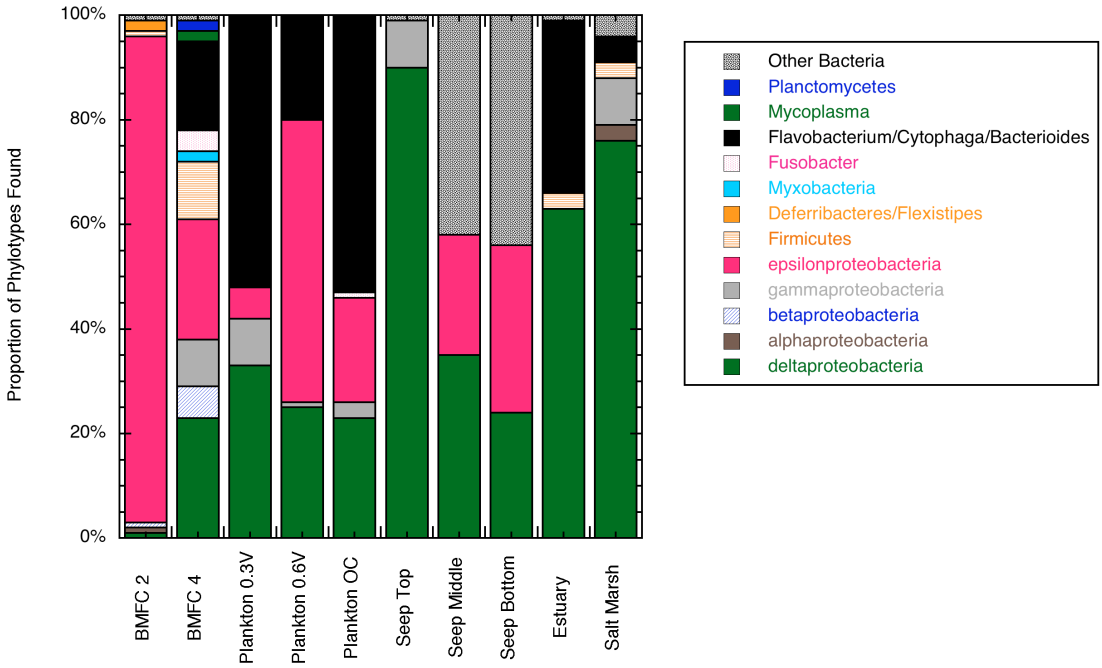


Figure 3.7 Comparison of phylogenetic communities found on anodes between this and previous experiments. Plankton data are from experiments at various controlled potentials (OC = open circuit) (Reimers et al., 2007), seep data are from experiments at a Monterey Canyon cold seep with a vertical buried anode that was sampled at three intervals (20-29 cm, 46-55 cm and 70-76 cm below the sediment-water interface) (Reimers et al., 2006), estuary and salt marsh data are from plate anodes buried horizontally in the sediment (Holmes et al., 2004a).

represent those present at the end of each experiment. In the case of BMFCs 2 and 4 the current being produced at the end of the experiment was representative of the long-term average of what could be produced by these BMFCs. In the other experiments the current profiles were more like BMFC 1 (a peak followed by a decay) and the communities represent the late-time low-current production phase rather than the peak current phase of the respective experiments. Therefore, the results from the BMFCs described in this paper might implicate new organisms that might participate in current generation that were not previously observed in marine microbial fuel cells (e.g. betaproteobacteria and firmicutes groups found on the BMFC 4 anode).

## 3.5 Conclusion

BMFCs with carbon-fiber brush anodes enclosed in chambers and suspended above the sediment water interface clearly outperformed a BMFC with a solid anode buried in the sediment. Based on the configurations in this investigation, 600 solid anodes would be required to generate power equivalent to one chambered BMFC with natural advection. Tender et al. (2008) described other configurations of solid anodes resulting in more anode surface area per device cross sectional area. However, it is unknown how their design might benefit, if at all, from advective processes in the sediment. Even under low-flow conditions (BMFCs 2 and 3) the chamber design behaved more like a well-mixed reactor in which the geochemical gradient of electron donors was maintained. The solid anode BMFC exhibited the characteristics of an unstirred reactor in which the concentration gradient of the electron donor away from the anode diminishes due to progressive depletion of electron donors around the anode.

One of the deployments produced an average of 56 mW of power, which is enough to power some off the shelf low-power oceanographic instruments. Lowering the power demands of sensors by adjusting their duty cycles is a way to increase the number and types of sensors that can practicably be powered by BMFCs. A remaining obstacle is that BMFCs generate power at a low voltage (0.4 V in these experiments) and

instruments typically require higher voltage inputs (3.5 V and greater) thus requiring a DC-DC converter to step up the voltage (Tender et al., 2008). We have already begun new experiments that include investigation of these devices coupled to BMFCs.

## 3.6 Acknowledgments

This research was supported by Award No. N00014-06-1-0212 from the U.S. Office of Naval Research. We are grateful to Monterey Bay Aquarium Research Institute, the crew of the Pt. Lobos and the pilots of the ROV Ventana for skilful and safe deployments. This paper was improved by helpful comments from J. Westall and an anonymous reviewer.

## 3.7 References

Aelterman P, Rabaey K, Pham HT, Boon N, Verstraete W. 2006. Continuous electricity generation at high voltages and currents using stacked microbial fuel cells. *Environmental Science & Technology* 40: 3388-3394

Bard AJ, Faulkner LR. 2001. *Electrochemical Methods*. New York: John Wiley & Sons, Inc.

Barry JP, Greene HG, Orange DL, Baxter CH, Robison BH, et al. 1996. Biological and geologic characteristics of cold seeps in Monterey Bay, California. *Deep-Sea Research Part I-Oceanographic Research Papers* 43: 1739-1762

Bond DR, Holmes DE, Tender LM, Lovley DR. 2002. Electrode-reducing microorganisms that harvest energy from marine sediments. *Science* 295: 483-485

Bond DR, Lovley DR. 2003. Electricity production by Geobacter sulfurreducens attached to electrodes. *Applied and Environmental Microbiology* 69: 1548-1555

Boudreau BP. 1997. *Diagenetic models and their implementation: modelling transport and reactions in aquatic sediments*. Heidleberg, NY: Springer-Verlag. 414 pp.

Campbell BJ, Engel AS, Porter ML, Takai K. 2006. The versatile epsilon-proteobacteria: key players in sulphidic habitats. *Nature Reviews Microbiology* 4: 458-468

Chaudhuri SK, Lovley DR. 2003. Electricity generation by direct oxidation of glucose in mediatorless microbial fuel cells. *Nature Biotechnology* 21: 1229-1232

Covert JS, Moran MA. 2001. Molecular characterization of estuarine bacterial communities that use high- and low-molecular weight fractions of dissolved organic carbon. *Aquatic Microbial Ecology* 25: 127-139

Dumas C, Mollica A, Feron D, Basseguy R, Etcheverry L, Bergel A. 2007. Marine microbial fuel cell: Use of stainless steel electrodes as anode and cathode materials. *Electrochimica Acta* 53: 468-473

Girguis PR, Orphan VJ, Hallam SJ, DeLong EF. 2003. Growth and methane oxidation rates of anaeoic methanotrophic archaea in a continuous-flow bioreactor. *Applied and Environmental Microbiology* 69: 5472-5482

Hasvold O, Henriksen H, Melvaer E, Citi G, Johansen BO, et al. 1997. Sea-water battery for subsea control systems. *Journal of Power Sources* 65: 253-261

Holmes DE, Bond DR, O'Neill RA, Reimers CE, Tender LR, Lovley DR. 2004a. Microbial communities associated with electrodes harvesting electricity from a variety of aquatic sediments. *Microbial Ecology* 48: 178-190

Holmes DE, Chaudhuri SK, Nevin KP, Mehta T, Methe BA, et al. 2006. Microarray and genetic analysis of electron transfer to electrodes in Geobacter sulfurreducens. *Environmental Microbiology* 8: 1805-1815

Holmes DE, Nicoll JS, Bond DR, Lovley DR. 2004b. Potential role of a novel psychrotolerant member of the family Geobacteraceae, Geopsychrobacter electrodiphilus gen. nov., sp nov., in electricity production by a marine sediment fuel cell. *Applied and Environmental Microbiology* 70: 6023-6030

Ioannis Ieropoulos JGCM. 2008. Microbial fuel cells based on carbon veil electrodes: Stack configuration and scalability. *International Journal of Energy Research* 9999: n/a

Jupp TE, Schultz A. 2004. A poroelastic model for the tidal modulation of seafloor hydrothermal systems. *Journal of Geophysical Research-Solid Earth* 109

Kim N, Choi Y, Jung S, Kim S. 2000. Effect of initial carbon sources on the performance of microbial fuel cells containing Proteus vulgaris. *Biotechnology and Bioengineering* 70: 109-114

Kirchman DL. 2002. The ecology of Cytophaga-Flavobacteria in aquatic environments. *Fems Microbiology Ecology* 39: 91-100

LaBonte AL, Brown KM, Tryon MD. 2007. Monitoring periodic and episodic flow events at Monterey Bay seeps using a new optical flow meter. *Journal of Geophysical Research-Solid Earth* 112

Logan BE, Hamelers B, Rozendal R, Schröder U, Keller J, et al. 2006. Microbial fuel cells: Methodology and technology. *Environmental Science & Technology* 40: 5181-5192

Logan BE, Regan JM. 2006. Microbial Fuel Cells: Challenges and Applications. *Environmental Science & Technology* 40: 5172-5180

Lovley DR. 2006a. Bug juice: harvesting electricity with microorganisms. *Nature Reviews Microbiology* 4: 497-508

Lovley DR. 2006b. Microbial fuel cells: novel microbial physiologies and engineering approaches. *Current Opinion in Biotechnology* 17: 327-332

Lowy DA, Tender LM, Zeikus JG, Park DH, Lovley DR. 2006. Harvesting energy from the marine sediment-water interface II - Kinetic activity of anode materials. *Biosensors & Bioelectronics* 21: 2058-2063

Martin JB, Orange DL, Lorenson TD, Kvenvolden KA. 1997. Chemical and isotopic evidence of gas-influenced flow at a transform plate boundary: Monterey Bay, California. *Journal of Geophysical Research-Solid Earth* 102: 24903-24915

Nielsen ME, Reimers CE, Stecher HA. 2007. Enhanced Power from Chambered Benthic Microbial Fuel Cells. *Environmental Science & Technology* 41: 7895-7900

Orange DL, Greene HG, Reed D, Martin JB, McHugh CM, et al. 1999. Widespread fluid expulsion on a translational continental margin: Mud volcanoes, fault zones, headless canyons, and organic-rich substrate in Monterey Bay, California. *Geological Society of America Bulletin* 111: 992-1009

Paull CK, Schlining B, Ussler W, Paduan JB, Caress D, Greene HG. 2005. Distribution of chemosynthetic biological communities in Monterey Bay, California. *Geology* 33: 85-88

Rathburn AE, Perez ME, Martin JB, Day SA, Mahn C, et al. 2003. Relationships between the distribution and stable isotopic composition of living benthic foraminifera and cold methane seep biogeochemistry in Monterey Bay, California. *Geochemistry Geophysics Geosystems* 4

Reguera G, Nevin KP, Nicoll JS, Covalla SF, Woodard TL, Lovley DR. 2006. Biofilm and nanowire production leads to increased current in Geobacter sulfurreducens fuel cells. *Applied and Environmental Microbiology* 72: 7345-7348

Reimers CE, Girguis P, Stecher HA, Tender LM, Ryckelynck N. 2006. Microbial fuel cell energy from an ocean cold seep. *Geobiology* 4: 123-136

Reimers CE, Jahnke RA, McCorkle D. 1992. Carbon fluxes and burial rates over the continental slope and rise off central California with implications for the global carbon cycle. *Global Biogeochemical Cycles* 6: 199-224

Reimers CE, Stecher HA, Westall JC, Alleau Y, Howell KA, et al. 2007. Substrate degradation kinetics, microbial diversity and current efficiency of microbial fuel cells supplied with marine plankton. *Applied and Environmental Microbiology* 73: 7029-7040

Reimers CE, Tender LM, Fertig S, Wang W. 2001. Harvesting energy from the marine sediment-water interface. *Environmental Science & Technology* 35: 192-195

Rezaei F, Richard TL, Brennan RA, Logan BE. 2007. Substrate-enhanced microbial fuel cells for improved remote power generation from sediment-based systems. *Environmental Science & Technology* 41: 4053-4058

Rhoads A, Beyenal H, Lewandowski Z. 2005. Microbial fuel cell using anaerobic respiration as an anodic reaction and biomineralized manganese as a cathodic reactant. *Environmental Science & Technology* 39: 4666-4671

Ryckelynck N, Stecher HA, Reimers CE. 2005. Understanding the anodic mechanism of a seafloor fuel cell: Interactions between geochemistry and microbial activity. *Biogeochemistry* 76: 113-139

Schröder U. 2007. Anodic electron transfer mechanisms in microbial fuel cells and their energy efficiency. *Physical Chemistry Chemical Physics* 9: 2619-2629

Schulz HD. 2006. Quantification of Early Diagenesis: Dissolved Constituents in Pore Water and Signals in the Solid Phase. In *Marine Geochemistry*, ed. HD Schulz, M Zabel. Berlin: Springer

Shantaram A, Beyenal H, Raajan R, Veluchamy A, Lewandowski Z. 2005. Wireless sensors powered by microbial fuel cells. *Environmental Science & Technology* 39: 5037-5042

Tender LM, Gray SA, Groveman E, Lowy DA, Kauffman P, et al. 2008. The first demonstration of a microbial fuel cell as a viable power supply: Powering a meterological buoy. *Journal of Power Sources* 179: 571-575

Tender LM, Reimers CE, Stecher HA, Holmes DE, Bond DR, et al. 2002. Harnessing microbially generated power on the seafloor. *Nature Biotechnology* 20: 821-825

Tivey MK, Bradley AM, Joyce TM, Kadko D. 2002. Insights into tide-related variability at seafloor hydrothermal vents from time-series temperature measurements. *Earth and Planetary Science Letters* 202: 693-707

Trauth M. 2006. *MATLAB Recipes for Earth Sciences*: Springer

Wang KL, Davis EE. 1996. Theory for the propagation of tidally induced pore pressure variations in layered subseafloor formations. *Journal of Geophysical Research-Solid Earth* 101: 11483-11495

# 4 Influence of Substrate on Electron Transfer Mechanisms in Chambered Benthic Microbial Fuel Cells

Mark E. Nielsen[1], Diane Wu[2], Clare E. Reimers[1], Peter R. Girguis[3]

[1]College of Oceanic & Atmospheric Sciences, Oregon State University, Corvallis, OR 97331, USA

[2]Cornell University, Ithaca, NY 14853, USA

[3]Harvard University, Biological Labs, 16 Divinity Avenue, Cambridge, MA 02138, USA

Biosensors and Bioelectronics
Elsevier B.V. Radarweg 29, 1043 NX Amsterdam, The Netherlands
In Preparation

## 4.1 Abstract

Different models for electron transfer to the anodes of benthic microbial fuel cells (BMFCs) have been proposed; including oxidation of organic carbon by electroactive bacteria that use the anode as a terminal electron acceptor and a sulfur-mediated process in which sulfate reducing bacteria produce sulfide that is subsequently oxidized at the anode. These two mechanisms have different inherent efficiencies and geochemical consequences. This research investigated whether the addition of an exogenous electron donor could select for one process over the other. Six small-scale BMFCs were operated for over one year in a temperature-controlled laboratory. Three BMFCs relied on endogenous electron donors, and three were supplemented with lactate. The supplemented BMFCs passed more cumulative current, but there did not appear to be a long-term benefit from the lactate injections. Coulombic efficiency of the lactate injections ranged from 25 to 65%. The cumulative flux of electrons resulting from lactate additions could not be explained by sulfide oxidation to sulfur without invoking an additional process such as sulfur disproportionation. Sulfate reduction and sulfur disproportionation were blocked with a specific inhibitor and all BMFCs continued to produce current. Possible alternative mechanisms of current production include an iron mediated process and/or fermentation of complex organic molecules. Chemical data support a two-step cycle in which endogenous organic carbon and/or supplemented lactate fuel dissimilatory iron reduction resulting in ferrous iron and simple organic molecules (such as acetate) that can act as the electron donors for the BMFC.

## 4.2 Introduction

A defining characteristic of microbial fuel cells (MFCs) is the exploitation of electrons liberated by microbial redox processes. This exploitation requires a mechanism for transferring available electrons between microorganisms and the electrodes of an MFC. Due to the fundamental importance of electron transfer processes at the anode this topic has received considerable attention in the MFC literature. Two main classifications for electron transfer are direct electron transfer (DET) and mediated

electron transfer (MET; Schröder, 2007). DET refers to cases where electrons are transferred directly from the microbial cell to the electrode via membrane bound proteins, such as multiheme cytochromes (Bond & Lovley, 2003; Chaudhuri & Lovley, 2003; Lovley, 2006a), or via electrically conductive appendages often called nanowires (Gorby et al., 2006; Reguera et al., 2006). MET refers to cases where electrons are transferred to the electrode via an electrochemically active compound, which could be a metabolite produced by microorganisms (e.g. hydrogen sulfide or reduced iron compounds; Reimers et al., 2001; Tender et al., 2002; Ryckelynck et al., 2005; Rabaey et al., 2006), or an endogenous redox mediator (e.g. phenazines, quinones, and flavins; Hernandez & Newman, 2001; Rabaey et al., 2005; Stams et al., 2006; Pham et al., 2008).

The mechanism that mediates electron transfer at the anode in benthic microbial fuel cells (BMFCs), has been proposed to influence the performance of the BMFC due to differing efficiencies and geochemical consequences (Ryckelynck et al., 2005; Reimers et al., 2007). For example, a DET process coupled to lactate oxidation by an organism (or group of organisms) using an anode as the terminal electron acceptor can be written simply as:

(4.1) $$C_3H_5O_3^{-} + 3H_2O \xrightarrow{\text{microbe(s)}} 3CO_2 + 11H^+ + 12e^-$$

In reaction (4.1), up to 12 $e^-$ may be transferred to the circuit for every molecule of substrate oxidized, and the production of protons would likely result in a decrease in pH near the anode. An alternative mechanism is a sulfur MET process at the anode of a BMFC (particularly for those immersed in a seawater medium). It can be described by two simplified reactions:

(4.2) $$2C_3H_5O_3^{-} + 3SO_4^{2-} \xrightarrow{\text{microbe(s)}} 6HCO_3^{-} + H^+ + 3HS^-$$

(4.3) $$3HS^- \rightarrow 3S^0 + 3H^+ + 6e^-$$

In equations (4.2) and (4.3) only three electrons are passed to the circuit through sulfide oxidation for every molecule of substrate oxidized. In some cases microbes capable of sulfur disproportionation have been isolated from BMFC anodes (Holmes et al., 2004b). This process could yield an additional six electrons to the circuit and help to buffer the pH, but the extent to which it occurs is unknown.

One objective of this investigation was to determine if we could promote one anode process over another with a goal of optimizing these systems in the natural environment. A key difference between BMFCs and many laboratory MFCs is that in BMFCs, the microbiological community develops spontaneously from the environmental medium (Holmes et al., 2004b) while laboratory MFCs often contain pure cultures or are inoculated with mixed cultures.

This paper describes the performance and efficiency of six laboratory-scale BMFCs operated for over one year, of which three were supplemented with an exogenous electron donor and three relied on endogenous electron donors. The electron donor additions resulted in short-term gains in current production, but benefits did not appear to last beyond the program of injections. Experiments to block sulfate reduction in the anode chambers yielded surprising results that raise questions about the role of sulfate reduction as the underlying process supporting current production from microbial fuel cells drawing energy from marine sediments.

## 4.3 Materials and methods

### *4.3.1 BMFC design and operation*

Six identical BMFCs were constructed based on a design developed in the course of field experiments (Nielsen et al., 2007; Nielsen et al., 2008). Sandy sediment was collected from the intertidal zone in Yaquina Bay, OR, and homogenized by mixing in a 5-gallon bucket and turning it with a shovel. Each BMFC was set up in a bucket with 4 L of homogenized sediment. An acrylic core tube (70 $cm^2$ cross-sectional area) pushed approximately 10 cm into the sediment served as the anode chamber (Figure 4.1). The top of the core tube extended approximately 4 cm above the sediment and

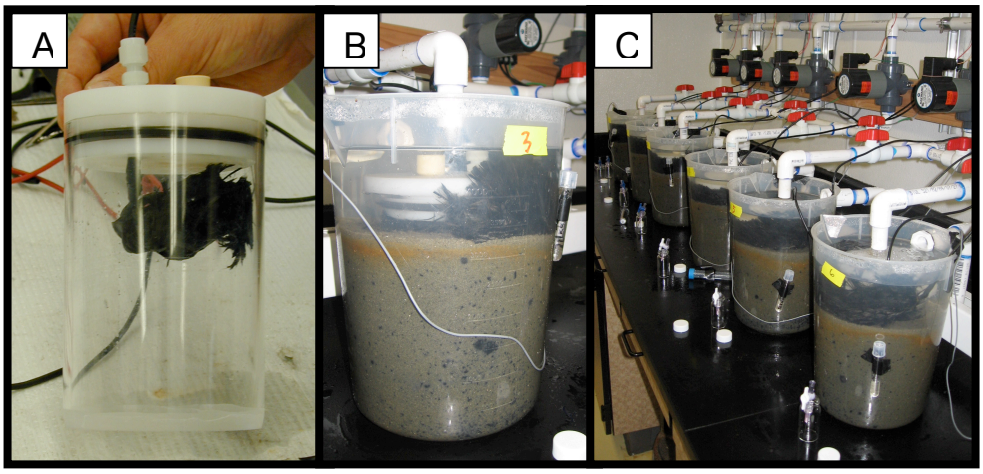


**Figure 4.1** Photographs of laboratory BMFC construction. A. Core tube and anode prior to insertion into sediment. B. Complete BMFC showing sediment, cathode in overlying water and anode chamber. C. Six BMFCs in climate controlled laboratory with seawater circulation system. Black spots in the sediment are pockets of organic material and a layer of iron oxide in each container indicates the iron reduction zone.

was capped with an o-ring sealed lid resulting in a chamber volume above the sediment of approximately 150 mL. The BMFCs were kept in a refrigerated laboratory at approximately 10°C equipped with a seawater circulation system that refreshed the overlying water approximately every 5 minutes. Carbon-fiber brush anodes (Hasvold et al., 1997) were positioned inside each chamber with a wire passing through a bulkhead fitting in the lid. Each anode was approximately 10-cm long with an estimated surface area of 2.6 $m^2$; however, it was not possible to evenly distribute the anode surface area within the chambers (which also explains some performance variability between replicates). Cathodes consisted of 20-cm lengths of the carbon-fiber electrode (5.2 $m^2$) positioned in the seawater overlying the sediment in each container. Each BMFC setup had a Ag/AgCl (3M KCl) reference electrode (Microelectrodes, Inc., Bedford, NH) positioned in the overlying seawater. Whole-cell potential ($E_{cell}$), anode potential ($E_{anode}$ vs. *Ag/AgCl*) and current ($I$) were monitored and logged every 10 minutes with a multi-channel datalogger (Agilent Technologies, Santa Clara, CA). Cathode potential ($E_{cath}$) was calculated according to $E_{cath} = E_{cell} + E_{anode}$. All BMFCs were operated at a constant $E_{cell}$ of 0.4 V that was controlled by a custom designed potentiostat (NW Metasystems, Bainbridge Island, WA). The potentiostat effectively operates like a variable external resistor that automatically adjusts the amount of current passed in order to maintain a pre-defined $E_{cell}$. If $E_{cell}$ falls below the setpoint, then the potentiostat opens the circuit to allow the redox gradient to recover.

Each BMFC chamber had a septum allowing sample collection or addition of supplemental electron donors and various chemicals according to the experimental plan. BMFCs 1, 3 and 5 did not receive supplements at any time during the course of the experiment. BMFCs 2, 4 and 6 received supplements approximately every two weeks during the experiment. Supplements were made with a 1- or 5-mL syringe and consisted of sodium lactate diluted with filtered and autoclaved $N_2$-sparged seawater. We selected lactate as an electron donor because it is a known substrate for some dissimilatory metal reducing bacteria (Lovley & Phillips, 1988) and sulfate reducing

bacteria (SRB; Kondo et al., 1993; Finke et al., 2007; Liamleam & Annachhatre, 2007). Typical injections consisted of 1 mL of 35 mM lactate giving a final concentration of approximately 0.23 mM in the anode chamber. During days 240 - 320 we varied the concentration of lactate injected into BMFC 4 to give a concentration range inside the chamber of 0.12 to 3.8 mM. During days 414 - 482 we conducted a series of 6 injections on BMFCs 3-6 that contained molybdate, a specific inhibitor of sulfate reduction (Oremland & Taylor, 1978) and sulfur disproportionation (Finster et al., 1998). Each BMFC received a 5 mL injection containing 1.6 M $Na_2MoO_4 \bullet 2H_2O$ giving a final concentration of approximately 50 mM inside the anode chambers. Molybdate alone was added to BMFCs 3 and 5, while lactate (to a final concentration of 0.23 mM) was co-injected with the molybdate in BMFCs 4 and 6. In addition to 6 molybdate injections, we also conducted two injections without molybdate to investigate the stirring effect of the injections themselves. On day 441 each cell was injected with 5 mL of $N_2$-sparged seawater and on day 470 we injected BMFCs 3 and 5 with $N_2$-sparged seawater and BMFCs 4 and 6 with $N_2$-sparged seawater + lactate to a final concentration of 0.23 mM.

### *4.3.2 Sampling*

Fluid samples were collected from each anode chamber with a syringe and a No. 18 needle inserted through a septum. Approximately 10 mL were collected and subsequently partitioned for sulfide, sulfate, dissolved organic carbon (DOC), total alkalinity, pH, iron, and molybdenum analyses. Sulfide samples were preserved with 20 μL 0.227 M zinc acetate and analyzed spectrophotometrically according to a method adapted from Cline (1969). Sulfate was determined with a turbidity method (Tabatabai, 1974). DOC samples were filtered (GF/F, Whatman, International, Maidstone, England) and preserved to pH<2 with $H_3PO_4$ and analyzed on a TOC-$V_{CSH}$ analyzer (Shimadzu Scientific Instruments, Columbia, MD). Alkalinity was determined through a Gran titration (Gieskes & Rogers, 1973), and pH was measured with a combination glass electrode (Denver Instruments, Denver, CO) calibrated with NBS buffers. Iron and molybdenum samples were preserved with HCl or $H_3PO_4$ to

pH < 2 and analyzed with an inductively coupled plasma-optical emission spectrometer (Prodigy ICP, Teledyne Leeman Labs, Hudson, NH). Metal samples collected on day 393 were filtered with the same apparatus as the DOC samples, and metal samples collected on day 460 were unfiltered.

Samples for microbial community analysis were collected from the anodes of BMFCs 1 and 2 by transferring the entire BMFC to a $N_2$ flushed glove bag, opening the anode chamber lid and clipping approximately 1 g of fibers with flame sterilized shears. Samples were placed in WhirlPak bags and flash frozen by immersing them in liquid $N_2$ and then stored at -50 ºC for later analysis. Clone libraries were constructed as described in Chapter 3 (Nielsen et al., 2008). Briefly, nucleic acids were extracted with the PowerSoil DNA extraction kit (MoBio Inc., San Diego, CA), modified to maximize yields. Small-subunit (SSU) rRNA bacterial genes from all samples were amplified by PCR with a bacterial targeted forward primer (B27f, 59-AGAGTTTGATCCTGGCTCAG-39) and a universal reverse primer (U1492r, 59-GGTTACCTTGTTACGACTT-39). Environmental rRNA clone libraries were constructed by cloning amplicons into a pCR4 TOPO vector and transforming into chemically competent Escherichia coli according to the manufacturer's protocol (TOPO TA cloning kit; Invitrogen Inc.).

## 4.4 Results and discussion

All BMFCs produced current for more than one year (Figure 4.2). Table 4.1 summarizes performance in terms of cumulative electrons passed by the circuit, integrated power and power density. It is notable that an average of 31± 4 mWhr of power was produced during the course of the experiment from sand with only endogenous electron donors. Apparently, there were enough electron donors in the sand to sustain current while maintaining a voltage difference between the anode and cathode of at least 0.4 V.

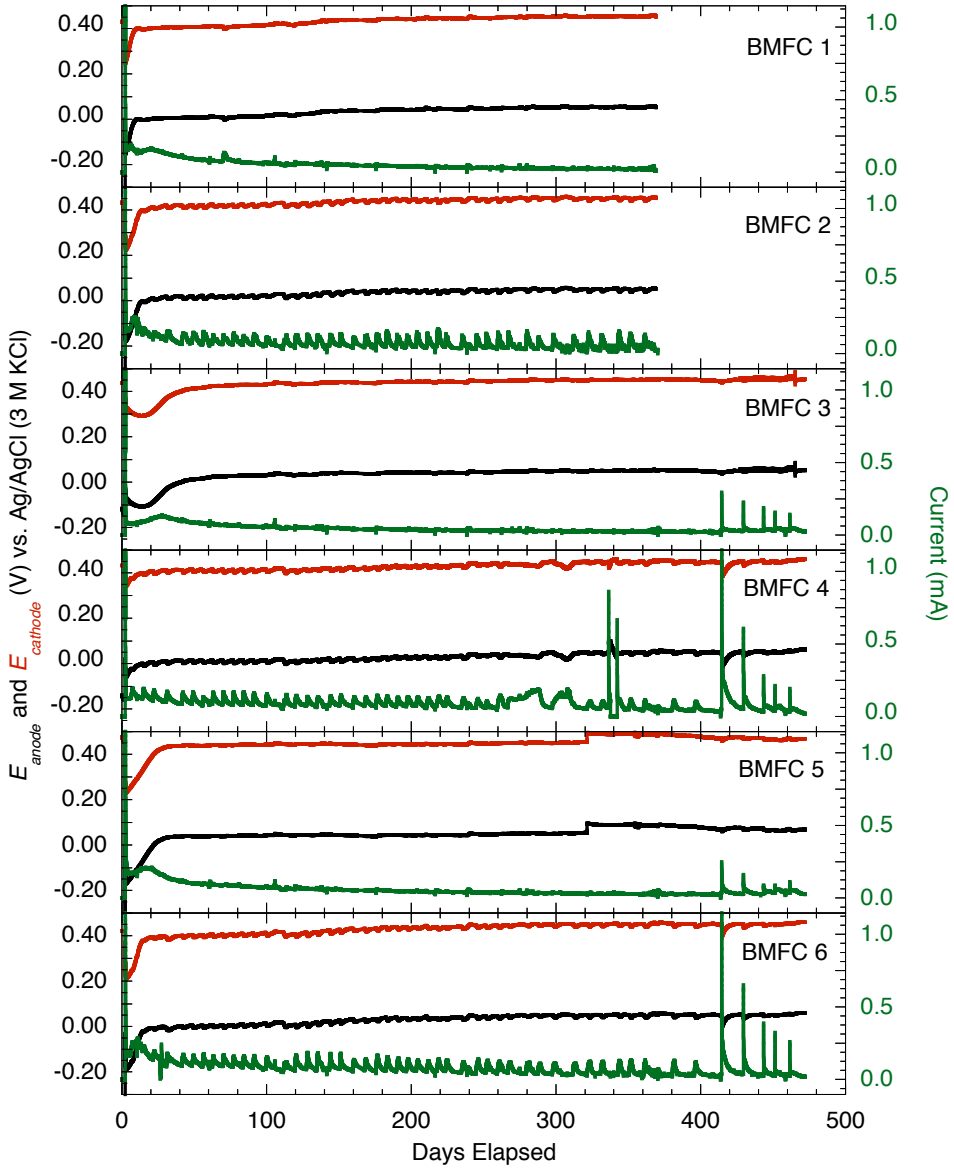


Figure 4.2 Electrode potential (left axis) and current (right axis) records for all BMFCs. $E_{anode}$ is shown in black, $E_{cathode}$ in red and current in green. Days indicate time since the circuits were closed and does not include the approximately 25 days required for the BMFCs to reach open circuit conditions. Current spikes correspond to injections - before day 400 lactate was injected and after day 400 lactate and molybdate were co-injected in BMFCs 4 and 6 and molybdate only was injected into BMFCs 3 and 5.

**Table 4.1. Summary of power production from laboratory scale BMFCs**

| BMFC | Total lactate added (mmoles) | No. of days operated | Cumulative electrons passed (mmol $e^-$) | Cumulative current efficiency* % | Integrated power (Whr) | Integrated power density** (Whr $m^{-2}$) |
|---|---|---|---|---|---|---|
| 1 | 0 | 372 | 18.4 | | 0.20 | 28 |
| 2 | 1.4 | 372 | 25.9 | 45 | 0.28 | 40 |
| 3 | 0 | 482 | 18.3 | | 0.20 | 28 |
| 4 | 2.3 | 482 | 36.9 | 58 | 0.40 | 57 |
| 5 | 0 | 482 | 24.0 | | 0.25 | 35 |
| 6 | 1.6 | 482 | 33.4 | 65 | 0.35 | 50 |

Notes: * cumulative current efficiency calculated relative to the lactate supply as described in section 4.4.1.
** Integrated power density based on cross-sectional area of chamber.

### *4.4.1 Effects of lactate addition*

Supplementation with lactate resulted in short-term peaks in current but did not apparently yield a long-term benefit. After the added lactate was consumed, current declined to levels similar to those in the unsupplemented cells. The cumulative amount of charge passed by supplemented BMFCs relative to unsupplemented BMFCs was consistent with the amount of lactate added, but not a clear indicator of the electron transfer process to the anode. For example, BMFC 6 received forty six 1-mL injections of 35 mM lactate solution totaling 1.6 mmol of added lactate. If the anode community were capable of direct lactate oxidation with 100% efficiency according to eq. (4.1), we would expect that BMFC 6 would pass approximately 19 mmol of electrons in excess of the amount passed due to background current. The average electron flux due to background current from BMFCs 3 and 5 (the two unsupplemented cells with the same period of operation) was about 21 mmol. Therefore, we would predict that BMFC 6 would pass about 40 mmol of electrons if all the lactate was oxidized to $CO_2$. The measured flux was 33.4 mmol implying 65% coulombic efficiency for the added lactate ((33.4-21)/19*100). Alternatively, if lactate stimulated SRB leading to an anode process consistent with eq. (4.3), then we would expect an excess of 5 mmol over the cumulative electron flux due to background current. The excess was more than double that amount. Thus, if we want to invoke eq. (4.3) it must have also been accompanied by another process such as sulfur

disproportionation to account for the excess cumulative electron flux. We will return to these considerations when examining further results.

### *4.4.2 Coulombic efficiency in cells with lactate supplements*

Section 4.4.1 describes lactate utilization averaged over the course of the entire experiment. We also calculated the efficiency of lactate conversion to current for individual injections. Figure 4.3 illustrates the calculation for one such injection for BMFC 4. The area under the current vs. time curve was used to determine the total amount of charge passed during one injection cycle ($q_{total}$). The baseline charge ($q_{base}$) was the area of a rectangle defined by the baseline current picked from the plot × the time between injections. The amount of charge resulting from the injection ($q_{peak}$) was the difference between $q_{total}$ and $q_{base}$. We performed this calculation for 5 peaks from the early (day 40 – 75), middle (day 110 – 150) and late (day 195 – 230) periods (15 peaks total) from BMFC 4. By this method, the average coulombic efficiency of the lactate injections was 34 ± 4%. There was no difference between the different periods examined indicating that there was not an evolution of microbial community in the anode chamber that had a significant effect on its ability to oxidize lactate. The apparent discrepancy between this method of determining coulombic efficiency and the method based on cumulative electron flux was probably caused by the frequency of lactate injections. If the instantaneous current was not at baseline level prior to an injection, then the contribution of baseline current would be overestimated and the contribution from the lactate injection would be underestimated.

### *4.4.3 Effect of varying concentrations of lactate*

During days 240 – 320 the concentration of lactate in BMFC 4 supplements was varied. As shown in Figure 4.4, the coulombic efficiency decreased with increasing lactate concentration. The coulombic efficiency (calculated as described in section 4.4.2) ranged from 25% with a lactate concentration of 3.8 mM to 58% with a lactate concentration of 0.12 mM. The inverse relationship between efficiency and lactate concentration suggests 1) lactate supplements promoted biomass growth or

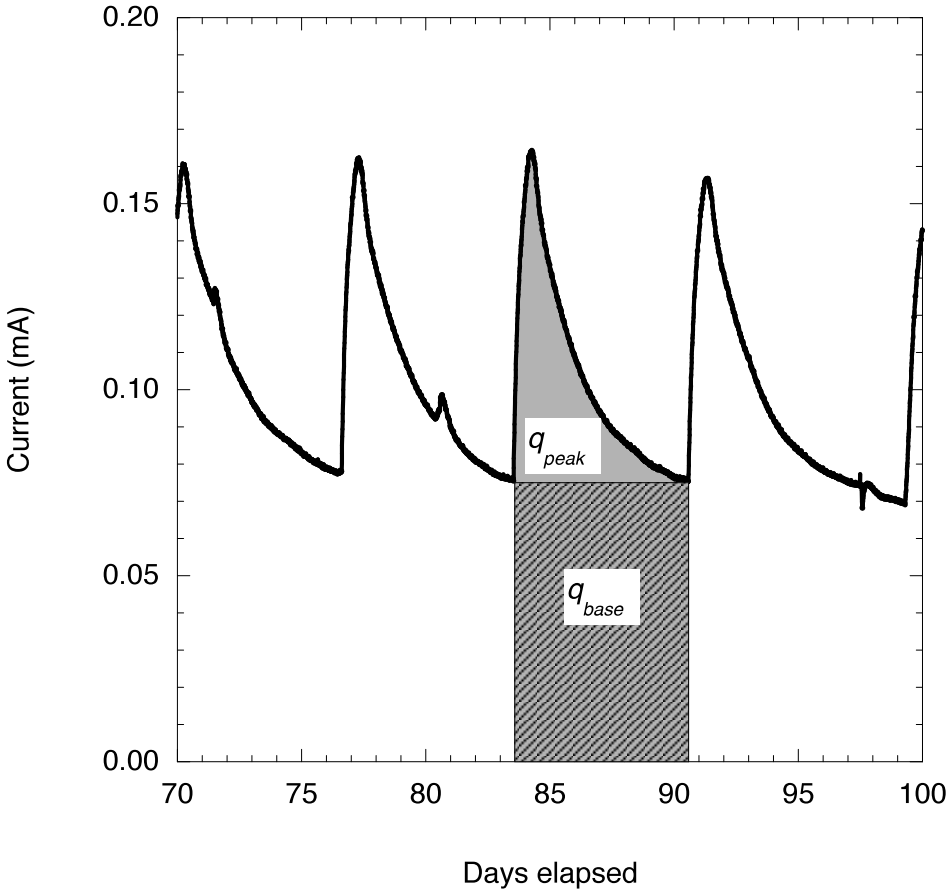


**Figure 4.3** Illustration of coulombic efficiency calculations. Area under curve was integrated to give $q_{peak}$. $q_{base}$ was subtracted from $q_{peak}$ to determine the amount of charge passed due to the lactate injection. This charge was divided by the number of electrons added as lactate to give efficiency.

metabolism that did not necessarily contribute to current generation and 2) at high lactate concentrations, current was limited by some factor other than the concentration of the electron donor. Figure 4.4 also shows $q_{peak}$ (c.f. Figure 4.3) as a function of lactate concentration and the $q_{peak}$ that would be expected based on the reactions shown in equations 4.1-4.3. At the higher concentrations of lactate, the observed electron flux was consistent with sulfate reduction to sulfide and subsequent oxidation of sulfide to elemental sulfur.

### *4.4.4 Current density*

The maximum current density in these laboratory BMFCs was 0.07 mA $m^{-2}$ anode surface area or 27 mA $m^{-2}$ seafloor. These values are at least an order of magnitude less than our previous experiments that used the same electrode materials and similar BMFC design. In Yaquina Bay we achieved current densities of 0.45 to 0.73 mA $m^{-2}$ anode (580 to 950 mA $m^{-2}$ seafloor) and in Monterey Canyon we achieved 1.8 mA $m^{-2}$ anode (350 mA $m^{-2}$ seafloor) (Nielsen et al., 2007). The reason for the low current density in these laboratory BMFCs under the conditions of the lactate additions may be found in the chemical data.

### *4.4.5 Chemical consequences of BMFC operation*

A difference between the earlier field studies and this laboratory study is that fluid advection (either mechanically induced or naturally forced) delivered electron donors to BMFCs in the field. The results of this study suggest that in the absence of advection, products of electrode reactions progressively change the chemical environment surrounding the anode, and this change may affect the long-term performance of BMFCs.

Figure 4.5 summarizes the results of the chemical analyses of anode fluid samples taken from the anode chambers near the beginning and end of the experiment. Samples were collected when BMFCs were as close to baseline condition as possible, usually at least one week after the most recent lactate injection. During the early

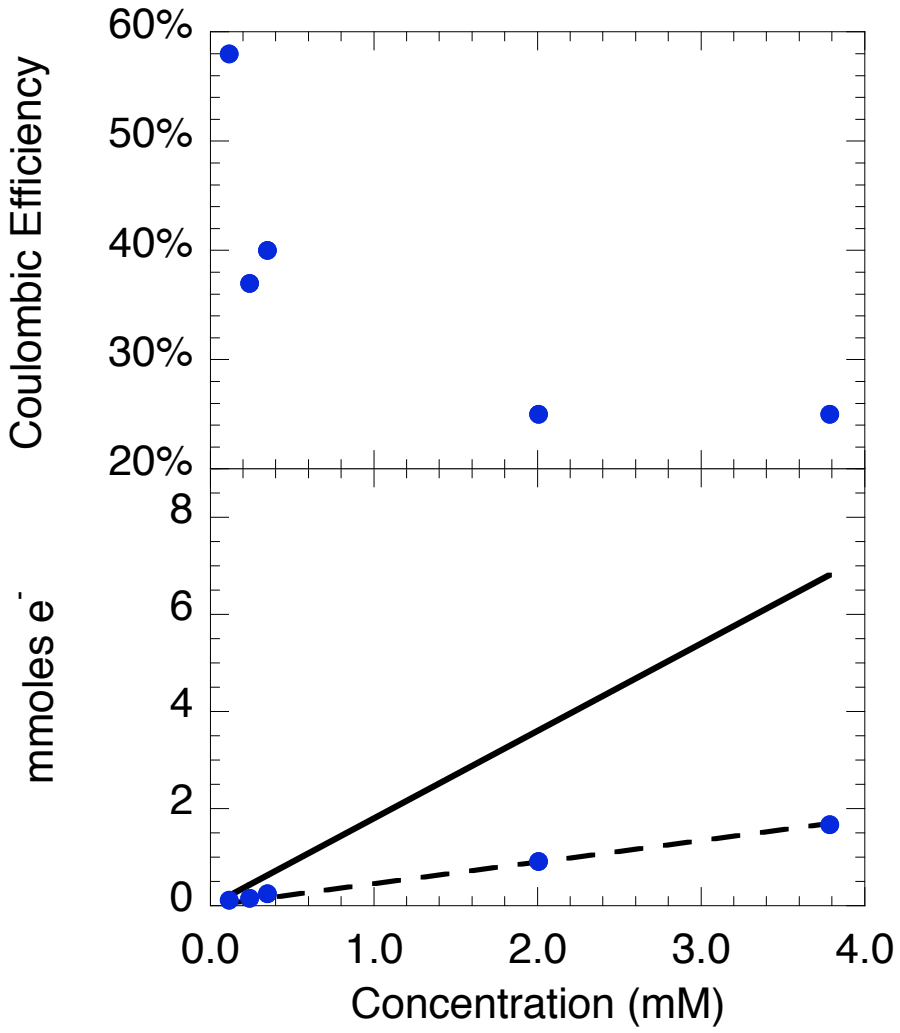


Figure 4.4 Coulombic efficiency and cumulative electron flux as a function of lactate concentration in the anode chamber of BMFC 4. Efficiency (upper panel) decreased with increasing concentration suggesting lactate fueled alternative processes that did not contribute to current production. Lower panel shows cumulative amount of electrons passed as a result of lactate injections. Symbols indicate the observed flux of electrons, the solid line represents the expected flux according to equation 4.1, and the dashed line represents the expected flux according to equations 4.2 and 4.3.

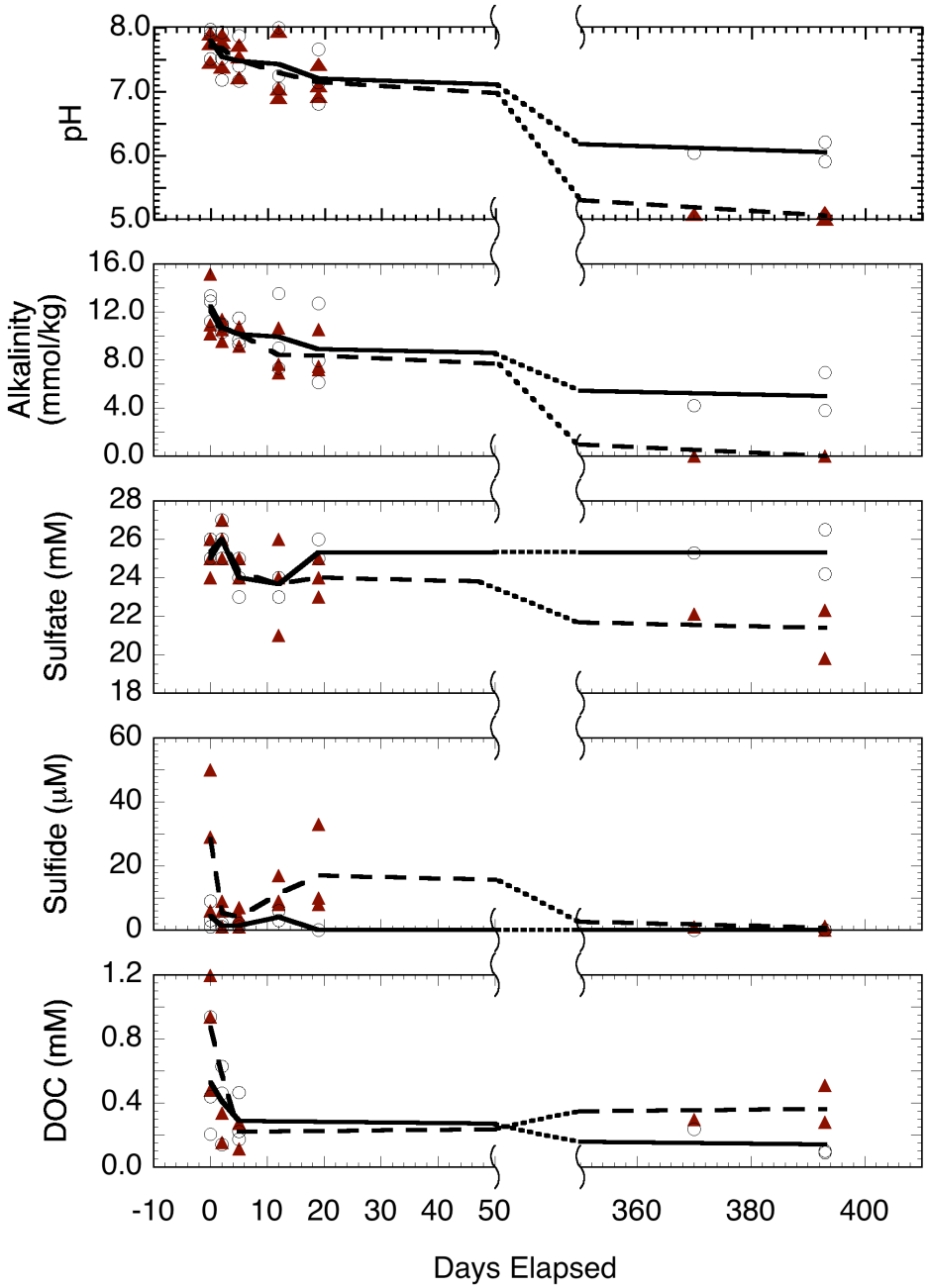


Figure 4.5 Summary of fluid chemistry from unsupplemented (open circles) and supplemented (filled triangles) BMFCs. Solid lines indicate the average for all unsupplemented results and dashed indicate the average for all supplemented results.

phase of the experiment, there is no apparent difference in fluid (anolyte) composition between the supplemented and unsupplemented BMFCs (except for detectable sulfide in the supplemented cells day 10-20). Samples collected toward the conclusion of the experiment did indicate differences. Supplemented BMFCs generally had lower pH, alkalinity and sulfate. All the BMFCs had less than 2 μM dissolved sulfide and the supplemented BMFCs had slightly higher DOC concentrations. The DOC concentrations do not show an increase resulting from repeated lactate injections suggesting that some process consumed the lactate. As shown in Table 4.2, the concentration of iron in the anode chambers was extremely enriched relative to seawater values. The enrichment of iron in the supplemented cells relative to the unsupplemented cells suggests that the added lactate promoted iron cycling. The supplemental lactate could have stimulated dissimilatory reduction (Lovley, 1991) of hydrous ferric oxide by a reaction such as:

(4.4) $C_3H_5O_3^- + 4Fe(OH)_3 + 7H^+ \rightarrow C_2H_3O_2^- + 4Fe^{2+} + 10H_2O + HCO_3^-$

The resulting ferrous iron could be an electron donor for the BMFC as shown by Ohmura, et al. (2002).

(4.5) $4Fe^{2+} \rightarrow 4Fe^{3+} + 4e^-$

The reactions proposed in equations (4.4) and (4.5) are analogous to the two-step MET process involving sulfur and would result in 4 out of 12 electrons being available to the circuit. The acetate produced by lactate oxidation in equation (4.4) could be a substrate for DET by anode-attached microorganisms or for reduction of the ferric iron produced by reaction (4.5). We favor the former explanation since it also could explain the low pH, alkalinity, and current efficiency of the supplemented cells.

**Table 4.2. Summary of iron and molybdenum analyses.**

| | | Fe (µM) | | |
|---|---|---|---|---|
| BMFC | pH** | Before $MoO_4^{2-}$ additions | After $MoO_4^{2-}$ additions | Mo (mM) |
| 3 | 6.2 | 38 | 9 | 30 |
| 4* | 5.1 | 3807 | 118 | 35 |
| 5 | 5.9 | 211 | 22 | 35 |
| 6* | 5.0 | 3682 | 51 | 44 |

Notes: *BMFCs 4 and 6 received lactate supplements
**pH data are from the same date as initial Fe samples
"Before" samples were filtered, "After" samples were unfiltered

In other recent MFC studies, pH was manipulated and current production decreased in treatments outside of circumneutral pH (Gil et al., 2003; Biffinger et al., 2008). Conversely, in this experiment the BMFCs that passed the most cumulative current had the lowest pH at the end. The low pH is not surprising given that the production of protons results from oxidation of electron donors at the anode surface. However, the accumulation of protons in excess of the buffering capacity of the anolyte (or sediments underlying the chamber) could have at least two detrimental effects. According to Finster et al. (1998) the growth range for a sulfur disproportionating organism (*Desulfocapsa* sp.) is pH 6.0 – 8.2. At the low pH that occurs in these BMFCs, sulfur disproportionation might be inhibited which would limit current and potentially result in a build-up of elemental sulfur on the anodes resulting in passivation of the surface. Furthermore, Biffinger et al. (2008) showed that low pH inhibits *Shewanella* sp. from excreting riboflavin which could serve as a redox mediator resulting in lower current production. The low pH in these BMFCs could have a similar inhibitory effect.

The low alkalinity observed in these BMFCs is inconsistent with sulfate reduction followed by sulfide oxidation at the anode being fully responsible for current. Even in the presence of an anode as an electron sink, we would expect a net increase in

alkalinity as a result of sulfate reduction according to equations 4.2 and 4.3. However, the low pH and alkalinity could be explained by an iron cycle in which lactate is oxidized to acetate which is then oxidized to $CO_2$ by anode-attached microorganisms (i.e., in a DET process similar to equation (4.1) except with acetate substituted for lactate).

### *4.4.6 Phylogenetic analyses of anode communities*

Table 4.3 summarizes the 16s rRNA clone libraries that were constructed from samples of the anodes from BMFCs 1 and 2. Phylogenetic identification does not indicate function but, when considered with electrochemical data and other studies from the literature, it does suggest possible processes. The communities from the two anodes were similar, but BMFC 1 (which was not supplemented) showed slightly more diversity. Deltaproteobacteria was the dominant class in both samples representing 37% and 66% of the phylotypes found in BMFC 1 and 2, respectively. In BMFC 1 the deltaproteobacteria were dominated by species within the desulfuromonales order and in BMFC 2 the desulfobacterales were the dominant order. Organisms within desulfuromonales are known to oxidize organic acids using Fe(III) or an electrode as the terminal electron acceptor (Holmes et al., 2004a; Holmes et al., 2004b). In contrast, some organisms within desulfobacterales are known for their ability to disproportionate sulfur (Bak & Cypionka, 1987; Finster et al., 1998). The phylogenetic communities from the respective BMFCs suggest that the supplemented BMFCs were more reliant on a sulfur cycle (eq. 4.2 – 4.3) than the unsupplemented BMFCs. We speculate that the unsupplemented BMFCs relied on a cycle in which complex organic material was broken down by various hydrolytic enzymes and fermentation processes and with the resulting products serving as substrates for bacteria capable of transferring electrons to an anode (Lovley, 2006b). To further investigate the role of sulfur in the unsupplemented BMFCs we conducted a series of molybdate injections to confirm whether sulfate reduction was contributing to current.

**Table 4.3. Summary of 16s rRNA clone libraries from BMFCs 1 and 2.**

| Phylum | Order | Proportion of Phylotypes found BMFC 1 | BMFC 2 |
|---|---|---|---|
| Alphaproteobacteria | | 8% | |
| Deltaproteobacteria | | | |
| | Desulfuromonales | 25% | 22% |
| | Desulfobacterales | 8% | 44% |
| | Desulfovibrionales | 2% | |
| | Syntrophobacterales | 2% | |
| Epsilonproteobacteria | | 5% | 2% |
| Gammaproteobacteria | | 11% | 4% |
| Flavobacteria | | 23% | 16% |
| Bacterioidetes | | 2% | 2% |
| Sphingobacteria | | 7% | 4% |
| Other | | 8% | 6% |

### *4.4.7 Effects of molybdate on BMFC current*

Figure 4.6 shows the current responses of the four BMFCs that received molybdate injections. All BMFCs showed an initial spike in current production followed by a secondary peak above baseline in response to repeated molybdate injections. Molybdate interrupts the synthesis of ATP in SRB thus leading to cell death, so we expected current to decline if sulfate reduction and subsequent oxidation of sulfide was the main process contributing to baseline current production. The main implication of the observed results is that some process other than sulfate reduction is responsible for maintaining the baseline current in these BMFCs. This implication is consistent with the observation of dissimilatory metal reducers and other bacterial groups capable of breaking down complex organic matter (e.g. flavobacteria) in the samples collected from the BMFC 1 anode.

BMFCs 4 and 6, which received regular lactate supplements, showed larger current spikes than BMFCs 3 and 5 which had not received any supplements. We hypothesize that there was a lactate-promoted community of SRB in BMFCs 4 and 6 that were killed during the first two molybdate injections and the biomass of the SRB fueled

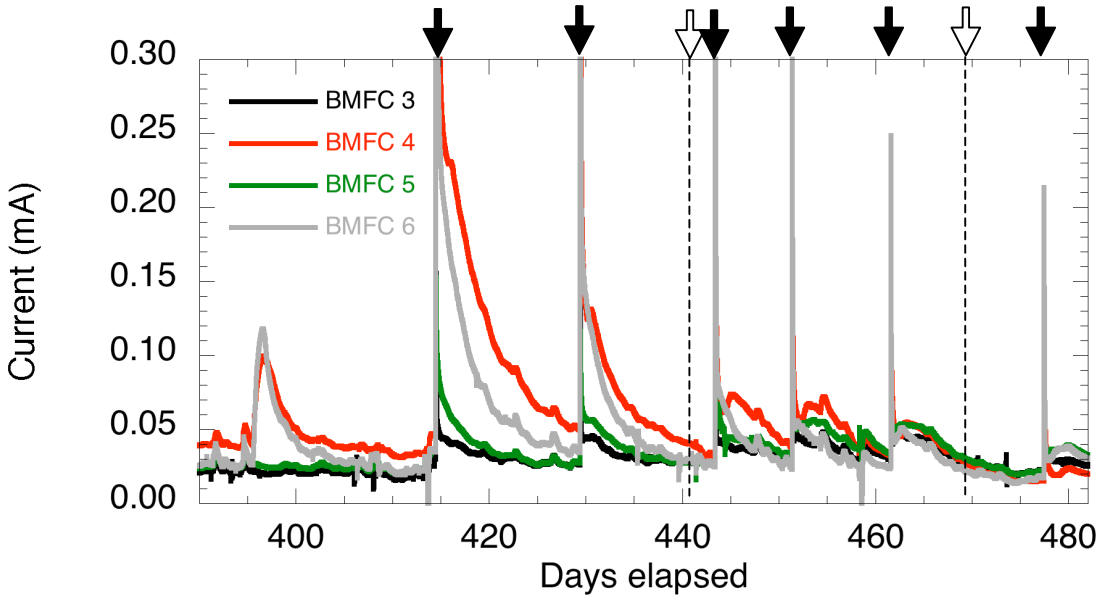


Figure 4.6 Current versus time for all BMFCs during the course of molybdate injections (days 414 – 470). BMFCs 3 and 5 were injected with molybdate only and BMFCs 4 and 6 were injected with molybdate and lactate. Peaks from days 394 – 404 in BMFCs 4 and 6 were typical lactate injections and are shown for comparison. Brief periods of zero current production (day 413 and 459) were caused by changing the cathode water in the circulation system and were not related to molybdate injections. Open arrows indicate blank injections of sparged SW without molybdate.

whatever geochemical cycle was the underlying current generating process. Subsequent molybdate + lactate injections to BMFCs 4 and 6 yielded progressively smaller current peaks until the peaks were nearly identical to the unsupplemented cells. On day 470, BMFCs 4 and 6 were injected with lactate only and there was no apparent response. The lack of response to lactate indicates that the earlier molybdate injections succeeded in killing off organisms that could use lactate (likely SRB) and the underlying process that supported current generation did not show a response to lactate. The microbiological sample from a supplemented BMFC (BMFC 2) was collected before any molybdate injections and indicated the presence of sulfur metabolizing bacteria within the deltaproteobacteria. The molybdate injections probably inhibited such bacteria leaving other members of the deltaproteobacteria that do not rely on a sulfur metabolism.

We can only speculate why molybdate injections caused immediate current spikes in both the supplemented and unsupplemented BMFCs. Molybdenum within the molybdate anion is fully oxidized as Mo(VI) and therefore could not be oxidized further at the anode surface. We can also rule out stirring effects because we observed no peaks when injections were made without molybdate on days 441 and 470. Potential explanations include: 1) the addition of molybdate disrupts the electric double layer at the anode surface resulting in a temporary non-faradaic current spike, and 2) the molybdate ion substitutes for an electrochemically active ion in a compound adsorbed to the anode surface (e.g. it liberates reduced sulfur from FeS or $FeS_2$). Targeted experiments will be required to assess these possibilities.

### 4.5 Conclusion

These experiments were motivated by the question: can we select for a particular electron transfer process at the anode of BMFCs by supplementing the cells with an exogenous electron donor? Apparently, the answer is yes because the supplemented BMFCs responded to additional electron donor and had a larger proportion of phylotypes that metabolize sulfur species (either sulfate reduction and/or sulfur

disproportionation). It is also likely that lactate additions stimulated sulfate reduction away from the anode surface resulting in a microbial community that was not necessarily represented by anode samples. After injections of supplemental electron donor, currents returned to baseline levels, particularly towards the end of the experiment.

Previous BMFC experiments have invoked a sulfur mediated system in which sulfate reducing bacteria generate sulfide that is subsequently oxidized at the anode surface to produce current. Results of molybdate injections showed that the BMFCs were able to continue to produce current even when sulfate reduction was inhibited. There was also an enrichment of iron in the anode chambers suggesting that the anode process could be mediated by an iron cycle analogous to the one proposed for sulfur. Fluid in the anode chambers of all the BMFCs had relatively low pH and alkalinity, which is contrary to expectations if the system were mediated solely by sulfur transformations. Coulombic efficiency was greater than can be explained by sulfate reduction and subsequent sulfide oxidation. Sulfur disproportionation could account for additional current, but pH in the cells were outside of the known range for sulfur disproportionators.

These experiments demonstrated that current could be generated from sandy sediments for over a year without added electron donors. The process responsible for current generation is mainly one that does not rely on cycling sulfur. This observation could be specific to the sandy sediments used in these experiments and may not apply to muddy environments where other BMFCs have been deployed. However, understanding the mechanisms in sandy environments will be important as this technology is further developed since a large proportion of continental margin sediments are sand rather than mud.

### 4.6 References:

Bak F, Cypionka H. 1987. A novel type of energy-metabolism involving fermentation of inorganic sulfur-compounds. *Nature* 326: 891-892

Biffinger JC, Pietron J, Bretschger O, Nadeau LJ, Johnson GR, et al. 2008. The influence of acidity on microbial fuel cells containing *Shewanella oneidensis*. *Biosensors and Bioelectronics* 24: 906-911

Bond DR, Lovley DR. 2003. Electricity production by Geobacter sulfurreducens attached to electrodes. *Applied and Environmental Microbiology* 69: 1548-1555

Chaudhuri SK, Lovley DR. 2003. Electricity generation by direct oxidation of glucose in mediatorless microbial fuel cells. *Nature Biotechnology* 21: 1229-1232

Cline JD. 1969. Spectrophotometric determination of hydrogen sulfide in natural waters. *Limnology and Oceanography* 14: 454-458

Finke N, Vandieken V, Jørgensen BB. 2007. Acetate, lactate, propionate, and isobutyrate as electron donors for iron and sulfate reduction in Arctic marine sediments, Svalbard. *Fems Microbiology Ecology* 59: 10-22

Finster K, Liesack W, Thamdrup B. 1998. Elemental sulfur and thiosulfate disproportionation by *Desulfocapsa sulfoexigens* sp. nov., a new anaerobic bacterium isolated from marine surface sediment. *Applied and Environmental Microbiology* 64: 119-125

Gieskes J, Rogers W. 1973. Alkalinity determination in interstitial waters of marine sediments. *Journal of Sedimentary Petrology* 43: 272-277

Gil GC, Chang IS, Kim BH, Kim M, Jang JK, et al. 2003. Operational parameters affecting the performance of a mediator-less microbial fuel cell. *Biosensors & Bioelectronics* 18: 327-334

Gorby YA, Yanina S, McLean JS, Rosso KM, Moyles D, et al. 2006. Electrically conductive bacterial nanowires produced by Shewanella oneidensis strain MR-1 and other microorganisms. *Proceedings of the National Academy of Sciences of the United States of America* 103: 11358-11363

Hasvold O, Henriksen H, Melvaer E, Citi G, Johansen BO, et al. 1997. Sea-water battery for subsea control systems. *Journal of Power Sources* 65: 253-261

Hernandez ME, Newman DK. 2001. Extracellular electron transfer. *Cellular and Molecular Life Sciences* 58: 1562-1571

Holmes DE, Bond DR, Lovley DR. 2004a. Electron transfer by Desulfobulbus propionicus to Fe(III) and graphite electrodes. *Applied and Environmental Microbiology* 70: 1234-1237

Holmes DE, Bond DR, O'Neill RA, Reimers CE, Tender LR, Lovley DR. 2004b. Microbial communities associated with electrodes harvesting electricity from a variety of aquatic sediments. *Microbial Ecology* 48: 178-190

Kondo R, Nishijima T, Hata Y. 1993. Mineralization process of glucose and low-molecular fatty-acid production in an anoxic marine sediment slurry. *Nippon Suisan Gakkaishi* 59: 105-109

Liamleam W, Annachhatre AP. 2007. Electron donors for biological sulfate reduction. *Biotechnology Advances* 25: 452-463

Lovley DR. 1991. Dissimilatory Fe(III) and Mn(IV) reduction. *Microbiological Reviews* 55: 259-287

Lovley DR. 2006a. Bug juice: harvesting electricity with microorganisms. *Nature Reviews Microbiology* 4: 497-508

Lovley DR. 2006b. Microbial fuel cells: novel microbial physiologies and engineering approaches. *Current Opinion in Biotechnology* 17: 327-332

Lovley DR, Phillips EJP. 1988. Novel mode of microbial energy metabolism - organic-carbon oxidation coupled to dissimilatory reduction of iron or manganese. *Applied and Environmental Microbiology* 54: 1472-1480

Nielsen ME, Reimers CE, Stecher HA. 2007. Enhanced Power from Chambered Benthic Microbial Fuel Cells. *Environmental Science & Technology* 41: 7895-7900

Nielsen ME, Reimers CE, White HK, Sharma S, Girguis PR. 2008. Sustainable energy from deep ocean cold seeps. *Energy & Environmental Science* 1: 584-593

Ohmura N, Matsumoto N, Sasaki K, Saiki H. 2002. Electrochemical regeneration of Fe(III) to support growth on anaerobic iron respiration. *Applied and Environmental Microbiology* 68: 405-407

Oremland RS, Taylor BF. 1978. Sulfate reduction and methanogenesis in marine sediments. *Geochimica et Cosmochimica Acta* 42: 209-214

Pham TH, Boon N, Aelterman P, Clauwaert P, De Schamphelaire L, et al. 2008. Metabolites produced by Pseudomonas sp enable a Gram-positive bacterium to achieve extracellular electron transfer. *Applied Microbiology and Biotechnology* 77: 1119-1129

Rabaey K, Boon N, Hofte M, Verstraete W. 2005. Microbial phenazine production enhances electron transfer in biofuel cells. *Environmental Science & Technology* 39: 3401-3408

Rabaey K, Van de Sompel K, Maignien L, Boon N, Aelterman P, et al. 2006. Microbial fuel cells for sulfide removal. *Environmental Science & Technology* 40: 5218-5224

Reguera G, Nevin KP, Nicoll JS, Covalla SF, Woodard TL, Lovley DR. 2006. Biofilm and nanowire production leads to increased current in Geobacter sulfurreducens fuel cells. *Applied and Environmental Microbiology* 72: 7345-7348

Reimers CE, Stecher HA, Westall JC, Alleau Y, Howell KA, et al. 2007. Substrate degradation kinetics, microbial diversity and current efficiency of microbial fuel cells supplied with marine plankton. *Applied and Environmental Microbiology* 73: 7029-7040

Reimers CE, Tender LM, Fertig S, Wang W. 2001. Harvesting energy from the marine sediment-water interface. *Environmental Science & Technology* 35: 192-195

Ryckelynck N, Stecher HA, Reimers CE. 2005. Understanding the anodic mechanism of a seafloor fuel cell: Interactions between geochemistry and microbial activity. *Biogeochemistry* 76: 113-139

Schröder U. 2007. Anodic electron transfer mechanisms in microbial fuel cells and their energy efficiency. *Physical Chemistry Chemical Physics* 9: 2619-2629

Stams AJM, de Bok FAM, Plugge CM, van Eekert MHA, Dolfing J, Schraa G. 2006. Exocellular electron transfer in anaerobic microbial communities. *Environmental Microbiology* 8: 371-382

Tabatabai M. 1974. A rapid method for determination of sulfate in water samples. *Environmental Letters* 7: 237-243

Tender LM, Reimers CE, Stecher HA, Holmes DE, Bond DR, et al. 2002. Harnessing microbially generated power on the seafloor. *Nature Biotechnology* 20: 821-825

# 5 Challenges and Approaches for Practical Power Production from Benthic Microbial Fuel Cells

Mark E. Nielsen[1], Peter Kauffman[2], Clare E. Reimers[1]

[1]College of Oceanic & Atmospheric Sciences, Oregon State University, Corvallis OR 97331, USA

[2]Northwest Metasystems, Inc., Bainbridge Island, WA 98110 USA

Environmental Science & Technology
American Chemical Society, Washington D.C. 20036
In preparation

## 5.1 Abstract

Benthic microbial fuel cells (BMFCs) have been proposed as long term power supplies to replace batteries for remote monitoring systems. An important aspect of this technology is the management of power and the storage of energy. Three conditions govern the approaches for implementation of this technology: 1) current is produced at a low voltage that requires conversion to higher voltages for practical use, 2) modest power production and variable load cycles require energy storage, and 3) BMFCs have a maximum power point that is defined by a constant cell voltage. A power converter/potentiostat (PCP) was designed in accordance with these conditions. The PCP uses a voltage comparator and an electrical switch to poise the cell potential at a user defined level (0.4 V for most BMFC applications). Current is stepped up in voltage through a DC-DC converter and then stored in a Li-ion rechargeable battery. The PCP was integrated with a chambered BMFC to power an acoustic receiver in a field demonstration. The BMFC provided intermittent power, and the PCP operated as expected and recharged the Li-ion battery after it was depleted. The field experiment demonstrates the practicality and limitations of using BMFCs to power off-the-shelf electronic devices.

## 5.2 Introduction

Benthic microbial fuel cells (BMFCs, also called sediment MFCs) generate electricity from the electrochemical gradient across the sediment-water interface in aquatic environments (Reimers et al., 2001; Tender et al., 2002). They produce modest power densities compared to other microbial fuel cell technologies (e.g. wastewater). However, due to low power requirements of sensors, BMFCs represent one of the earliest practical applications of MFCs (Lovley, 2006). To date, most work describing BMFCs (also called sediment MFCs) has focused on processes, mechanisms and BMFC design; including investigations of anode materials and kinetics (Lowy et al., 2006; Dumas et al., 2007; Scott et al., 2008a), cathode materials (He et al., 2007; Scott et al., 2008b), microbiological communities (Bond et al., 2002; Holmes et al., 2004); geochemical interactions (Ryckelynck et al., 2005; Reimers et al., 2006), and mass

transport limitations (Nielsen et al., 2007). Comparatively little effort has focused on the practical conversion of that energy for use in powering instruments, and only four papers describe systems for using power (Shantaram et al., 2005; McBride et al., 2006; Donovan et al., 2008; Tender et al., 2008). The work by Donovan et al. (2008) provides specific details about a custom-designed power management system (PMS). They identify the low potential available from sediment MFCs and the ability to repower the sensor at low potential as the guiding design criteria for their PMS, and they present data from a demonstration in a freshwater stream.

Building on the work of Donovan et al., we identify three conditions that govern approaches for practical implementation of BMFCs for powering sensors in remote environments: 1) current is produced at a low voltage that requires conversion to higher voltages for practical use, 2) modest power production and variable load cycles require energy storage, and 3) BMFCs have a maximum power point that is defined by a constant cell voltage. This paper elaborates on these considerations, describes a power converter/potentiostat-like (PCP) device based on these considerations, and presents a demonstration of the technology in a field setting. A similar PCP design was used in the demonstration reported by Tender et al. (2008), but they focused on BMFC design and performance rather than power management and energy storage.

### *5.2.1 Nature of the voltage gradient in BMFCs*

A BMFC bridges the redox gradient across the sediment-water interface and converts this potential energy into useful electrical energy. Many texts describe sediment biogeochemical processes and resulting pore water composition and redox profiles (Froelich et al., 1979; Berner, 1980; Burdige, 2006; Schulz, 2006). The redox gradient is established because bacteria use a succession of oxidants as the terminal electron acceptor to remineralize organic detritus delivered to the sediment-water interface. The sequence is ordered such that the reaction that yields the greatest free energy change per mole of organic carbon occurs first (i.e. at the delivery site of organic material – the sediment water interface). When the oxidant becomes limiting, the next most favorable reaction dominates and so on until either all the organic carbon is

remineralized or all the oxidants are depleted (Froelich et al., 1979). The result is a sediment profile with redox potentials ranging from positive (oxidizing conditions) in the overlying water and at the sediment water interface to negative (reducing) in deeper, anoxic sediments (Whitfield, 1972; Burdige, 2006). The resulting redox gradient in typical continental margin sediments is approximately 0.8 V (Figure 5.1). In the presence of a benthic chamber, a similar redox gradient develops over time rather than space (Nielsen et al., 2007). At the time of deployment, a chamber encloses bottom seawater and there is no difference between the inside and outside of the chamber. As time passes, aerobic processes consume the oxygen in the chamber and are then followed by anaerobic processes, and the electrode potential becomes increasingly negative. The voltage difference between the anaerobic anode chamber and the aerobic cathode outside of the chamber represents the open circuit condition in a chambered BMFC. When a circuit is closed so as to produce current, the cell voltage ($E_{cell}$) typically drops to some value less than the open circuit value.

Low-power sensors and/or instruments generally require at least 3.5 V (and often more). Consequently, the voltage delivered by BMFCs (< 0.8 V) must be stepped up. Unlike laboratory or wastewater MFCs, multiple BMFCs cannot be connected in series to increase voltage because conduction through seawater would short-circuit the cells in series. Alternative devices for stepping up the voltage are required, and in this paper we describe the use of a DC-DC converter for that purpose.

### *5.2.2 Energy storage*

Recently, BMFCs have produced relatively modest amounts of power (2 to 60 mW; Donovan et al., 2008; Nielsen et al., 2008; Tender et al., 2008). They characteristically deliver some average level of power with fluctuations caused by

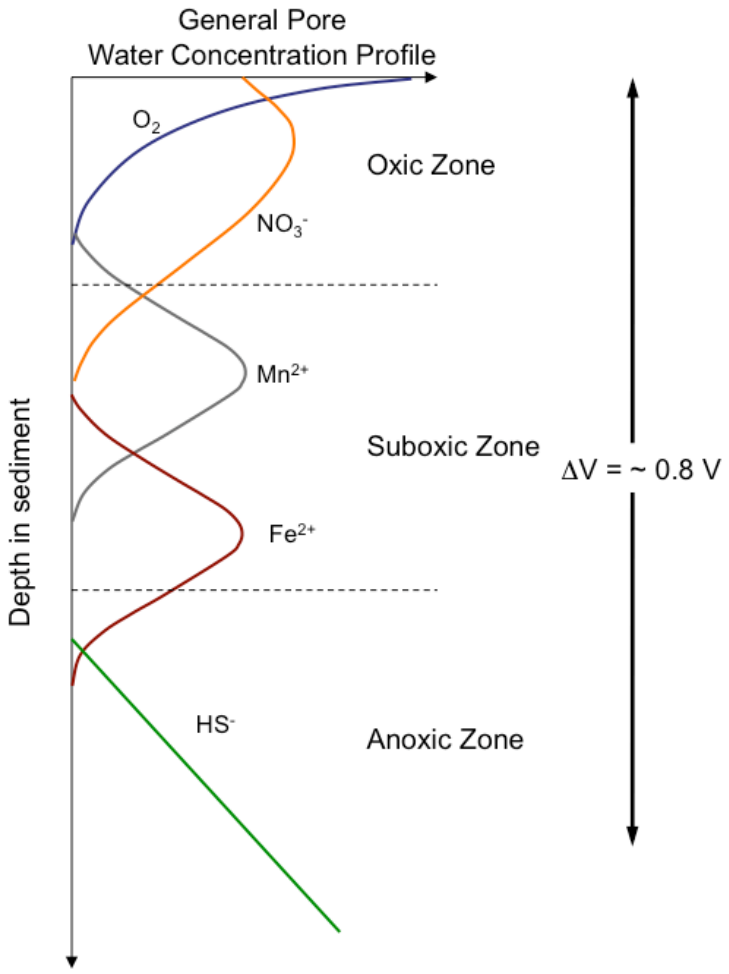


Figure 5.1 Schematic representation of pore water composition for a column of marine sediment. Deposition of organic matter drives aerobic respiration in the surface layer followed by nitrate reduction, manganese reduction, iron reduction, sulfate reduction and methanogenesis. Sulfate reduction tends to dominate in coastal sediments (Burdige, 2006). There is typically a redox gradient of 0.7 to 0.8 V between overlying seawater and sulfidic sediments. Modified from Froelich et al. (1979).

environmental factors such as tidal fluctuations, water current, salinity, temperature, variable inputs of electron donors, etc. Furthermore, BMFCs deliver power based on what the environment can sustain; they can not readily deliver bursts of power in response to varying load cycles. Most off-the-shelf sensors and communication devices have variable power requirements; alternating between stand-by modes and peak (sampling or transmitting) modes, and often the peak power requirements are in excess of what typical BMFCs can produce. Thus, energy storage is required in order for BMFCs to power such devices.

Figure 5.2 illustrates an example of how power demand can be managed so that a BMFC that supplies 16 mW could power a hypothetical instrument that draws 28 mW in peak mode and 14 mW in stand-by mode. These values were selected for illustrative purposes based on typical BMFC performance and reasonable low-power instrument demands (Table 3.1; Nielsen et al., 2008).

For a given BMFC output and known power demands, the optimal interval for drawing peak power ($\Delta t$) can be determined by the following equation:

$$\Delta t = t_p \times (P_p - P_s)/(P_{BMFC} - P_s) \quad (1)$$

where, $t_p$ is the duration of a demand spike, $P_p$ is the peak power requirement, $P_s$ is the stand-by power requirement, and $P_{BMFC}$ is the average power produced by the BMFC (mW). The critical requirement is that the cumulative power generated over time exceeds the cumulative demand for the device. For the example values given above and a $t_p$ of 5s, the optimum timing interval would be 35 s.

Two principal devices for storing electrical energy are batteries and capacitors (Winter & Brodd, 2004). We opted to use a rechargeable battery due to the ability to produce power at a relatively constant voltage (compared to capacitors) and appropriate voltage ($\approx$ 3.7 V) for a variety of sensor applications. There are many

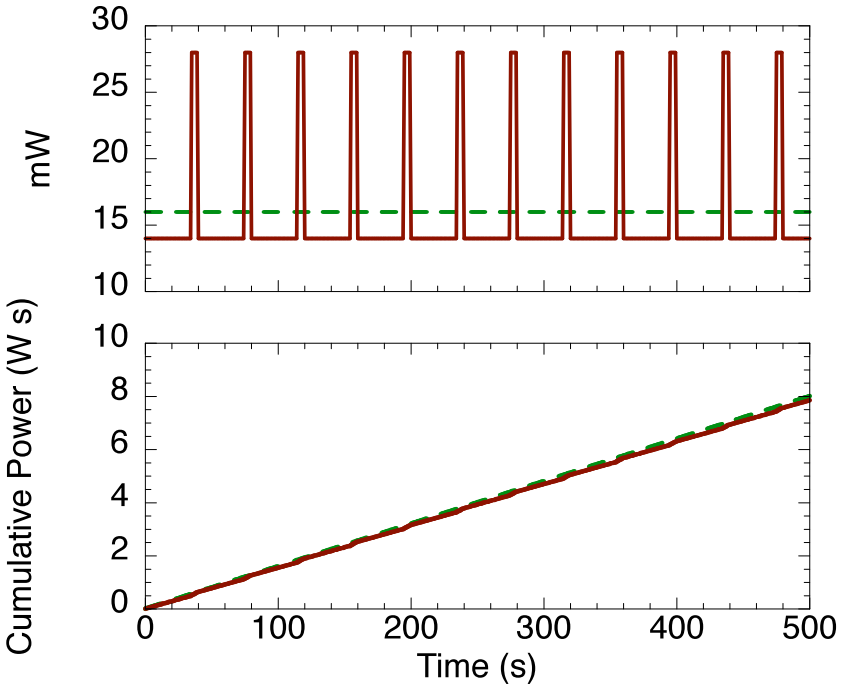


Figure 5.2 Example of how a BMFC with low steady-state power production can meet variable demands. The solid line represents instantaneous (upper panel) and cumulative power demands for a sensor that requires 28 mW in active scanning mode and 14 mW in stand-by mode. The dashed line represents a BMFC that can deliver an average of 16 mW. The cumulative power generated must always be greater than the cumulative demand for the system to operate. The cumulative demand can be adjusted by adjusting the time between scanning intervals.

types of rechargeable batteries, and we selected a Li-ion version based on the advantages they have over other rechargeables (Table 5.1).

Table 5.1 Advantages and Disadvantages of Li-ion Batteries (from Linden & Reddy, 2002)

| Advantages | Disadvantages |
|---|---|
| Sealed cells (no maintenance) | Moderate initial cost |
| Long cycle life | Degrade at high temperatures |
| Broad temperature range of operation | Require protective circuitry |
| Long shelf life | Capacity loss or thermal runaway when over-charged |
| Low self-discharge rate | Venting and possible thermal runaway when crushed |
| Rapid charge capability | Lower power density than NiCd or NiMH |
| High rate and high power discharge capability | |
| High coulombic and energy efficiency | |
| High specific energy and energy density | |
| No memory effect | |

The advantages listed in Table 5.1 have led to Li-ion batteries becoming the technology of choice for consumer electronics and other portable applications and made them an appropriate choice for powering sensors in remote settings. The most significant disadvantage for our systems is the requirement for protective circuitry to protect against full discharge or over-charging, which we took into account and included in our PCP.

### *5.2.3 Poising a BMFC at the optimal voltage for power generation*

An objective for the development of any power source, including BMFCs, is to generate the maximum amount of sustainable power. Since power is the product of voltage and current, which are inversely related in BMFCs, maximizing power production requires an optimization between $E_{cell}$ and $I$. For a given BMFC, the optimum voltage for power production is called the maximum power point (MPP) and can be determined from polarization experiments (Logan et al., 2006). Polarization

curves from a variety of BMFCs are similar (Reimers et al., 2001; Tender et al., 2002; Lowy et al., 2006; Reimers et al., 2006; Dumas et al., 2007; He et al., 2007; Nielsen et al., 2007; Donovan et al., 2008; Scott et al., 2008a; Scott et al., 2008b) and commonly have an MPP that corresponds to an $E_{cell}$ of 0.2 to 0.4 V. Therefore, to get the best performance out of a BMFC, it should be operated at a constant $E_{cell}$ corresponding to its MPP. In research applications, $E_{cell}$ is often controlled with an external resistor, but this does not make sense for practical application since energy is wasted as heat emitted by the resistor. Also, the resistance required to poise the potential at the optimum output level would be different from deployment to deployment and would change over time during a single deployment. Our system uses a capacitor, voltage comparator and an electrical switch to effectively poise the $E_{cell}$ at a predetermined level.

## 5.3 Materials and Methods

### *5.3.1 Potentiostat and DC-DC Converter*

Figure 5.3 shows a block diagram and a photograph of the PCP (custom design, Northwest Metasystems, Bainbridge Island, WA). As $E_{cell}$ increases, charge is stored in a 10K μF capacitor. When $E_{cell}$ reaches a predetermined voltage (set on an adjustable voltage comparator biased by a 3.5 V coin battery) a switch closes thus discharging the capacitor. The switch opens again when the charge on the capacitor falls below a user-defined low voltage cutoff. By selecting a narrow voltage range for the opening and closing of the switch that discharges the capacitor this design behaves like a potentiostat that poises $E_{cell}$ at the desired level (Figure 5.4). Based on polarization curves, the MPP for chambered BMFCs of similar design is about 0.4 V (Nielsen et al., 2007) so this is the $E_{cell}$ that we selected for this demonstration. The current from the discharge of the capacitor passes through an inverter to convert it to AC current so it can be stepped up to approximately 5 V. After conversion, the AC current passes through a rectifier that converts it back to DC current. The resulting

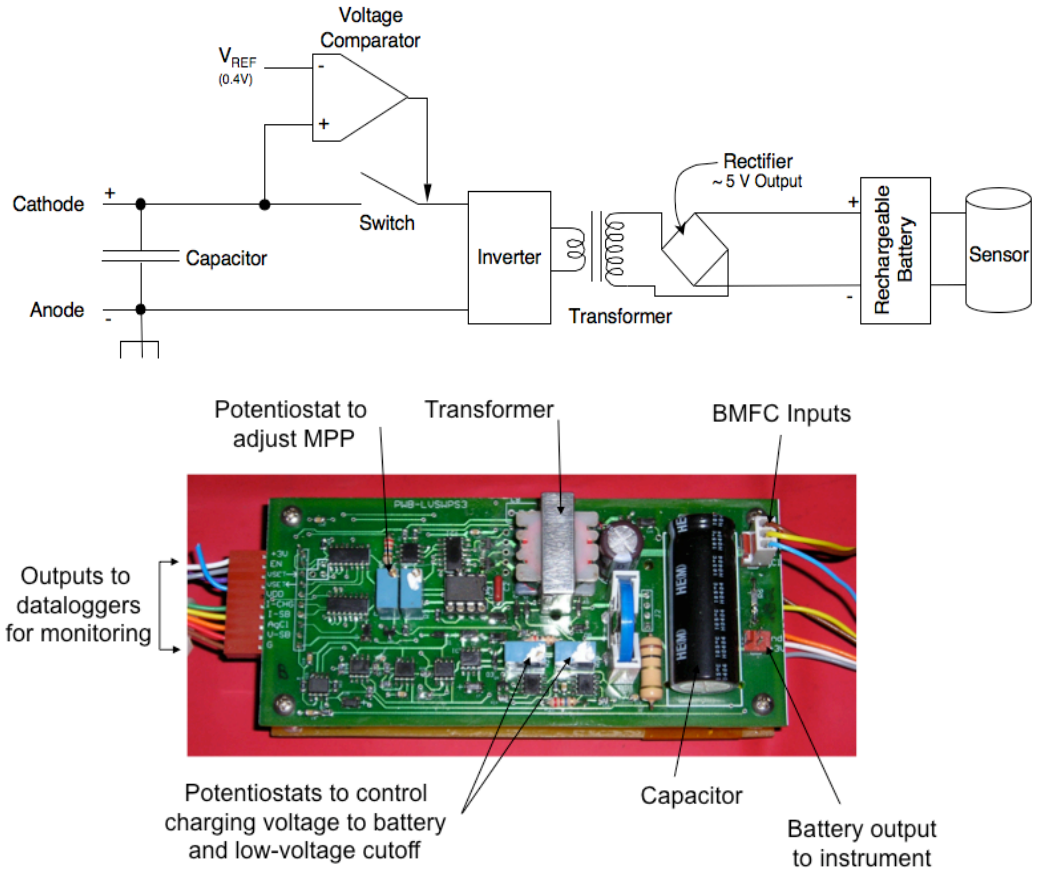


Figure 5.3 Block diagram (top) and photograph (bottom) of PCP.

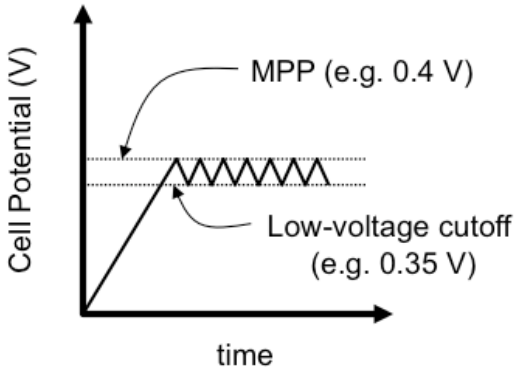


Figure 5.4 Graphical representation of how PCP controls BMFC potential. $E_{cell}$ is initially 0 V and increases as the concentration of electron donors increases inside the chamber. Charge is stored in a capacitor until $E_{cell}$ reaches the MPP at which time it discharges to the DC-DC converter. When $E_{cell}$ reaches the low-voltage cutoff point the circuit opens until $E_{cell}$ recover to the MPP. The frequency of oscillation is a function of the size of the capacitor and how much current draw can be supported by the microbial biofilm.

DC current is finally routed to a rechargeable Li-ion battery (UBBP01, Ultralife Batteries, Newark, NY). The battery has a nominal voltage of 3.5 V and a capacity of 1.8 Ah when fully charged, which provides power for the selected sensor/device for the deployment. The PCP includes a "low-battery" cutoff feature that cuts off the current supply to the sensor from the rechargeable battery when the voltage of the battery falls below 2.9 V. This protects the Li-ion battery from a total discharge that can cause damage. The PCP also includes a mechanism that switches the BMFC to open circuit conditions if the rechargeable battery is charged to capacity. This feature has the effect of saving "fuel" by leaving electron donors unreacted if there is no useful purpose for the current, and it protects the battery from over-charge. The PCP consumes approximately 400 μW when it is running (i.e. charging the battery) and approximately 100 μW when it is in stand by mode (i.e. when $E_{cell} < 0.4$ V).

The PCP is equipped with output pins for monitoring of $E_{cell}$, anode potential vs. Ag/AgCl ($E_{anode}$), current before conversion ($I_{BFMC}$), charging current after conversion ($I_{ch}$), and battery voltage ($V_{batt}$). For this study the current channels were converted to voltage and all data were recorded every 10 minutes with dataloggers (Madgetech, Warner, NH) mounted in a submersible pressure housing with the PCP. Cathode potential vs. Ag/AgCl is equal to the sum of $E_{cell}$ and $E_{anode}$.

The PCP was calibrated and tested in the laboratory prior to field testing with a BMFC. An alkaline "D" cell battery and a variable resistor (R = 0.1 – 26 Ω) were used to simulate varying levels of current from a BMFC. The PCP automatically limits the input voltage to the $E_{cell}$ set by the user, and we conducted tests at three different values of $E_{cell}$ to determine the effect on efficiency of the DC-DC conversion. The calibrations were required because $I_{BMFC}$ and $I_{ch}$ are converted to voltages using resistors on the PCP circuit board to enable logging by voltage recorders, and we required an independent measurement to relate recorded data to BMFC performance. Input current (analogous to $I_{BMFC}$) was calculated by measuring voltage drop across a 0.2 Ω resistor and $I_{ch}$ (after passing through the DC-DC converter portion of the PCP)

was calculated by measuring the voltage drop across a 1 Ω resistor. $I_{BMFC}$ and $I_{ch}$ were converted to power by multiplying by $E_{cell}$ and 3.5 V, respectively. PCP efficiency was calculated as input power divided by the charging power × 100 and ranged from 53% to 93% (Figure 5.5, Table A.4). The efficiency was the highest for an $E_{cell}$ value of 0.3 V (81 – 93%) and lowest for an $E_{cell}$ of 0.5 V (53 – 68%) and as a rule efficiency increased with BMFC power output.

For a field demonstration we selected an ultrasonic receiver (SUR-1, Sonotronics, Inc. Tuscon, AZ) as the target application. We modified the SUR-1 by removing the integrated batteries and replacing them with an underwater pluggable connector so power could be delivered through a cable from a BMFC. Bench tests indicated that the power demand for the SUR-1 was 14 mW in standby mode and 28 mW in scanning mode. The receiver was set to scan 16 different frequencies (each corresponding to a different acoustic tag) for 2 s with a 1 s pause between scans. There was also a 10 s pause at the end of each set of 16 frequencies. The average power demand in this configuration was approximately 22 mW.

### *5.3.2 BMFC Design and Operation*

We previously described the development of a chambered design for our BMFCs (Nielsen et al., 2007; Nielsen et al., 2008). Chambered BMFCs differ from those with buried anodes in that the anodes are suspended above the sediment water interface rather than buried in the sediment. This design permits the use of high surface area anodes and enables fluid advection to participate in delivery of electron donors to the anode. To test our PCP design under field conditions we deployed a chambered BMFC in sandy sediments in Yaquina Bay, OR at a water depth of approximately 6.5 m with a tidal fluctuation of up to 3 m.

The BMFC was designed according to estimated power demand for the acoustic receiver and previous BMFC results. Previous BMFCs in Yaquina Bay produced 13 mW $m^{-2}$ seafloor in the absence of mechanically enhanced transport (Nielsen et al., 2007). Based on those results, we estimated that a footprint of 0.5 $m^2$ should give us

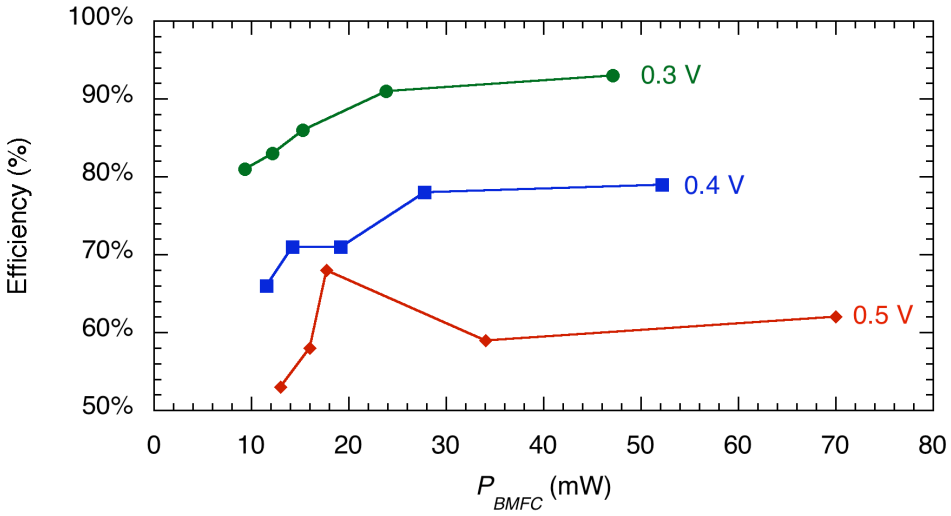


Figure 5.5 Efficiency of the PCP at various values of $E_{cell}$. An external battery and variable resistor was used to simulate a BMFC in the laboratory.

at least 6.5 mW and probably more due to other design improvements such as an increased amount of anode surface area and the addition of a low-pressure check valve to facilitate natural transport through the chamber. Our objective was to meet an average power requirement of 22 mW while still maintaining a size that could be easily deployed without any special requirements other than SCUBA equipment.

The chamber consists of a PVC cylinder 0.5 m tall × 0.4 m inside diameter giving a cross sectional area of 0.5 $m^2$ (Figure 5.6). The cylinder has a domed top and an open bottom. The volume of the chamber depends on how far the base is pushed into the sediment. During this deployment, the cylinder was pushed approximately 0.2 m into the sediment resulting in a chamber volume of ~0.175 $m^3$ (including the domed top that has a volume of 0.025 $m^3$). Divers facilitated deployment with a standard garden hose fitted with a 1-m length of PVC to fluidize the sediment. The lid has a one-way valve that allows fluid flow from inside to outside the chamber. The chamber was bolted to a trawl-resistant aluminum frame that aided in pushing the cylinder into the sediment. The anode was attached to anchor points inside the lid and was assembled from four 1-m sections of carbon fiber brush electrode taken from a commercially available seawater battery (SWB 1200; Kongsberg Maritime AS, Norway; Hasvold et al., 1997). The cathode also consisted of four 1-m sections of identical carbon fiber electrode and was attached to the aluminum frame of the fuel cell. Rubber sleeves insulated the aluminum frame from the cathodes. After deployment, divers added 11 kg of weight to each foot of the frame to ensure the BMFC remained in place. Syntactic foam aided flotation of the cathode in order to keep it above the sediment-water interface. The electrodes have a manufacturer reported surface area of 26 $m^2$ per meter of length resulting in a total estimated surface area of 104 $m^2$ for both anode and cathode. A bare-wire Ag/AgCl reference electrode was used to determine anode and cathode potentials and was attached to the frame of the BMFC. We estimate the reference electrode has an average potential of 0.248 V versus SHE at an average temperature of 12 °C and a salinity of 21. All three electrodes were wired to

Figure 5.6 Photographs of chambered BMFC. Top panel: Frame is made of aluminum and is designed to be trawl-resistant. The frame is insulated from the cathode with rubber. The chamber has an open bottom and encloses the anodes so that they are positioned above the sediment when the BMFC is deployed. The one-way valve can be seen on the top of the chamber and the pressure housing that contains the PCP and dataloggers is attached to the frame in the left foreground. Bottom panel: Carbon-fiber brush anodes inside the chamber.

underwater pluggable connectors (Impulse, San Diego, CA) for connection to the PCP in the submersible pressure housing. Two additional underwater pluggable connectors on the pressure housing carried power from the Li-ion battery to the SUR-1 and enabled data recovery through a cable from the dataloggers to the surface without needing to recover the pressure housing.

On day 56 of the deployment we replaced the check valve with a 500 mL reservoir of a supplemental electron donor (HRC-X, Regenesis, San Clemente, CA). HRC-X is a glycerol tripolylactate that releases lactate upon hydration. It has viscosity of 200,000 centipoise (compared to 1 centipoise for water at 20 °C). The reservoir was a 500 mL Teflon-FEP gas-sampling bag connected to the chamber with 50 cm of 0.635-cm (ID) PVC tubing.

### 5.4 Results and Discussion

Data from the field deployment in Yaquina Bay are shown in Figure 5.7. When the chamber was deployed, there was no difference between $E_{anode}$ and $E_{cathode}$ so $E_{cell}$ was equal to zero. Only after oxygen in the chamber was depleted did the anode potential begin to decline (approximately day 5). It took approximately 9 days for $E_{cell}$ to reach 0.4 V at which point it began to generate current. $I_{BMFC}$ steadily increased during days 9 – 20 until it reached approximately 60 mA (24 mW). Current then decreased to less than 10 mA (4 mW) before increasing again to approximately 50 mA (20 mW). The early peak was probably due to abiotic oxidation of Fe(II) or sulfide that accumulated from anaerobic respiration fueled by excess organic material enclosed by the chamber at the time of deployment (e.g. algae and seaweed). The later peak probably represents the establishment of an electrochemically active microbial community on the anode. Several days after the second peak began to appear, divers replaced the check valve with a reservoir of supplemental electron donor. The donor may or may not have caused the rise in current observed from day 56 to 64. We observed a similar double peak pattern in previous chambered BMFC experiments in Yaquina Bay without adding a supplemental electron donor (Nielsen et al., 2007). It is also unclear

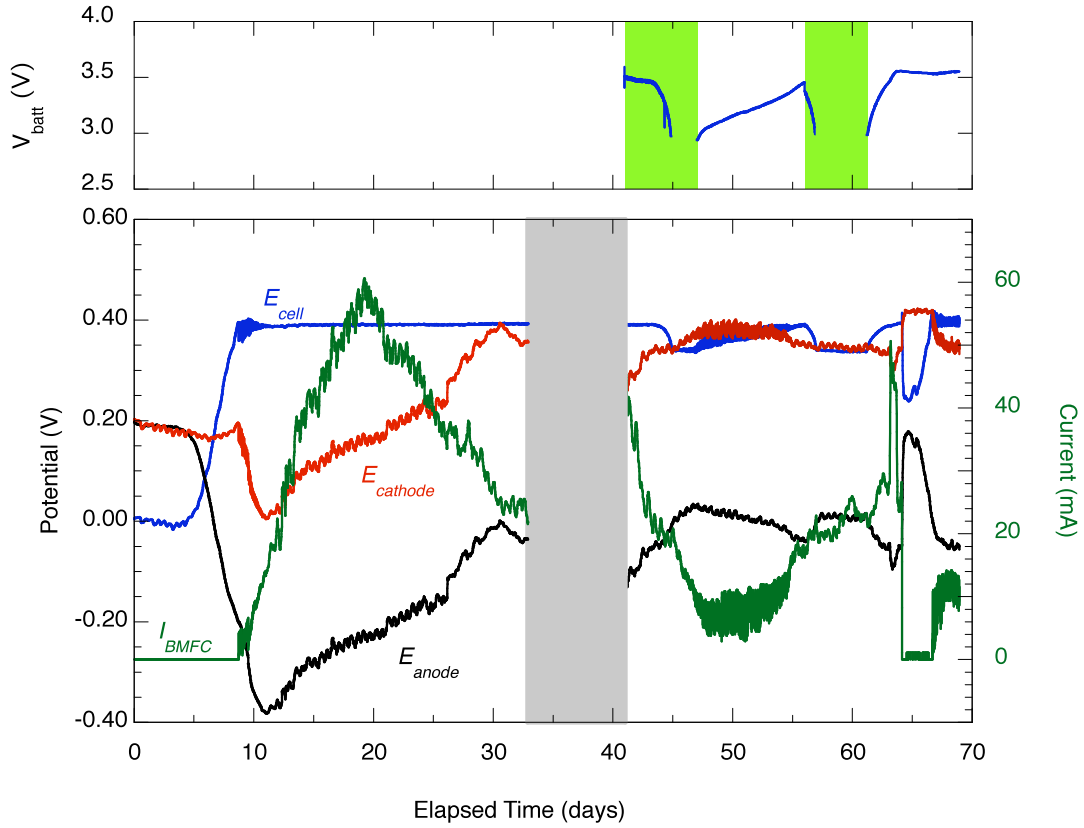


Figure 5.7 Field demonstration of the BMFC and PCP being used to power an acoustic receiver. $V_{batt}$ is the state of the Li-ion rechargeable battery (top panel). No data is shown when $V_{batt} < 2.9$ V because the PCP includes a low voltage threshold to protect the battery from being completely discharged. BMFC performance is shown in the lower panel. PCP was removed from the BMFC over days 33 – 41 to repair a faulty connection.

how much of the electron donor actually entered the chamber. Due to the high viscosity of the HRC-X, low water temperature (~12 °C), and relatively long delivery tube, divers were not able to observe any electron donor entering the chamber. Around day 64 current dropped to zero for about 2 days. This coincided with a sharp but temporary rise in $E_{anode}$. The potential rose to ~ 0.2 V and caused $E_{cell}$ to drop below 0.4 V thus cutting current from the BMFC. We observed a similar phenomenon in previous experiments at this location and hypothesized that it was caused by a temporary bioturbation event that opened a conduit between the anode chamber and the overlying water (Nielsen et al., 2007). It is possible that a similar event occurred here, but it also could have been due to physical scouring by tidal currents temporarily breaking the seal between the sediment and the anode chamber. On repeated dives we observed effects of scouring around the chamber. After two months of deployment the sediment had been partially winnowed away from the base of the chamber resulting in a crater extending approximately 0.75 m beyond the chamber on all sides. The chamber was still sealed but only about 10 cm of the cylinder remained in the sediment.

Initially the BMFC was cathode limited as indicated by the drop in $E_{cathode}$ relative to the expected value of approximately 0.4 vs Ag/AgCl. The initial cathode overpotential indicates that the concentration of electron donors or kinetics of electron transfer at the anode exceeded the corresponding factors at the cathode. Over time, the rapid oxidation of electron donors in the anode chamber depleted the initial concentration and the current became limited by the transport of electron donors into the anode chamber. Another factor that might shift the BMFC from cathode limitation to apparent anode limitation is the development of a cathode biofilm consisting of biomineralized manganese that subsequently catalyzes the reduction of oxygen at the cathode (Rhoads et al., 2005). The small-scale variability in the potentials and $I_{BMFC}$ match the frequency of tidal fluctuations as has been observed previously (Tender et al., 2002; Nielsen et al., 2007) and appear to be caused by water velocity in this case.

At slack tide, we observe dips in current followed by peaks during flood or ebb tidal periods.

Prior to day 33, the PCP had a faulty connection to the datalogger recording $V_{batt}$ so we recovered the PCP to the laboratory to repair the connection. During this period, indicated by the gray rectangle on Figure 5.7, the BMFC returned to open circuit conditions. When we replaced the PCP, the current was higher than it had been when it was disconnected. This suggests reduced compounds (most likely sulfide or Fe(II)) accumulated in the chamber under open circuit condition resulting from continuing anaerobic respiration (Nielsen et al., 2007; Chapter 4).

The green shaded areas on Figure 5.7 indicate the periods when the SUR-1 was connected to the BMFC. The load depleted the battery faster than it was recharged by the BMFC and after four days the voltage fell below the low voltage threshold thus cutting power to the acoustic receiver. The short battery life is inconsistent with the expected battery life of about 11 days based on a capacity of 1.8 amp-hours and an average demand of 22 mW. It is possible that either the battery was not fully charged at the time of deployment or there is an undetected loss in the system. We suspect the latter because we have observed the same discrepancy between expected and observed battery life in other experiments with a similar PCP (results not shown). In each case we charged the battery for 24 to 72 hours with a 4.1 V power supply prior to deployment. During the initial connection to the BMFC the acoustic receiver recorded 496 pings from an acoustic tag located in the water adjacent to the receiver. On day 45 the receiver was unplugged and the battery began to recover. It passed above the low voltage threshold after 2.5 days and continued to charge even though the BMFC was generating less than 10 mA (4 mW). We connected the SUR-1 again on day 56, and it depleted the available battery power within two days. When the load was disconnected, the battery recovered in approximately 3 days.

### *5.4.1 Limitations and improvement strategies*

We demonstrated a power converter/potentiostat system capable of managing power produced by a BMFC in sandy estuarine sediments. The PCP poised the BMFC at 0.4 V, which has previously been shown to correspond to the maximum power point for BMFCs. The BMFC supplied 0 – 60 mA at 0.4 V (0 – 24 mW) which was stepped up by the PCP to recharge a Li-ion battery. The PCP performed as expected, but the BMFC did not provide sufficient primary power to continuously power an acoustic receiver that drew an average of 22 mW. Strategies to provide sustained power to the receiver include lowering the demand by lengthening the time between scans, and boosting power from the BMFC by adding a supplemental electron donor or moving it to a location with muddier more organic-rich sediments. One advantage of the PCP described in this paper is that the rechargeable battery remained charged despite a period of time late in the deployment when the BMFC did not produce current.

The cold temperature of the water at the field site hindered delivery of the supplemental electron donor and future experiments will utilize a donor with lower viscosity or a different delivery method. Scouring also appeared to a potential problem based on diver observations and a short period when $E_{cell}$ fell below 0.4 V. Pushing the chamber deeper into the sediments could minimize this problem, but divers were not able to do this without special equipment. Future experiments should consider other methods for sealing the chambered BMFC to the sediments including adding weight and possibly employing an auger.

## 5.5 References:

Berner RA. 1980. *Early Diagenesis: A Theoretical Approach*. Princeton, N.J.: Princeton University Press. 241 pp.

Bond DR, Holmes DE, Tender LM, Lovley DR. 2002. Electrode-reducing microorganisms that harvest energy from marine sediments. *Science* 295: 483-485

Burdige DJ. 2006. *Geochemistry of Marine Sediments*: Princeton University Press. 609 pp.

Donovan C, Dewan A, Heo D, Beyenal H. 2008. Batteryless, Wireless Sensor Powered by a Sediment Microbial Fuel Cell. *Environmental Science & Technology* In Press

Dumas C, Mollica A, Feron D, Basseguy R, Etcheverry L, Bergel A. 2007. Marine microbial fuel cell: Use of stainless steel electrodes as anode and cathode materials. *Electrochimica Acta* 53: 468-473

Froelich PN, Klinkhammer GP, Bender ML, Luedtke NA, Heath GR, et al. 1979. Early oxidation of organic matter in pelagic sediments of the eastern equatorial Atlantic: suboxic diagenesis. *Geochimica Et Cosmochimica Acta* 43: 1075-1090

Hasvold O, Henriksen H, Melvaer E, Citi G, Johansen BO, et al. 1997. Sea-water battery for subsea control systems. *Journal of Power Sources* 65: 253-261

He Z, Haibo S, Angenent LT. 2007. Increased power production from a sediment microbial fuel cell with a rotating cathode. *Biosensors and Bioelectronics* 22: 3252-3255

Holmes DE, Bond DR, O'Neill RA, Reimers CE, Tender LR, Lovley DR. 2004. Microbial communities associated with electrodes harvesting electricity from a variety of aquatic sediments. *Microbial Ecology* 48: 178-190

Linden D, Reddy TB, eds. 2002. *Handbook of Batteries*. New York City: McGraw-Hill

Logan BE, Hamelers B, Rozendal R, Schrorder U, Keller J, et al. 2006. Microbial fuel cells: Methodology and technology. *Environmental Science & Technology* 40: 5181-5192

Lovley DR. 2006. Microbial fuel cells: novel microbial physiologies and engineering approaches. *Current Opinion in Biotechnology* 17: 327-332

Lowy DA, Tender LM, Zeikus JG, Park DH, Lovley DR. 2006. Harvesting energy from the marine sediment-water interface II - Kinetic activity of anode materials. *Biosensors & Bioelectronics* 21: 2058-2063

McBride LR, Girguis P, Reimers CE. 2006. *Power Storage and Conversion from an Ocean Microbial Energy Source*. Presented at OCEANS 2006

Nielsen ME, Reimers CE, Stecher HA. 2007. Enhanced Power from Chambered Benthic Microbial Fuel Cells. *Environmental Science & Technology* 41: 7895-7900

Nielsen ME, Reimers CE, White HK, Sharma S, Girguis PR. 2008. Sustainable energy from deep ocean cold seeps. *Energy & Environmental Science* 1: 584-593

Reimers CE, Girguis P, Stecher HA, Tender LM, Ryckelynck N. 2006. Microbial fuel cell energy from an ocean cold seep. *Geobiology* 4: 123-136

Reimers CE, Tender LM, Fertig S, Wang W. 2001. Harvesting energy from the marine sediment-water interface. *Environmental Science & Technology* 35: 192-195

Rhoads A, Beyenal H, Lewandowski Z. 2005. Microbial fuel cell using anaerobic respiration as an anodic reaction and biomineralized manganese as a cathodic reactant. *Environmental Science & Technology* 39: 4666-4671

Ryckelynck N, Stecher HA, Reimers CE. 2005. Understanding the anodic mechanism of a seafloor fuel cell: Interactions between geochemistry and microbial activity. *Biogeochemistry* 76: 113-139

Schulz HD. 2006. Quantification of Early Diagenesis: Dissolved Constituents in Pore Water and Signals in the Solid Phase. In *Marine Geochemistry*, ed. HD Schulz, M Zabel. Berlin: Springer

Scott K, Cotlarciuc I, Hall D, Lakeman JB, Browning D. 2008a. Power from marine sediment fuel cells: the influence of anode material. *Journal of Applied Electrochemistry* 38: 1313-1319

Scott K, Cotlarciuc I, Head I, Katuri KP, Hall D, et al. 2008b. Fuel cell power generation from marine sediments: Investigation of cathode materials. *Journal of Chemical Technology and Biotechnology* 83: 1244-1254

Shantaram A, Beyenal H, Raajan R, Veluchamy A, Lewandowski Z. 2005. Wireless sensors powered by microbial fuel cells. *Environmental Science & Technology* 39: 5037-5042

Tender LM, Gray SA, Groveman E, Lowy DA, Kauffman P, et al. 2008. The first demonstration of a microbial fuel cell as a viable power supply: Powering a meteorological buoy. *Journal of Power Sources* 179: 571-575

Tender LM, Reimers CE, Stecher HA, Holmes DE, Bond DR, et al. 2002. Harnessing microbially generated power on the seafloor. *Nature Biotechnology* 20: 821-825

Whitfield M. 1972. The electrochemical characteristics of natural redox cells. *Limnology and Oceanography* 17: 383-393

Winter M, Brodd RJ. 2004. What Are Batteries, Fuel Cells, and Supercapacitors? *Chemical Reviews* 104: 4245-4270

# 6 Conclusion

## 6.1 Summary of conclusions

A unique aspect of the BMFCs described in this dissertation is the incorporation of a benthic chamber design. Five experiments were conducted to study and improve chambered BMFCs. A combination of laboratory and field studies investigated: factors that limit current production, the feasibility of scaling up BMFCs for practical use, mechanisms of electron transfer at the anode, and a novel power management system.

An experiment in Yaquina Bay, OR compared BMFC internal resistance with and without enhanced mass transport of porewater solutes to the anode chamber. Without added transport, the internal resistance was approximately 577 Ω. When a peristaltic pump was used to pump sediment porewater through the anode chamber, internal resistance decreased to approximately 38 Ω. Pumping also yielded an 18-fold increase in power. In that experiment, the energy cost of pumping offset the power gains and was not a viable long-term solution. To investigate chamber performance in an area with natural pore fluid advection, two chambered BMFCs and one solid anode BMFC were deployed at cold seeps in Monterey Canyon, CA. The chambers produced an average of about 30 mW $m^{-2}$, which was consistent with estimated diffusive transport rates. However, power increased by a factor of five when one-way valves on one of the chambers were replaced to allow advective flow through the chamber. The latter deployment produced an average of 56 mW, which is adequate to power a variety of off-the-shelf electronic devices.

The Monterey Canyon experiments highlighted a key difference between chambered BMFCs and solid anode BMFCs. A solid anode BMFC was co-located at a cold seep with a chambered BMFC. When normalized to cross-sectional area, the solid anode BMFC (which had a vertically oriented cylindrical anode) produced roughly the same amount of power as the chambered BMFC. However, the chambered BMFCs

produced 55 to 600 times more absolute power (i.e., when not normalized to cross sectional area). Power records were also distinctly different between the solid-anode and chambered BMFCs. The solid-anode BMFC showed a power peak approximately 20 days into the deployment and then a decay to a constant level about one-tenth of the peak level. On the other hand, the chambered BMFCs did not show the same peak and decay pattern. They were highly variable, but two of the three chamber deployments did not show any systematic degradation in power production.

Laboratory experiments were conducted to investigate the effect of adding a supplemental electron donor to the anode chambers of BMFCs. Intermittent lactate injections resulted in short-term current increases but did not apparently affect the process that supports the baseline current level in these BMFCs. Each injection resulted in a distinct current peak, which then declined to a level similar to unsupplemented BMFCs. At the end of the experiment, molybdate was added to block sulfate reduction. The molybdate eliminated any current response due to lactate supplementation, but baseline current production increased slightly as a result of the molybdate injections; raising questions about the role of sulfate reduction as the process that supports the baseline current in BMFCs.

For BMFCs to be put to practical use, the produced energy must be stepped up in voltage and stored. I tested and described a novel power converter/potentiostat and energy storage system. The power converter was approximately 75% efficient (at an $E_{cell}$ of 0.4 V) and used a combination of a voltage comparator and switch to poise the BMFC potential at the maximum power point. The power converter system was demonstrated with a BMFC deployed in Yaquina Bay that was used to power an acoustic receiver.

## 6.2 Future work

Each of the experiments and demonstrations generated new questions for future study. For example, given the demonstrated advantages of advective transport of electron

donors to the anode, chambered BMFCs would benefit from a pumping system that required little or no electrical energy. Possibilities include a system that uses tidal pumping to enhance fluid exchange, a mechanical device that converts energy from water currents to mechanical energy for a pumping system (e.g. a savonius rotor), or an osmotic pump.

Phylogenetic analyses of anode fibers from two Monterey Canyon BMFCs showed significant differences. BMFC 2 was dominated by epsilonproteobacteria and BMFC 4 had a more diverse community with representatives from deltaproteobacteria, epsilonproteobacteria, firmicutes and flavobacterium/cytophaga/bacterioides. Due to different transport processes, BMFC 4 produced about five times more power than BMFC 2. In general, power gains were attributed to increased transport of electron donors to the anode, however, different transport processes might also cause a shift to a different microbial community with a different electroactive potential. A new experiment with more comprehensive microbial community sampling and analysis could shed insights on the relationship between transport processes, microbial community and power production.

The laboratory experiments in which sulfate reduction was blocked with molybdate raised questions about the role of sulfur in these systems. Previous evidence suggested current was mediated by a sulfur cycle in which sediment organic matter fueled sulfate reduction resulting in sulfide, which was oxidized to sulfur at the surface of the anode. The presence of sulfur-disproportionating organisms suggested that the sulfur was oxidized back to sulfate with the anode serving as an electron acceptor. However, all laboratory BMFCs in this study continued to generate current even when sulfate reduction and sulfur disproportionation were blocked. Future experiments may investigate the role of fermentation in the anode chambers and the possibility of microbiologically produced hydrogen as an electron donor.

Future chambered BMFCs would benefit from a better seal with the sediment, which might be accomplished with additional weight or designing the chamber to be driven into the sediment like an auger. The use of supplemental electron donors in the field should also be investigated with a focus on sustainability of current generation. There was also an apparent discrepancy between the rated capacity of the rechargeable battery and the amount of time that it could power the acoustic receiver. Future designs could benefit from increased storage capacity.

BMFCs represent a novel technology with the potential for powering a variety of electronic devices in aquatic settings. If employed successfully, BMFCs could extend the range of ocean observing programs by powering a host of distributed sensors and communication devices. While the primary motivation for the development of BMFCs is oriented towards practical implementation, research and development of this technology also generates novel findings in the fields of electrochemistry, sediment biogeochemistry, microbial ecology and engineering.

# 7 Bibliography

Aelterman P, Rabaey K, Pham HT, Boon N, Verstraete W. 2006. Continuous electricity generation at high voltages and currents using stacked microbial fuel cells. *Environmental Science & Technology* 40: 3388-3394

Alberte R, Bright H, Reimers C, Tender L. 2005. Method and apparatus for generating power from voltage gradients at sediment-water interfaces. *United States Patent No. US 6,913,854 B1*

Bak F, Cypionka H. 1987. A novel type of energy-metabolism involving fermentation of inorganic sulfur-compounds. *Nature* 326: 891-892

Bard AJ, Faulkner LR. 2001. *Electrochemical Methods*. New York: John Wiley & Sons, Inc.

Barry JP, Greene HG, Orange DL, Baxter CH, Robison BH, et al. 1996. Biological and geologic characteristics of cold seeps in Monterey Bay, California. *Deep-Sea Research Part I-Oceanographic Research Papers* 43: 1739-1762

Bergel A, Feron D, Mollica A. 2005. Catalysis of oxygen reduction in PEM fuel cell by seawater biofilm. *Electrochemistry Communications* 7: 900-904

Berner RA. 1980. *Early Diagenesis: A Theoretical Approach*. Princeton, N.J.: Princeton University Press. 241 pp.

Biffinger JC, Pietron J, Bretschger O, Nadeau LJ, Johnson GR, et al. 2008. The influence of acidity on microbial fuel cells containing *Shewanella oneidensis*. *Biosensors and Bioelectronics* 24: 906-911

Bond DR, Holmes DE, Tender LM, Lovley DR. 2002. Electrode-reducing microorganisms that harvest energy from marine sediments. *Science* 295: 483-485

Bond DR, Lovley DR. 2003. Electricity production by Geobacter sulfurreducens attached to electrodes. *Applied and Environmental Microbiology* 69: 1548-1555

Boudreau BP. 1997. *Diagenetic models and their implementation: modelling transport and reactions in aquatic sediments*. Heidleberg, NY: Springer-Verlag. 414 pp.

Bullen RA, Arnot TC, Lakeman JB, Walsh FC. 2006. Biofuel cells and their development. *Biosensors and Bioelectronics* 21: 2015-2045

Burdige DJ. 2006. *Geochemistry of Marine Sediments*: Princeton University Press. 609 pp.

Campbell BJ, Engel AS, Porter ML, Takai K. 2006. The versatile epsilon-proteobacteria: key players in sulphidic habitats. *Nature Reviews Microbiology* 4: 458-468

Chaudhuri SK, Lovley DR. 2003. Electricity generation by direct oxidation of glucose

in mediatorless microbial fuel cells. *Nature Biotechnology* 21: 1229-1232

Cheng S, Liu H, Logan BE. 2006. Increased power generation in a continuous flow MFC with advective flow through the porous anode and reduced electrode spacing. *Environmental Science & Technology* 40: 2426-2432

Cline JD. 1969. Spectrophotometric determination of hydrogen sulfide in natural waters. *Limnology and Oceanography* 14: 454-458

Covert JS, Moran MA. 2001. Molecular characterization of estuarine bacterial communities that use high- and low-molecular weight fractions of dissolved organic carbon. *Aquatic Microbial Ecology* 25: 127-139

Dewan A, Beyenal H, Lewandowski Z. 2008. Scaling up microbial fule cells. *Environmental Science and Technology* 42: 7643-7648

Donovan C, Dewan A, Heo D, Beyenal H. 2008. Batteryless, Wireless Sensor Powered by a Sediment Microbial Fuel Cell. *Environmental Science & Technology* In Press

Du ZW, Li HR, Gu TY. 2007. A state of the art review on microbial fuel cells: A promising technology for wastewater treatment and bioenergy. *Biotechnology Advances* 25: 464-482

Dumas C, Mollica A, Feron D, Basseguy R, Etcheverry L, Bergel A. 2007. Marine microbial fuel cell: Use of stainless steel electrodes as anode and cathode materials. *Electrochimica Acta* 53: 468-473

Dumbauld BR, Armstrong DA, Feldman KL. 1996. Life-History of Two Sympatric Thalassinidean Shrimps, Neotrypaea californiensis and Upogebia pugettensis, with implications for Oyster Culture. *Journal of Crustacean Biology* 16: 689-708

Elderfield H, Schultz A. 1996. Mid-ocean ridge hydrothermal fluxes and the chemical composition of the ocean. *Annual Review of Earth and Planetary Sciences* 24: 191-224

Finke N, Vandieken V, Jørgensen BB. 2007. Acetate, lactate, propionate, and isobutyrate as electron donors for iron and sulfate reduction in Arctic marine sediments, Svalbard. *Fems Microbiology Ecology* 59: 10-22

Finkelstein DA, Tender LM, Zeikus JG. 2006. Effect of electrode potential on electrode-reducing microbiota. *Environmental Science & Technology* 40: 6990-6995

Finster K, Liesack W, Thamdrup B. 1998. Elemental sulfur and thiosulfate disproportionation by *Desulfocapsa sulfoexigens* sp. nov., a new anaerobic bacterium isolated from marine surface sediment. *Applied and Environmental Microbiology* 64: 119-125

Froelich PN, Klinkhammer GP, Bender ML, Luedtke NA, Heath GR, et al. 1979. Early oxidation of organic matter in pelagic sediments of the eastern equatorial

Atlantic: suboxic diagenesis. *Geochimica et Cosmochimica Acta* 43: 1075-1090

Gieskes J, Rogers W. 1973. Alkalinity determination in interstitial waters of marine sediments. *Journal of Sedimentary Petrology* 43: 272-277

Gil GC, Chang IS, Kim BH, Kim M, Jang JK, et al. 2003. Operational parameters affecting the performance of a mediator-less microbial fuel cell. *Biosensors and Bioelectronics* 18: 327-334

Girguis PR, Orphan VJ, Hallam SJ, DeLong EF. 2003. Growth and methane oxidation rates of anaeoic methanotrophic archaea in a continuous-flow bioreactor. *Applied and Environmental Microbiology* 69: 5472-5482

Gorby YA, Yanina S, McLean JS, Rosso KM, Moyles D, et al. 2006. Electrically conductive bacterial nanowires produced by Shewanella oneidensis strain MR-1 and other microorganisms. *Proceedings of the National Academy of Sciences of the United States of America* 103: 11358-11363

Hasvold O, Henriksen H, Melvaer E, Citi G, Johansen BO, et al. 1997. Sea-water battery for subsea control systems. *Journal of Power Sources* 65: 253-261

He Z, Haibo S, Angenent LT. 2007. Increased power production from a sediment microbial fuel cell with a rotating cathode. *Biosensors and Bioelectronics* 22: 3252-3255

He Z, Minteer SD, Angenent LT. 2005. Electricity generation from artificial wastewater using an upflow microbial fuel cell. *Environmental Science & Technology* 39: 5262-5267

Hernandez ME, Newman DK. 2001. Extracellular electron transfer. *Cellular and Molecular Life Sciences* 58: 1562-1571

Holmes DE, Bond DR, Lovley DR. 2004. Electron transfer by Desulfobulbus propionicus to Fe(III) and graphite electrodes. *Applied and Environmental Microbiology* 70: 1234-1237

Holmes DE, Bond DR, O'Neill RA, Reimers CE, Tender LR, Lovley DR. 2004. Microbial communities associated with electrodes harvesting electricity from a variety of aquatic sediments. *Microbial Ecology* 48: 178-190

Holmes DE, Chaudhuri SK, Nevin KP, Mehta T, Methe BA, et al. 2006. Microarray and genetic analysis of electron transfer to electrodes in Geobacter sulfurreducens. *Environmental Microbiology* 8: 1805-1815

Holmes DE, Nicoll JS, Bond DR, Lovley DR. 2004. Potential role of a novel psychrotolerant member of the family Geobacteraceae, Geopsychrobacter electrodiphilus gen. nov., sp nov., in electricity production by a marine sediment fuel cell. *Applied and Environmental Microbiology* 70: 6023-6030

Huettel M, Ziebis W, Forster S, Luther GW. 1998. Advective transport affecting metal and nutrient distributions and interfacial fluxes in permeable sediments.

*Geochimica et Cosmochimica Acta* 62: 613-631

Ioannis Ieropoulos JGCM. 2008. Microbial fuel cells based on carbon veil electrodes: Stack configuration and scalability. *International Journal of Energy Research* 9999: n/a

Jang JK, Pham TH, Chang IS, Kang KH, Moon H, et al. 2004. Construction and operation of a novel mediator- and membrane-less microbial fuel cell. *Process Biochemistry* 39: 1007-1012

Johnson KM, King AE, Sieburth JM. 1985. Coulometric DIC analyses for marine studies: An introduction. *Marine Chemistry* 16: 61-82

Jørgensen BB. 2006. Bacteria and Marine Biogeochemistry. In *Marine Geochemistry*, ed. HD Schulz, M Zabel. Berlin: Springer

Jupp TE, Schultz A. 2004. A poroelastic model for the tidal modulation of seafloor hydrothermal systems. *Journal of Geophysical Research-Solid Earth* 109

Kim N, Choi Y, Jung S, Kim S. 2000. Effect of initial carbon sources on the performance of microbial fuel cells containing Proteus vulgaris. *Biotechnology and Bioengineering* 70: 109-114

Kirchman DL. 2002. The ecology of Cytophaga-Flavobacteria in aquatic environments. *Fems Microbiology Ecology* 39: 91-100

Kondo R, Nishijima T, Hata Y. 1993. Mineralization process of glucose and low-molecular fatty-acid production in an anoxic marine sediment slurry. *Nippon Suisan Gakkaishi* 59: 105-109

LaBonte AL, Brown KM, Tryon MD. 2007. Monitoring periodic and episodic flow events at Monterey Bay seeps using a new optical flow meter. *Journal of Geophysical Research-Solid Earth* 112

Larminie J, Dicks A. 2000. *Fuel Cell Systems Explained*. Chichester: John Wiley & Sons Ltd.

Liamleam W, Annachhatre AP. 2007. Electron donors for biological sulfate reduction. *Biotechnology Advances* 25: 452-463

Linden D, Reddy TB, eds. 2002. *Handbook of Batteries*. New York City: McGraw-Hill

Logan BE. 2008. *Microbial Fuel Cells*. Hoboken, N.J., U.S.A.: John Wiley & Sons, Inc.

Logan BE, Cheng S, Watson V, Estadt G. 2007. Graphite fiber brush anodes for increased power production in air-cathode microbial fuel cells. *Environmental Science & Technology* 41: 3341-3346

Logan BE, Hamelers B, Rozendal R, Schröder U, Keller J, et al. 2006. Microbial fuel cells: Methodology and technology. *Environmental Science & Technology* 40: 5181-5192

Logan BE, Regan JM. 2006. Microbial Fuel Cells: Challenges and Applications. *Environmental Science & Technology* 40: 5172-5180

Lovley DR. 1991. Dissimilatory Fe(III) and Mn(IV) reduction. *Microbiological Reviews* 55: 259-287

Lovley DR. 2006. Bug juice: harvesting electricity with microorganisms. *Nature Reviews Microbiology* 4: 497-508

Lovley DR. 2006. Microbial fuel cells: novel microbial physiologies and engineering approaches. *Current Opinion in Biotechnology* 17: 327-332

Lovley DR, Phillips EJP. 1988. Novel mode of microbial energy metabolism - organic-carbon oxidation coupled to dissimilatory reduction of iron or manganese. *Applied and Environmental Microbiology* 54: 1472-1480

Lowy DA, Tender LM, Zeikus JG, Park DH, Lovley DR. 2006. Harvesting energy from the marine sediment-water interface II - Kinetic activity of anode materials. *Biosensors and Bioelectronics* 21: 2058-2063

Martin JB, Orange DL, Lorenson TD, Kvenvolden KA. 1997. Chemical and isotopic evidence of gas-influenced flow at a transform plate boundary: Monterey Bay, California. *Journal of Geophysical Research-Solid Earth* 102: 24903-24915

McBride LR, Girguis P, Reimers CE. 2006. *Power Storage and Conversion from an Ocean Microbial Energy Source*. Presented at OCEANS 2006

Moon H, Chang IS, Kim BH. 2006. Continuous electricity production from artificial wastewater using a mediator-less microbial fuel cell. *Bioresource Technology* 97: 621-627

Nealson KH. 1997. Sediment bacteria: Who's there, what are they doing, and what's new? *Annual Review of Earth and Planetary Sciences* 25: 403-434

Nielsen ME, Reimers CE, Stecher HA. 2007. Enhanced Power from Chambered Benthic Microbial Fuel Cells. *Environmental Science & Technology* 41: 7895-7900

Nielsen ME, Reimers CE, White HK, Sharma S, Girguis PR. 2008. Sustainable energy from deep ocean cold seeps. *Energy & Environmental Science* 1: 584-593

Ohmura N, Matsumoto N, Sasaki K, Saiki H. 2002. Electrochemical regeneration of Fe(III) to support growth on anaerobic iron respiration. *Applied and Environmental Microbiology* 68: 405-407

Orange DL, Greene HG, Reed D, Martin JB, McHugh CM, et al. 1999. Widespread fluid expulsion on a translational continental margin: Mud volcanoes, fault zones, headless canyons, and organic-rich substrate in Monterey Bay, California. *Geological Society of America Bulletin* 111: 992-1009

Oremland RS, Taylor BF. 1978. Sulfate reduction and methanogenesis in marine sediments. *Geochimica et Cosmochimica Acta* 42: 209-214

Paull CK, Schlining B, Ussler W, Paduan JB, Caress D, Greene HG. 2005. Distribution of chemosynthetic biological communities in Monterey Bay, California. *Geology* 33: 85-88

Pham TH, Boon N, Aelterman P, Clauwaert P, De Schamphelaire L, et al. 2008. Metabolites produced by Pseudomonas sp enable a Gram-positive bacterium to achieve extracellular electron transfer. *Applied Microbiology and Biotechnology* 77: 1119-1129

Pilson MEQ. 1998. *An Introduction to Chemistry of the Sea*. Upper Saddle River, NJ: Prentice Hall. 431 pp.

Rabaey K, Boon N, Hofte M, Verstraete W. 2005. Microbial phenazine production enhances electron transfer in biofuel cells. *Environmental Science & Technology* 39: 3401-3408

Rabaey K, Clauwaert P, Aelterman P, Verstraete W. 2005. Tubular Microbial Fuel Cells for Efficient Electricity Generation. *Environmental Science & Technology* 39: 8077-8082

Rabaey K, Rodriguez J, Blackall LL, Keller J, Gross P, et al. 2007. Microbial ecology meets electrochemistry: electricity-driven and driving communities. *Isme Journal* 1: 9-18

Rabaey K, Van de Sompel K, Maignien L, Boon N, Aelterman P, et al. 2006. Microbial fuel cells for sulfide removal. *Environmental Science & Technology* 40: 5218-5224

Rathburn AE, Perez ME, Martin JB, Day SA, Mahn C, et al. 2003. Relationships between the distribution and stable isotopic composition of living benthic foraminifera and cold methane seep biogeochemistry in Monterey Bay, California. *Geochemistry Geophysics Geosystems* 4

Reguera G, Nevin KP, Nicoll JS, Covalla SF, Woodard TL, Lovley DR. 2006. Biofilm and nanowire production leads to increased current in Geobacter sulfurreducens fuel cells. *Applied and Environmental Microbiology* 72: 7345-7348

Reimers CE, Girguis P, Stecher HA, Tender LM, Ryckelynck N. 2006. Microbial fuel cell energy from an ocean cold seep. *Geobiology* 4: 123-136

Reimers CE, Jahnke RA, McCorkle D. 1992. Carbon fluxes and burial rates over the continental slope and rise off central California with implications for the global carbon cycle. *Global Biogeochemical Cycles* 6: 199-224

Reimers CE, Stecher HA, Westall JC, Alleau Y, Howell KA, et al. 2007. Substrate degradation kinetics, microbial diversity and current efficiency of microbial fuel cells supplied with marine plankton. *Applied and Environmental Microbiology* 73: 7029-7040

Reimers CE, Tender LM, Fertig S, Wang W. 2001. Harvesting energy from the marine sediment-water interface. *Environmental Science & Technology* 35: 192-195

Rezaei F, Richard TL, Brennan RA, Logan BE. 2007. Substrate-enhanced microbial fuel cells for improved remote power generation from sediment-based systems. *Environmental Science & Technology* 41: 4053-4058

Rhoads A, Beyenal H, Lewandowski Z. 2005. Microbial fuel cell using anaerobic respiration as an anodic reaction and biomineralized manganese as a cathodic reactant. *Environmental Science & Technology* 39: 4666-4671

Ryckelynck N, Stecher HA, Reimers CE. 2005. Understanding the anodic mechanism of a seafloor fuel cell: Interactions between geochemistry and microbial activity. *Biogeochemistry* 76: 113-139

Schröder U. 2007. Anodic electron transfer mechanisms in microbial fuel cells and their energy efficiency. *Physical Chemistry Chemical Physics* 9: 2619-2629

Schulz HD. 2006. Quantification of Early Diagenesis: Dissolved Constituents in Pore Water and Signals in the Solid Phase. In *Marine Geochemistry*, ed. HD Schulz, M Zabel. Berlin: Springer

Scott K, Cotlarciuc I, Hall D, Lakeman JB, Browning D. 2008. Power from marine sediment fuel cells: the influence of anode material. *Journal of Applied Electrochemistry* 38: 1313-1319

Scott K, Cotlarciuc I, Head I, Katuri KP, Hall D, et al. 2008. Fuel cell power generation from marine sediments: Investigation of cathode materials. *Journal of Chemical Technology and Biotechnology* 83: 1244-1254

Shantaram A, Beyenal H, Raajan R, Veluchamy A, Lewandowski Z. 2005. Wireless sensors powered by microbial fuel cells. *Environmental Science & Technology* 39: 5037-5042

Solorzano L. 1969. Determination of ammonia in natural waters by the phenolhypochlorite method. *Limnology and Oceanography* 14: 799-801

Stams AJM, de Bok FAM, Plugge CM, van Eekert MHA, Dolfing J, Schraa G. 2006. Exocellular electron transfer in anaerobic microbial communities. *Environmental Microbiology* 8: 371-382

Stumm W, Morgan JJ. 1996. *Aquatic Chemistry: Chemical Equilibria and Rates in Natural Waters*: Wiley-Interscience

Tabatabai M. 1974. A rapid method for determination of sulfate in water samples. *Environmental Letters* 7: 237-243

Tender LM, Gray SA, Groveman E, Lowy DA, Kauffman P, et al. 2008. The first demonstration of a microbial fuel cell as a viable power supply: Powering a meteorological buoy. *Journal of Power Sources* 179: 571-575

Tender LM, Gray SA, Groveman E, Lowy DA, Kauffman P, et al. 2008. The first demonstration of a microbial fuel cell as a viable power supply: Powering a meterological buoy. *Journal of Power Sources* 179: 571-575

Tender LM, Reimers CE, Stecher HA, Holmes DE, Bond DR, et al. 2002. Harnessing

microbially generated power on the seafloor. *Nature Biotechnology* 20: 821-825

Thauer RK, Jungermann K, Decker K. 1977. Energy conservation in chemotrophic anaerobic bacteria. *Bacteriological Reviews* 41: 100-180

Tivey MK, Bradley AM, Joyce TM, Kadko D. 2002. Insights into tide-related variability at seafloor hydrothermal vents from time-series temperature measurements. *Earth and Planetary Science Letters* 202: 693-707

Torres ME, McManus J, Hammond DE, de Angelis MA, Heeschen KU, et al. 2002. Fluid and chemical fluxes in and out of sediments hosting methane hydrate deposits on Hydrate Ridge, OR, I: Hydrological provinces. *Earth and Planetary Science Letters* 201: 525-540

Trauth M. 2006. *MATLAB Recipes for Earth Sciences*: Springer

Wang KL, Davis EE. 1996. Theory for the propagation of tidally induced pore pressure variations in layered subseafloor formations. *Journal of Geophysical Research-Solid Earth* 101: 11483-11495

Whitfield M. 1972. The electrochemical characteristics of natural redox cells. *Limnology and Oceanography* 17: 383-393

Winter M, Brodd RJ. 2004. What Are Batteries, Fuel Cells, and Supercapacitors? *Chemical Reviews* 104: 4245-4270

# Appendices

# Appendix A: Supplementary figures from Chapter 2.

Figure S1

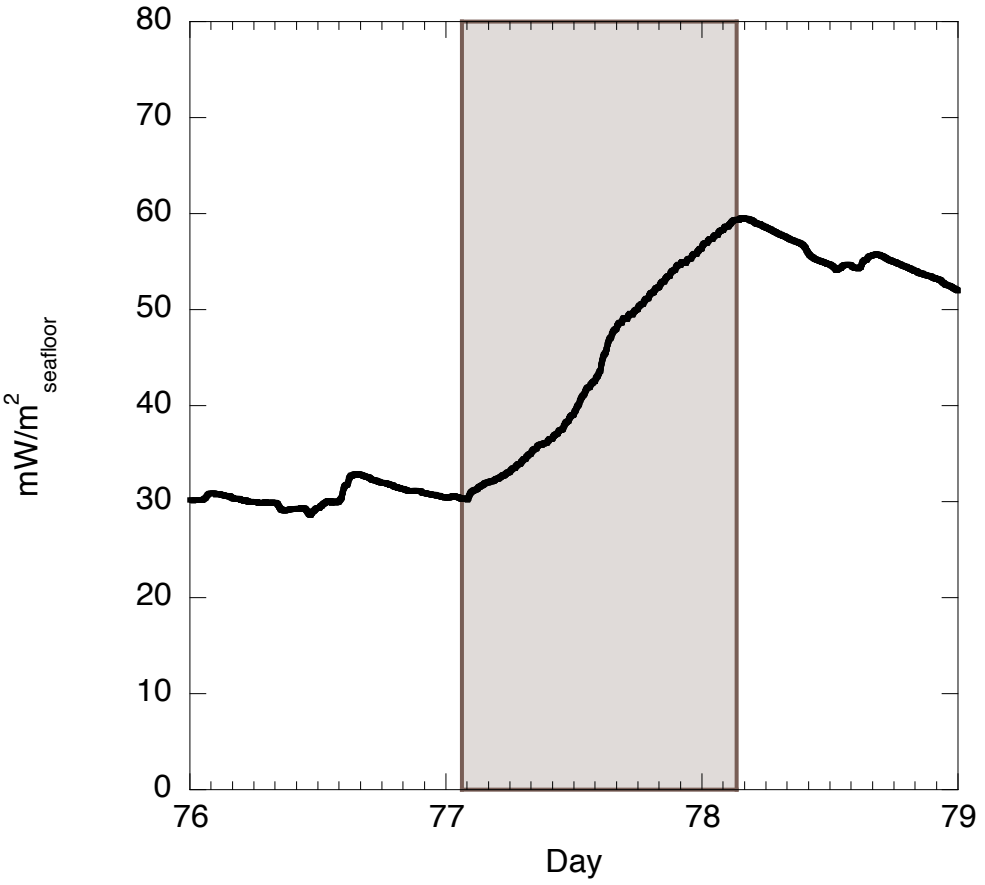


Figure A.1 24-Hour pumping experiment on Yaquina Bay BMFC. Beginning on Day 77, we conducted a 24-hour interval pumping experiment (shaded area). Using a laboratory timer, BMFC B was pumped at intervals of 1 minute on and 29 minutes off. Figure B.1 shows the power density determined from measurements made at one minute intervals during this experiment. The steady increase in power during the experiment confirms that the concentration effect is responsible for the rise in power due to advection. If hydrodynamics were responsible then the one minute pumping intervals would be evident in this plot.

Figure S2

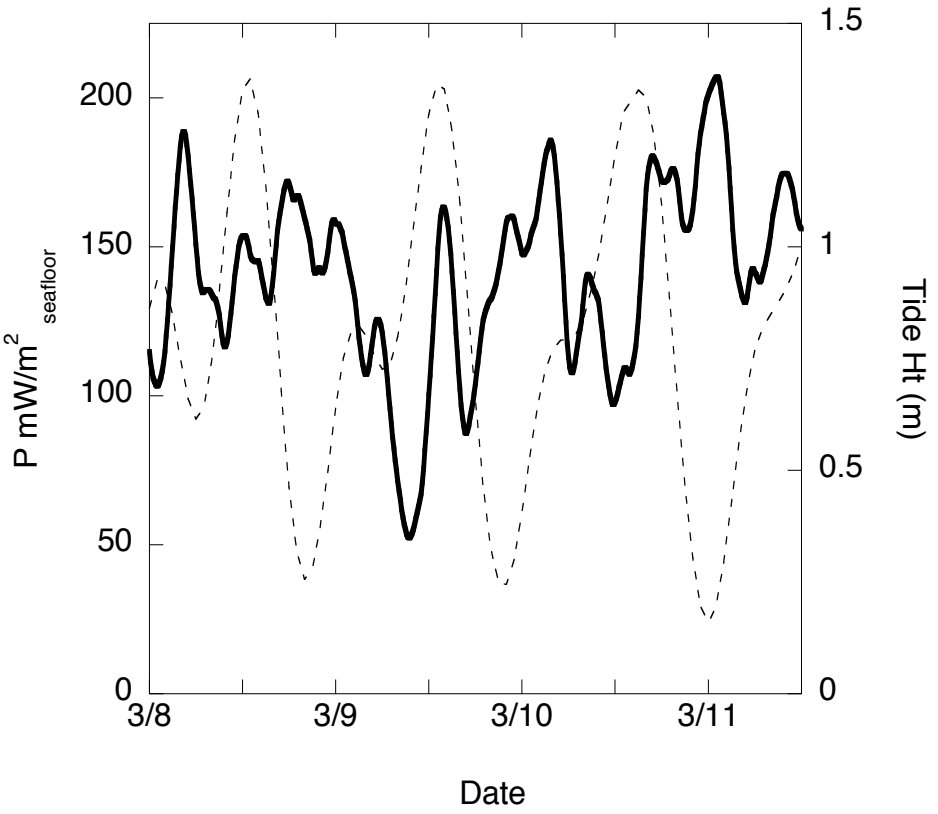


Figure A.2 Magnified portion of the power density record from the Monterey Canyon BMFC compared to the tide data from Moss Landing, CA (Station No. 9413616, www.tidesandcurrents.noaa.gov). The frequency of power peaks (solid line) is similar to the tidal signal (dashed line), but may be slightly out of phase due to the distance between the deployment site and the nearest tide gage. At a water depth of 960 m and a distance of 27 km from shore, the only effect that tides could have on the BMFC would be pressure changes or advection through the seeps driven by pressure changes. Other factors such as bottom water salinity, oxygen and temperature do not change significantly with the tides at this location.

# Appedix B: Data for selected figures from Chapters 2 through 5

**Table B.1 Chemical data from pumped and unpumped Yaquina Bay BMFCs (Figure 2.3)**

| Date/Time | Day | BMFC | T (°C) | pH | Sulfide (μM) | Ammonia (μM) | DIC (mM $CO_2$) | DOC (μM) | Cl (mM) | SO4 (mM) | SO4:Cl |
|---|---|---|---|---|---|---|---|---|---|---|---|
| 12/14/05 8:15 | 15 | Pumped | 7.5 | | 0 | 1906 | 8.7 | 275 | 561 | 18.3 | 0.033 |
| 12/14/05 9:00 | 15 | Unpumped | | | 0 | 3820 | 13.2 | 548 | 584 | 15.7 | 0.027 |
| 12/14/05 9:35 | 15 | Pumped | 10.5 | 7.34 | 0 | 1684 | 9.9 | 254 | 559 | 17.5 | 0.031 |
| 12/14/05 10:24 | 15 | Pumped | 11.1 | 7.32 | 0 | 1774 | 9.9 | 252 | 568 | 18.2 | 0.032 |
| 12/14/05 11:20 | 15 | Pumped | 11.1 | 7.32 | 0 | 1829 | 10.1 | 240 | 568 | 18.1 | 0.032 |
| 12/14/05 12:28 | 15 | Pumped | 10.2 | 7.35 | 0 | 1883 | 10.4 | 247 | 558 | 17.8 | 0.032 |
| 12/14/05 13:22 | 15 | Pumped | 10.2 | 7.33 | 24 | 1940 | 10.6 | 220 | 558 | 18.3 | 0.033 |
| 12/14/05 14:22 | 15 | Pumped | 10.9 | 7.33 | 42 | 1870 | 10.2 | 214 | 562 | 18.8 | 0.033 |
| 12/14/05 16:20 | 15 | Pumped | 10.8 | 7.33 | 127 | 1509 | 10.2 | 186 | 567 | 20.8 | 0.037 |
| 12/14/05 18:22 | 15 | Pumped | 10.7 | 7.33 | 226 | 1116 | 8.6 | 171 | 555 | 22.4 | 0.040 |

**Table B.1 (Continued)**

| Date/Time | Day | BMFC | T (°C) | pH | Sulfide (μM) | Ammonia (μM) | DIC (mM $CO_2$) | DOC (μM) | Cl (mM) | SO4 (mM) | SO4:Cl |
|---|---|---|---|---|---|---|---|---|---|---|---|
| 12/15/05 7:40 | 16 | Pumped | 8.8 | 7.38 | 321 | 816 | 7.1 | 143 | 546 | 23.8 | 0.044 |
| 12/15/05 15:00 | 16 | Pumped | 11.1 | 7.26 | 307 | 772 | 6.5 | 206 | 547 | 24.4 | 0.045 |
| 12/16/05 11:25 | 17 | Pumped | 7.4 | 7.32 | 394 | 760 | 6.4 | 209 | 539 | 23.7 | 0.044 |
| 1/4/06 14:00 | 36 | Pumped | 13.8 | 7.26 | 0 | 1122 | 3.1 | 331 | 535 | 23.3 | 0.044 |
| 1/5/06 12:40 | 37 | Pumped | 16.6 | 7.23 | 497 | 782 | 8.4 | 278 | 533 | 23.2 | 0.044 |
| 1/6/06 11:57 | 38 | Pumped | 14.9 | 7.3 | 528 | 639 | 8.6 | 324 | 510 | 22.0 | 0.043 |
| 1/9/06 13:10 | 41 | Pumped | 14.8 | 7.32 | 242 | 472 | 6.6 | 239 | 475 | 21.3 | 0.045 |
| 1/11/06 12:33 | 43 | Pumped | 13.9 | 7.15 | 14 | 78 | 3.4 | 189 | 422 | 20.4 | 0.048 |
| 1/13/06 12:55 | 45 | Pumped | 14.5 | 7.14 | 12 | 0 | 1.9 | 156 | 390 | 19.6 | 0.050 |
| 1/15/06 10:00 | 47 | Pumped | 11.2 | 7.19 | 12 | 51 | 2.6 | 217 | 440 | 21.8 | 0.049 |
| 1/17/06 9:00 | 49 | Pumped | 12.9 | 7.17 | 281 | 612 | 14.1 | 257 | 507 | 22.6 | 0.045 |
| 1/19/06 12:30 | 51 | Pumped | 12.8 | 7.17 | 250 | 492 | 7.5 | 204 | 498 | 22.5 | 0.045 |

**Table B.2 Polarization data from Yaquina Bay BMFCs (Figure 2.4)**

| Unpumped Chamber | | Pumped Chamber | | Plate Anode (Tender et al.(2002)) | |
|---|---|---|---|---|---|
| Current Density ($mA\ m^{-2}$) | Power Density ($mW\ m^{-2}$) | Current Density ($mA\ m^{-2}$) | Power Density ($mW\ m^{-2}$) | Current Density ($mA\ m^{-2}$) | Power Density ($mW\ m^{-2}$) |
| 0.1 | 0.1 | 0.0 | 0.0 | 0 | 0 |
| 35 | 26 | 40 | 34 | 17 | 11 |
| 70 | 51 | 79 | 66 | 46 | 25 |
| 131 | 92 | 149 | 120 | 70 | 31 |
| 202 | 135 | 232 | 178 | 84 | 29 |
| 284 | 179 | 329 | 239 | 94 | 23 |
| 357 | 211 | 411 | 282 | 99 | 20 |
| 467 | 249 | 547 | 341 | 107 | 16 |
| 552 | 267 | 630 | 366 | | |
| 625 | 273 | 745 | 387 | | |
| 768 | 270 | 918 | 393 | | |
| 979 | 213 | 1212 | 314 | | |
| 1162 | 95 | 1464 | 134 | | |

**Table B.3 Chemical data from laboratory BMFCs (Figure 4.5)**

| Date | Days | pH | Alkalinity (mM/kg) | Sulfate (mM) | Sulfide (μM) | DOC (mM) |
|---|---|---|---|---|---|---|
| | | | BMFC 1 | | | |
| 07/18/07 | 0 | 7.5 | 12.9 | 25 | 9 | 0.939 |
| 07/20/07 | 2 | 7.17 | 10.9 | 25 | 2 | 0.630 |
| 07/23/07 | 5 | 7.16 | 9.7 | 23 | 2 | 0.466 |
| 07/30/07 | 12 | 7.04 | 9.0 | 24 | 6 | |
| 08/06/07 | 19 | 7.13 | 8.0 | 25 | 0 | |
| 07/22/08 | 370 | 6.03 | 4.2 | 25.3 | 0 | 0.237 |
| | | | BMFC 2 | | | |
| 07/18/07 | 0 | 7.45 | 10.2 | 26 | 50 | 1.197 |
| 07/20/07 | 2 | 7.37 | 9.6 | 27 | 9 | 1.243 |
| 07/23/07 | 5 | 7.21 | 9.1 | 24 | 7 | 0.276 |
| 07/30/07 | 12 | 6.90 | 7.6 | 26 | 17 | |
| 08/06/07 | 19 | 7.08 | 7.5 | 25 | 33 | |
| 07/22/08 | 370 | 5.07 | 0.0 | 22.1 | 1 | 0.295 |
| | | | BMFC 3 | | | |
| 07/18/07 | 0 | 7.89 | 11.2 | 26 | 1 | 0.205 |
| 07/20/07 | 2 | 7.92 | 11.0 | 27 | 1 | 0.140 |
| 07/23/07 | 5 | 7.86 | 11.5 | 24 | 1 | 0.174 |
| 07/30/07 | 12 | 7.99 | 13.5 | 24 | 3 | |
| 08/06/07 | 19 | 7.65 | 12.7 | 26 | 0 | |
| 08/14/08 | 393 | 6.20 | 7.0 | 26.5 | 0 | 0.090 |

**Table B.3 (Continued)**

| Date | Days | pH | Alkalinity (mM/kg) | Sulfate (mM) | Sulfide (μM) | DOC (mM) |
|---|---|---|---|---|---|---|
| | | | BMFC 4 | | | |
| 07/18/07 | 0 | 7.74 | 11.0 | 25 | 29 | 0.935 |
| 07/20/07 | 2 | 7.87 | 10.5 | 26 | 6 | 0.153 |
| 07/23/07 | 5 | 7.72 | 10.7 | 25 | 4 | 0.113 |
| 07/30/07 | 12 | 7.93 | 10.7 | 24 | 9 | |
| 08/06/07 | 19 | 7.42 | 10.5 | 24 | 10 | |
| 08/14/08 | 393 | 5.10 | 0.0 | 22.3 | 1.19 | 0.510 |
| | | | BMFC 5 | | | |
| 07/18/07 | 0 | 7.96 | 13.4 | 25 | 3 | 0.441 |
| 07/20/07 | 2 | 7.51 | 10.3 | 26 | 1 | 0.460 |
| 07/23/07 | 5 | 7.39 | 9.3 | 25 | 1 | 0.223 |
| 07/30/07 | 12 | 7.24 | 7.3 | 23 | 3 | |
| 08/06/07 | 19 | 6.80 | 6.1 | 25 | 0 | |
| 08/14/08 | 393 | 5.90 | 3.8 | 24.2 | 0 | 0.100 |
| | | | BMFC 6 | | | |
| 07/18/07 | 0 | 7.89 | 15.1 | 24 | 6 | 0.479 |
| 07/20/07 | 2 | 7.76 | 11.3 | 25 | 1 | 0.336 |
| 07/23/07 | 5 | 7.53 | 10.8 | 24 | 1 | 0.274 |
| 07/30/07 | 12 | 7.03 | 6.9 | 21 | 8 | |
| 08/06/07 | 19 | 6.92 | 7.2 | 23 | 8 | |
| 08/14/08 | 393 | 5.00 | 0.0 | 19.8 | 0 | 0.280 |

**Table B.4 Power converter calibration data (Figure 5.5)**

| $E_{cell}$ | $I_{BMFC}$ (mA) | $P_{BMFC}$ (mW)* | $I_{ch}$ (mA) | $P_{ch}$ (mW)** | Efficiency (%) |
|---|---|---|---|---|---|
| 0.3 | 0 | 0 | 0 | 0 | |
| 0.3 | 31 | 9 | 2 | 8 | 81% |
| 0.3 | 41 | 12 | 3 | 10 | 83% |
| 0.3 | 51 | 15 | 4 | 13 | 86% |
| 0.3 | 80 | 24 | 6 | 22 | 91% |
| 0.3 | 157 | 47 | 12 | 44 | 93% |
| 0.4 | 0 | 0 | 0 | 0 | |
| 0.4 | 29 | 12 | 2 | 8 | 66% |
| 0.4 | 36 | 14 | 3 | 10 | 71% |
| 0.4 | 48 | 19 | 4 | 14 | 71% |
| 0.4 | 70 | 28 | 6 | 22 | 78% |
| 0.4 | 131 | 52 | 12 | 41 | 79% |
| 0.5 | 0 | 0 | 0 | 0 | |
| 0.5 | 26 | 13 | 2 | 7 | 53% |
| 0.5 | 32 | 16 | 3 | 9 | 58% |
| 0.5 | 35 | 18 | 3 | 12 | 68% |
| 0.5 | 68 | 34 | 6 | 20 | 59% |
| 0.5 | 140 | 70 | 12 | 43 | 62% |

Notes: * $P_{BMFC} = I_{BMFC} \times E_{cell}$

** $P_{ch} = I_{ch} \times 3.5$ V